

**DYNAMIC BEHAVIOUR OF  
LVL-CONCRETE COMPOSITE  
FLOORING SYSTEMS**

**Ph.D Thesis**

**Nor Hayati Abd. Ghafar**

**2015**

**Supervisors**

Prof. Andy Buchanan

Assoc. Prof. Massimo Fragiacomò

Dr Zainah Ibrahim

*Special dedication to  
my late mum, your love always with us  
'FARIDAH SALLEH'  
(1959-2010)*

## Abstract

An LVL-concrete composite floor (LCC) is a hybrid flooring system, which was adapted from a timber-concrete composite (TCC) floor system. By replacing the timber or glulam joists with LVL joists, the strength of the floor was increased. However, the demand nowadays is to build longer spans and this may reduce the stiffness and lead to the floor being more susceptible to vibration problems.

While the vibration problem may not be as critical as other structural issues, people could feel sick and not comfortable if the floor vibrates at the resonant frequency of the human body. Hence, this research focuses on the dynamic behaviour of long span LCC flooring systems. Experimental testing and finite element modelling was used to determine the dynamic behaviour, with particular regard to the natural frequency,  $f_n$  and mode shape of an LCC floor.

Initially, a representative series of LVL-concrete composite specimen types were built starting from (1) full-scale T-joist specimens, (2) reduced-scale (one-third) multi-span T-joist specimens and (3) reduced-scale (one-third) 3m x 3 m floor. The specimens were tested using an electrodynamic shaker. The SAP 2000 finite element modelling package was used to model and evaluate the full- and reduced-scale LVL-concrete composite T-joist experimental results. Additionally, a 8m x 7.8 m LCC floor was modelled and analysed using SAP 2000. The behaviour of the 8m LCC floor was investigated through the changing of (1) concrete topping thickness, (2) depth of LVL joist, (3) different types of boundary conditions, and (4) the stiffness of the connectors.

Both the experimental results and the finite element analyses agreed and showed that increased stiffness increased the natural frequency of the floor, and the boundary conditions influenced the dynamic behaviour of the LCC floor. Providing more restraint increased the stiffness of the floor system. The connectors' stiffness did not influence the dynamic performance of the floor.

The study outcomes were based on a 8 Hz natural frequency limitation where the fundamental natural frequency of the LCC floor must exceed 8 Hz in order to prevent vibration problems. The research showed that a 8 m LCC long span floor can be constructed using LVL joists of between 300 mm to 400 mm depth with a concrete thickness of 65 mm for the longer spans, and joists of between 150 mm to 240 mm depth in conjunction with a concrete topping thickness of 100 mm for the shorter spans.

## **Acknowledgments**

First and foremost to the great Allah Almighty, for giving me the strength to face all the obstacles and challenges, including two major earthquakes for me to complete this research successfully.

I would like to thank University Tun Hussein Onn Malaysia and the Ministry of High Education, Malaysia for giving me a big opportunity to further my study and for providing the scholarship.

The big thanks are to my supervisors, Prof. Andy Buchanan, Assoc. Prof Massimo Fragiacommo and Dr Zainah Ibrahim who never stopped giving me their knowledge for all the time of the research. Also to Dr. Bruce Deam and Assoc. Professor Peter Moss for your help and encouragement, insight and advice that have been invaluable to the success of this work. Also to Dr. David Carradine for your kindness helping me in the laboratory and being a part of this project.

Thanks are also expressed to David Yeoh, Marta Martalli and Kyle Channing-Pearch who were directly involved during the experimental phase in this project. Also thanks to John Maley, Tim Perigo, Gavin Keats, Nigel Dixon and other UC technicians who were directly and indirectly involved. Special thanks to Vinod Sadashiva and Charlotte Brown for their kindness.

In a addition, I would like to thank my family specially for dad, Asyikin (adik), Ain, Azli and Saaidah (Ucu), my best friends ever (Hartini, Mariyam, Farah Dina and Nastaein), and my flatmates (Fatanah, Shazlina and Ummu) for their support and putting up with me during the ups and downs of the last four years.

Finally, very deep appreciation to my husband, Wan Afnizan for always being there to support, encourage and be patient throughout the course of this work for the last few years.

## TABLE OF CONTENTS

<b>ABSTRACT.....</b>	<b>I</b>
<b>ACKNOWLEDGMENTS .....</b>	<b>II</b>
<b>TABLE OF CONTENTS .....</b>	<b>III</b>
<b>LIST OF FIGURES .....</b>	<b>VI</b>
<b>LIST OF TABLES .....</b>	<b>VIII</b>
<b>LIST OF SYMBOLS .....</b>	<b>IX</b>
<b>CHAPTER 1 INTRODUCTION.....</b>	<b>1</b>
<b>1.1 Aims and Objectives of the Research</b>	<b>2</b>
<b>1.2 Scope of the Research</b>	<b>2</b>
<b>1.3 Methodology of the Research</b>	<b>4</b>
<b>1.4 Significance of the study</b>	<b>4</b>
<b>1.5 Outline of Thesis</b>	<b>5</b>
<b>CHAPTER 2 LITERATURE REVIEW .....</b>	<b>8</b>
<b>2.1 Timber-concrete composite (TCC) floor system</b>	<b>8</b>
<b>2.1.1 Development of TCC</b>	<b>11</b>
<b>2.1.2 Design of TCC floors</b>	<b>14</b>
<b>2.1.3 LVL-Concrete Composite Flooring System</b>	<b>15</b>
<b>2.2 Floor Vibration</b>	<b>18</b>
<b>2.2.1 Floor Vibration Assessment</b>	<b>19</b>
<b>2.2.2 Vibration Assessment on Timber-Concrete Composite (TCC) Floor</b>	<b>21</b>
<b>2.2.3 Human Perception of Floor Vibration</b>	<b>22</b>
<b>2.2.4 Design Criteria for Floor Vibration</b>	<b>24</b>
<b>2.2.5 Use of Dampers to Control Floor Vibrations</b>	<b>37</b>
<b>2.3 Summary</b>	<b>37</b>
<b>CHAPTER 3 FULL-SCALE LCC T-JOIST SPECIMENS.....</b>	<b>39</b>
<b>3.1 LCC T-joist Specimen Details</b>	<b>40</b>
<b>3.2 Experiment Modal Testing Method</b>	<b>44</b>

<b>3.3</b>	<b>Modal Parameter Extraction Method</b>	<b>46</b>
<b>3.4</b>	<b>Dynamic performance of LCC T-joist specimens</b>	<b>49</b>
<b>3.5</b>	<b>Effect of span length</b>	<b>54</b>
<b>3.6</b>	<b>Effect of topping width</b>	<b>54</b>
<b>3.7</b>	<b>Effect of support stiffness</b>	<b>55</b>
<b>3.8</b>	<b>Finite Element Modelling of LCC T-joist specimens</b>	<b>58</b>
<b>3.9</b>	<b>Comparison between the modal test (EMA) and finite element modelling (FEA)</b>	<b>63</b>
<b>3.10</b>	<b>Damping from Impact Hammer Test</b>	<b>65</b>
<b>3.11</b>	<b>Conclusion and Summary</b>	<b>68</b>

**CHAPTER 4 EXPERIMENTAL MODAL ANALYSIS (EMA) ON REDUCED SCALE LVL-CONCRETE COMPOSITE (LCC) T-JOIST SPECIMENS .....70**

<b>4.1</b>	<b>Construction Detail of Reduced Scale specimens</b>	<b>71</b>
<b>4.1.1</b>	<b>Multi-span specimen detail</b>	<b>71</b>
<b>4.1.2</b>	<b>Multi-storey specimen detail</b>	<b>73</b>
<b>4.1.3</b>	<b>Single-bay T-joist floor details</b>	<b>75</b>
<b>4.2</b>	<b>Dynamic performance of multi-span specimens</b>	<b>76</b>
<b>4.3</b>	<b>Dynamic performance of multi-storey specimens</b>	<b>78</b>
<b>4.4</b>	<b>Dynamic performance of a single-bay floor</b>	<b>80</b>
<b>4.5</b>	<b>Conclusion and Summary</b>	<b>82</b>

**CHAPTER 5 ANALYTICAL MODELLING OF REDUCED SCALE LCC T-JOIST SPECIMENS AND FLOORS .....84**

<b>5.1</b>	<b>Multi-span specimens</b>	<b>88</b>
<b>5.2</b>	<b>Multi-storey specimens</b>	<b>96</b>
<b>5.3</b>	<b>Single-bay T-joist floor</b>	<b>100</b>
<b>5.4</b>	<b>Discussion</b>	<b>101</b>
<b>5.5</b>	<b>Summary and Conclusions</b>	<b>105</b>

**CHAPTER 6 ANALYTICAL MODELLING OF FULL-SCALE T-JOIST LCC FLOOR .....107**

<b>6.1</b>	<b>8 m x 7.8 m T-joist LCC floor model</b>	<b>107</b>
<b>6.2</b>	<b>8 m x 7.8 m T-joist LCC floor behaviour</b>	<b>110</b>
<b>6.3</b>	<b>Effect of connector stiffness</b>	<b>116</b>
<b>6.4</b>	<b>Effect of concrete topping thickness</b>	<b>117</b>
<b>6.5</b>	<b>Effect of LVL joist depth</b>	<b>118</b>
<b>6.6</b>	<b>Relationship between concrete topping thickness and LVL joist depth</b>	<b>120</b>
<b>6.7</b>	<b>Conclusion and Summary</b>	<b>125</b>

<b>CHAPTER 7 DESIGN FOR VIBRATION OF LVL- CONCRETE COMPOSITE (LCC) FLOORS .....</b>	<b>126</b>
<b>7.1 Introduction</b>	<b>126</b>
<b>7.2 Design criteria</b>	<b>127</b>
<b>7.3 Preliminary design</b>	<b>127</b>
<b>7.4 Advanced design method</b>	<b>128</b>
<b>7.5 Simple design method</b>	<b>132</b>
<b>7.6 Worked Example</b>	<b>134</b>
<b>7.7 Summary</b>	<b>137</b>
<b>CHAPTER 8 CONCLUSIONS AND RECOMMENDATIONS FOR FURTHER WORK .....</b>	<b>138</b>
<b>8.1 Research objectives</b>	<b>138</b>
<b>8.2 Research Summary</b>	<b>138</b>
<b>8.3 Recommendations for designers</b>	<b>140</b>
<b>8.4 Recommendation for Further Research</b>	<b>141</b>
<b>REFERENCES.....</b>	<b>142</b>
<b>APPENDIX A MATERIAL PROPERTIES .....</b>	<b>147</b>
<b>APPENDIX B WORKED EXAMPLE .....</b>	<b>148</b>

## LIST OF FIGURES

Figure 2-1 Timber-concrete interlayer connections .....	13
Figure 2-2 Proposed semi-prefabricated TCC floor system (Yeoh, 2008).....	17
Figure 2-3 Layout details of semi-prefabricated 'M' panel (a) off-site panel, .....	17
Figure 2-4 A person perform the heel drop test and the time history of the test .....	20
Figure 2-5 Evaluation of human sensitivity by acceleration or velocity response versus natural frequency, $f_n$ .....	23
Figure 2-6 Reiher-Meister scale .....	25
Figure 2-7 Modified Reiher-Meister scale .....	26
Figure 2-8 Recommended peak acceleration for human comfort for vibration due to human activity (source : Murray et al.,2003) .....	28
Figure 2-9 Relationship between a and b (CEN, 2008b) .....	31
Figure 3-1 (a) LVL-concrete composite specimen detail and.....	41
Figure 3-2 (a) 8 m LVL-concrete composite specimen with single LVL and .....	41
Figure 3-3 (a) 8 m LVL-concrete composite specimen with double LVL and .....	42
Figure 3-4 (a) 10 m LVL-concrete composite specimen and.....	42
Figure 3-5 Layout of 6 m beam .....	43
Figure 3-6 Different types of support condition .....	43
Figure 3-7 Location of exciter and node points along the LVL joist.....	44
Figure 3-8 Response of Specimen A.....	48
Figure 3-9 Theoretical mode shape for simply supported beam.....	51
Figure 3-10 The first three mode shape of 6 m and 8 m specimens from vibration tests .....	51
Figure 3-11 End support condition before and after being fixed to the ground .....	53
Figure 3-12 (a) Boundary stiffness a timber block as support and (b) mesh model.....	57
Figure 3-13 Finite element model.....	57
Figure 3-14 Support effective width .....	58
Figure 3-15 Lumped mass system.....	59
Figure 3-16 LCC finite element models .....	60
Figure 3-17 Connection experimental load-slip curve (source: Yeoh (2010)) .....	60
Figure 3-18 Mode shapes from finite element modelling for 6 m and 8 m specimens.....	62
Figure 3-19 Comparison of 6 m specimens with and without cantilever arm.....	62
Figure 3-20 A person striking the specimen and the time history of the impact force.....	65
Figure 3-21 Beam responses from impact hammer test .....	66
Figure 3-22 Decay of motion.....	67
Figure 3-23 Critical damping ratio.....	67
Figure 3-24 Natural frequency limitation for a LCC flooring system .....	69
Figure 4-1 Photographs of the multi-span system.....	72
Figure 4-2 Concrete topping being cut to split the beams .....	73
Figure 4-3 Multi-storey single-bay systems.....	74
Figure 4-4 2-storey, 2-bay T-joist beams .....	74
Figure 4-5 Floor plan layout (dimension in mm).....	75
Figure 4-6 Cross-section A - A .....	75
Figure 4-7 Multi-span mode shape.....	78

Figure 4-8 Multi-storey mode shape .....	80
Figure 4-9 Vibration test layout for single-bay floor.....	81
Figure 4-10 Mode shape for single-bay floor.....	81
Figure 4-11 Mode shapes curve to the perpendicular of the joist span.....	82
Figure 5-1 FE modelling elements representing structure components .....	84
Figure 5-2 FE model for continuous T-joist specimen .....	85
Figure 5-3 Details of timber block, joist and joist hanger (unit in mm) .....	86
Figure 5-4 Natural frequency and mode shape for 1-span specimen .....	90
Figure 5-5 Natural frequency and mode shape for 2-span specimen .....	91
Figure 5-6 Natural frequency and mode shape for 3-span specimen .....	92
Figure 5-7 Natural frequency and mode shape for 3-span specimen (cont').....	93
Figure 5-8 Natural frequency and mode shape for 4-span specimen .....	94
Figure 5-9 Natural frequency and mode shape for 4-span specimen (cont').....	95
Figure 5-10 Natural frequencies and mode shapes for a 2-storey specimen.....	96
Figure 5-11 Natural frequencies and mode shapes for a 3-storey specimen.....	97
Figure 5-12 Natural frequencies and mode shapes for a 4-storey specimen.....	98
Figure 5-13 Mode shape behaviour for a 2-bay, 2-storey specimen.....	99
Figure 5-14 Natural frequencies and mode shapes for a single-bay 3 m x 3 m floor .....	100
Figure 5-15 Comparative mode shapes for multi-span LCC specimens.....	103
Figure 5-16 Comparative mode shapes for multi-storey LCC specimens .....	104
Figure 5-17 Comparative mode shapes for the single-bay LCC floor.....	105
Figure 6-1 FE model of a floor strip of 8 m x 0.6.....	108
Figure 6-2 The model of an 8 m x 7.8 m T-joist LCC floor .....	108
Figure 6-3 Natural frequency vs number of nodes for mesh size of the floor strip .....	109
Figure 6-4 Different types of support system .....	111
Figure 6-5 Natural frequency of different types of support systems .....	113
Figure 6-6 Mode shapes of LCC floor with different types of support system .....	114
Figure 6-7 Comparison of natural frequency for different types of connector stiffness.....	117
Figure 6-8 The first six modes of vibration with increasing concrete topping thickness .....	118
Figure 6-9 The first six modes of vibration with increasing depth of LVL joist .....	119
Figure 6-10 Comparison of natural frequencies for different concrete topping thickness.....	122
Figure 6-11 Comparison of natural frequencies for different LVL joist depths .....	123

## LIST OF TABLES

Table 2-1 Advantages of TCC Floor System.....	10
Table 2-2 Recommended Values of Parameters, $P_o$ , $\beta$ , and $a_o/g$ limit.....	27
Table 2-3 Recommended Acceleration Limits for Vibrations Due to Rhythmic Activities (Murray et.al, 2003).....	28
Table 2-4 Summary of design methods to control vibrations in timber floors .....	35
Table 2-5 Acceptance criteria over time (Murray et.al, 2003).....	36
Table 3-1 Detail of LCC T-joist specimens .....	40
Table 3-2 Main digital data acquisition parameters adopted for FRF measurements .....	47
Table 3-3 Results of vibration tests on LCC simply supported specimens.....	49
Table 3-4 Comparison of modal properties between a single and a sweep sinusoidal vibration test on 8 m specimen .....	52
Table 3-5 Comparison of modal properties between a non-fixed and a fixed support .....	53
Table 3-6 Comparison of modal properties between different span lengths .....	54
Table 3-7 Comparison of modal properties between different topping widths .....	55
Table 3-8 Comparison of natural frequencies between different support conditions.....	56
Table 3-9 Summary of results from the finite element modelling .....	61
Table 3-10 Comparison between FEA and EMA for different support stiffnesses .....	64
Table 4-1 Results of vibration test on LCC multi-span specimens .....	76
Table 4-2 Result summary of multi-storey specimens.....	79
Table 5-1 Stiffness properties of the springs .....	86
Table 5-2 Prediction of natural frequency for multi-span specimens .....	88
Table 5-3 Comparison of fundamental natural frequency, $f_1$ .....	101
Table 5-4 Comparison of the natural frequencies of a single-bay LCC floor .....	101
Table 6-1 Limitation of concrete topping thickness for 8 m x 7.8 m LCC floor.....	121
Table 6-2 Percentage difference between SAP model and Eurocode 5 formula .....	124
Table 7-1 Suggested topping thickness for LCC floors based on 8 Hz limitation.....	128

## LIST OF SYMBOLS

$a_c, a_t$	Distance between the centroid of the timber-concrete composite section to the centroid of the concrete or timber section, respectively.
$b_1$	Spacing of joist (m)
$d$	Width of floor (m)
$d_t$	Width of joist (m)
$f, f_n$	Natural frequency, fundamental natural frequency (Hz)
$h_c, h_t$	Thickness that define different materials (with subscript c for concrete and t for LVL) (m)
$k, k_j, k_b, k_c$	Spring stiffness that define different properties (with subscript j for joist, b for timber block and c for screw) (N/m)
$k_{com}$	Slip modulus stiffness of composite system (N/m)
$n$	Number of mode shape
$n_{40}$	Number of first-order modes with natural frequencies up to 40 (Hz)
$m$	Distributed mass (kg)
$m_{com}$	Distributed mass of composite (kg)
$m_j$	per unit length of joist (kg/m)
$m_t$	Mass per unit length of joist (kg/m)
$l$	Span length (m)
$l_t$	Spacing of joist (m)
$s_{eff}$	Effective spacing (m)
$s_{max}$	Maximum spacing of connection (m)
$s_{min}$	Minimum spacing of connection (m)
$t_c, t_s, t_p$	Thickness of concrete topping , sub-floor and permanent formwork (m)
$w$	Weight per unit length
$w_n$	Circular natural frequency (rad/s)

$A, A_c, A_t$	Area that define different materials (with subscript c for concrete and t for LVL) ( $m^2$ )
BW	Usable frequency bandwidth (Hz)
C	Joist torsional constant
$E, E_b, E_j, E_c, E_t$	Elastic modulus that define different materials and properties (with subscript b for timber block, j for joist, c for concrete and t for LVL) ( $N/m^2$ )
EI	Effective stiffness (N/m)
$(EI)_b$	Equivalent plate bending stiffness ( $Nm^2/m$ )
$(EI)_i$	Bending stiffness of the floor about an axis perpendicular to the beam direction ( $Nm^2/m$ )
$EI_x$	Flexural stiffness in x-direction (Nm)
$EI_y$	Flexural stiffness in y-direction (Nm)
$(EI)_{com}$	Effective stiffness for composite (N/m)
FR	Frequency resolution
$G_c$	Shear modulus of concrete topping ( $N/m^2$ )
H	Floor thickness (concrete topping + joist depth) (m)
$K_j$	Joist spring constant (N/m)
$K_L$	Spring constant of subfloor and topping (N/m)
$L_n$	Generalised excitation
$M_n$	Generalised mass
P	Force (N)
RL	Record length
SR	Sample rate (Hz)
T	Period (s)
$\xi$	Modal damping ratio (%)
$\delta$	Deflection (mm)
$\rho, \rho_c, \rho_t, \rho_s$	Density that define different materials (with subscript c for concrete, t for timber and s for sub-floor) ( $kg/m^3$ )
$\Phi$	Characteristic mode shape
$\Gamma$	Participation factor

EMA	Experimental Modal Analysis
FEA	Finite Element Analysis
LCC	LVL Concrete Composite
LVL	Laminated Veneer Lumber
TCC	Timber Concrete Composite

## CHAPTER 1 INTRODUCTION

This thesis considers the dynamic performance of LVL-concrete composite (LCC) floor systems. LCC floor systems are hybrid structures in which solid timber or glued laminated timber beams are connected to a concrete slab in order to develop composite action. The new application of laminated veneer lumber (LVL) instead of sawn timber or glued laminated timber can further improve the performance of the timber-concrete composite (TCC) system. TCC and LCC are nearly the same, but LVL has higher strength and reduced variability, as a more reliable engineering material.

The composite action has to resist slip forces between timber and concrete. According to Ceccotti (1995), the TCC structure is distinguished by a bending stiffness much higher than the simple timber beam or concrete slab on their own. In comparison with reinforced concrete floors, the TCC floors are lighter and more sustainable. In comparison with timber floors, they are characterised by greater strength and stiffness, increased thermal mass, better acoustic separation and they are less susceptible to vibration.

These systems are an innovative system of timber structures to meet the demand for high-performance long-span floors. However, there is still a concern about serviceability vibration in the case of medium to long span LCC floors. These serviceability vibration problems can occur due to human activities like walking, running and jumping, which provide a repetitive loading on the floor. When the load variation has the same frequency as the natural frequency of the floor, resonance can occur and make other users feel uncomfortable and annoyed.

As retrofitting the floor to eliminate resonance can be quite expensive and difficult, the best way is to design the floor properly at the start by having an adequate understanding of the physical phenomena and a regard for the consequences of poor design. Thus, a LCC floor system has been constructed and tested at the University of Canterbury in collaboration with Carter Holt Harvey Wood products, a local New Zealand manufacturer of LVL. The performance of dynamic behaviour, natural

frequency and mode shape of the LCC floor was investigated. The study was continued by carrying out finite element modelling using SAP 2000 software to verify the experimental work as well as to explore the influences of concrete topping thickness, LVL joist depth, boundary conditions and connection stiffness. A simple design method proposed for predicting the response of the LCC floor, for a complicated flooring system is discussed at the end of this research.

## **1.1 Aims and Objectives of the Research**

The main objective for this research is to provide a better understanding of the vibration performance of LCC floors. The investigation is focussed on the dynamic behaviour of LCC floors, including natural frequencies, damping ratio and mode behaviours, and also the effect of boundary conditions.

In order to improve the knowledge of the dynamic behaviour of LVL-concrete composite T-joist floors and to provide some recommendations to control the vibration of these floors, the following specific research objectives were developed:

1. Experimentally characterise the dynamic performance (specifically the natural frequencies, equivalent viscous damping ratios and mode shapes) of full- and reduced-scale LVL-concrete composite floor system beams and floors.
2. Implement numerical finite element modelling of the tested structures, full- and reduced-scale beams and floors, using the results from experimental modal analysis to verify the models.
3. Propose a simple design method for control of vibration at the serviceability limit state based on finite element modelling results.

## **1.2 Scope of the Research**

The scope of the investigation of the dynamic behaviour of LCC T-joist specimens and floors covered:

- i) Experimental testing using experimental modal analysis (EMA):

- a. Full-scale, long-span beams with a representative range of cross-section and shear connector arrangements and positions.
  - b. Full-scale, long-span beams in order to predict the dynamic stiffness from the service stiffness that others have shown can be reliably calculated from the mechanical properties of the composite system.
  - c. Full-scale, long-span beams of varying lengths to verify the predictions for a range of span lengths.
  - d. Full-scale long-span beams with different supports in order to indentify how the support stiffness affected the dynamic response.
  - e. One-third (dimensionally) scaled beams in order investigate how the joist hanger properties affect the performance.
  - f. One-third (dimensionally) scaled multiple-span beams to estimate the junction stiffness and its effects.
  - g. One-third (dimensionally) scaled multiple-span beams to investigate the dynamic behaviour of adjacent beams.
  - h. One-third (dimensionally) scaled multi-storey beams in order to investigate how the coupling moment at the ends of the beams affects the performance.
  - i. One-third (dimensionally) scaled multi-storey beams to study the vibration energy transmitted between floors above and below.
- ii) Numerical finite element modelling:
- a. Modelling of all the tested floor systems which are listed above.
  - b. Modelling of full-scale floors to investigate the dynamic performance behaviour while changing the parameters, including the boundary conditions of the system.
  - c. Modelling of full-scale floors to study the relationship between the deflection under a 1 kN applied at mid-span and the fundamental natural frequency,  $f_1$ , of the LCC flooring system.

### **1.3 Methodology of the Research**

In order to achieve the research objectives, a series of LCC floor specimens were built as follows. Details of these specimens are described in Chapters 3 and 4.

- Specimen A : 8 m x 0.6 m full-scale LCC T-joist specimen.
- Specimen B : 8 m x 1.2 m full-scale LCC T-joist specimen.
- Specimen C : 10 m x 0.6 m full-scale LCC T-joist specimen.
- Specimen D : 3 m x 0.5 m x 4 span reduced-scale LCC T-joist specimen.
- Specimen E : One-third scale LCC T-joist floor.

Experimental modal analysis (EMA) was performed to determine the dynamic parameters of LCC flooring systems. An electrodynamic shaker was used to excite the specimens, for which the harmonic signal was supplied through a signal generator. Beforehand, grid lines were drawn on the concrete slab to collect the required data at suitable points. The number of points was selected so as to obtain the mode shapes of all vibration modes of interest.

The finite element SAP 2000 software package was utilised to model the specimens, to obtain the modal parameters as well as to verify the experimental results. Furthermore, the numerical investigations focussed on concrete topping thickness, LVL joist depth, boundary conditions and the overall stiffness of the system, which affect the modal parameters of the LCC floors.

### **1.4 Significance of the study**

Vibration serviceability issues are a concern in the case of medium to long span LCC floors. The problem may be even increased when LVL is used instead of sawn timber, due to the relatively high ratio of strength to Young's modulus. Timber is characterised by a high strength to weight ratio, which leads to reduced mass, but low Young's modulus which leads to reduced stiffness and susceptibility to vibration problems. The concrete slab, in fact, is relatively thin (40 to 70 mm) and the timber joists are quite flexible because of the low Young's modulus of timber.

Full assessment of long span LCC beams and floor were conducted through EMA and FEA procedures. The purpose of the assessment was to investigate the

dynamic behaviour of the LCC floor and to ensure the LCC floor met the vibration serviceability limitation as suggested in Euro code 5 (CEN, 2005). Thus, the main contributions of this research include:

1. The assessment was conducted with different span lengths of LCC beams. The results show that the longest span for an LCC beam of the dimensions tested in this thesis is 8 m as the fundamental natural frequency is more than 8 Hz. The natural frequency for a 10 m beam was found to be less than 8 Hz. The greater deflection and rotation of the 10 m beam could be seen during the experimental work. Thus, a 10 m beam floor is not recommended unless larger LVL beams are used, possibly in conjunction with a thicker concrete slab.
2. According to the parametric study on an 8m x 7.8 m LCC floor, a minimum concrete topping thickness is proposed based on the standard size of LVL joist from a manufacturer. For an LVL joist depth of 150 mm to 240 mm with 63 mm breath, the minimum concrete thickness is 100 mm and for LVL joist depth 300 mm to 400 mm with 63 mm breath, the minimum concrete thickness is 65 mm. This is a guide for a designer to estimate the size of LCC floor to meet the vibration serviceability limit.
3. A simple design method is recommended for controlling vibration based on the vibration serviceability limit state. The design method is based on finite element modelling (FEM). The FEM was better than hand calculation in terms of time and difficulty, especially for complex structures.

## **1.5 Outline of Thesis**

Eight chapters are used to present the research work in this thesis. A brief summary of each chapter is discussed in this section.

This Chapter 1 gives a brief introduction to this research including the research background, problems, and objectives and scope of the studies. The research was focused on serviceability problems of LCC floors.

Chapter 2 discusses previous research results that focus on (1) timber-concrete composite floor systems and (2) floor vibrations. The discussion begins with the development of timber-concrete composite systems, including background details and development of this system by other researchers. The connection between timber and concrete becomes the most important part of the system. Thus, most of the studies focus on the shear connectors, which are made from mechanical or adhesive fasteners.

Later, the discussions concentrate on the investigation of floor vibration, including timber, steel, concrete and composite flooring systems. The design of vibration control recommended for each type of flooring system will give guidance to this research to generate a new guideline for vibration control of LCC flooring systems.

Chapter 3 represents a step by step preliminary study on dynamic performance of full-scale LCC floors, including the vertical vibration methodology and data analysis, which will give guidance to the investigations of the multi-span and multi-storey reduced-scale LCC specimens. To verify the experimental data, finite element modelling used the SAP 2000 software package to generate the predicted behaviour. Comparisons between experimental and modelling investigations on dynamic behaviour are discussed later in this chapter.

Chapter 4 describes detailed construction of reduced-scale LCC T-joist specimens and LCC T-joist floors. The details were implemented from full-scale specimens, where 4 spans of LCC T-joist specimens were built with 2.8 m span length for each T-joist specimen. The four T-joist specimens were connected to each other with timber blocks (which act as columns) and the concrete was poured on the top as a continuous slab, to study the dynamic performance of multi-span behaviour. Later, the 4-span specimens were cut and stacked on top of each other to study the vibration behaviour of a multi-storey building. To understand more about the vibration behaviour on large scale flooring systems, a 3m x 3m simply supported floor T-joist floor built by others was tested as part of this research programme. Later, Chapter 4 discusses the results of the experimental investigation into reduced-scale LCC T-joist specimens and LCC T-joist floors. The vibration parameters, including natural frequencies and damping ratios of the principal modes of the specimens were obtained. Also, the transmissibility of the vibration energy between spans and storeys was investigated, with recommendations for design and construction of real buildings.

Chapter 5 discusses the correlation between finite element modelling and forced vibration test results, including natural frequencies and damping ratios of the principal modes of vibration. The vibration transmissibility between spans and storeys was also investigated.

Chapter 6 discusses the dynamic behaviour of a full-scale 8 m x 7.8 m LCC floor. The floor was modelled using the SAP 2000 software package and the modelling parameters were adopted from the previous model described in Chapter 4. The investigations were expanded by changing some parameters, including different types of boundary conditions, to get a better understanding of the vibration behaviour of these systems.

Chapter 7 introduces new design proposals for limiting the vibrations of LCC flooring systems, including a proposed step-by-step method to design the floor using finite element software. This guide also presents what designers should have to know and what not to do in the process of designing for the serviceability limit of LCC flooring systems.

Chapter 8 summarises and concludes the complete work in this research project. The recommendations for future research, which are mainly findings from this project, are also provided in this chapter.

## **CHAPTER 2 LITERATURE REVIEW**

This chapter discusses previous research that focused on timber-concrete composite (TCC) floor systems, and floor vibration. The discussion begins with the development of timber-concrete, including background details and development of this system by a number of researchers. The connection between timber and concrete is the most important part of the system, thus, most of the studies focus on the shear connectors, which are made from mechanical or adhesive fasteners. The new system of TCC by replacing traditional timber joists by laminated veneer lumber (LVL) was introduced by Yeoh (2008), known as an LVL-concrete composite (LCC) floor in this study, is also discussed in this chapter.

Later, the discussions concentrate on the investigation of floor vibration, including timber, steel, concrete and composite flooring systems. The design limitations for vibration control for each type of flooring system are used to generate a new guideline for LCC flooring systems

### **2.1 Timber-concrete composite (TCC) floor system**

TCC floors are an efficient system to replace the traditional flooring systems. This system has improved the stiffness of the floors and can fulfil the latest requirements for flooring systems which require long spans and lightweight systems (Natterer et.al., 1996). TCC floor systems are a hybrid between concrete and timber adopted from stressed skin floor systems, where the upper timber flanges are replaced with concrete. This system requires shear connectors to transfer forces from the concrete slab to the timber joists. (Ceccotti, 1995) explained that timber-concrete composite structures represent a construction technique that can be used for both strength and stiffness upgrading of existing timber floors as well as in new buildings. This technique connected a solid or glued laminated timber beam with a concrete slab cast above, and included shear connectors to resist differential movement between the timber and concrete.

The coupling of a concrete layer on the compression side and a timber beam on the tension side of the composite cross section makes use of the advantageous properties of these materials in terms of strength and stiffness. In this way an effective structure characterized by relatively low weight can be obtained (Stojić and Cvetković, 2001). The idea of using concrete and timber in a composite cross-section is a natural extension of an old technique, and it is even possible to attain full composite action if 'non-slip' connections are used.

The combination of the concrete and timber gave extra advantages that produced a structurally efficient section, rigid and light at the same time. Additionally, composite systems can have triple the load-carrying capability and up to six times the flexural rigidity of traditional timber floor systems, if the timber and concrete are well connected. A concrete topping increases the stiffness and strength of the floors, and can be used to construct up to 15 m long-span flooring systems. (Ceccotti, 1995).

The advantages of the TCC systems and comparison between reinforced concrete and timber only systems are summarised in Table 2-1.

Table 2-1 Advantages of TCC Floor System

Parameter	Type of floor material			Remarks
	Concrete	TCC	Timber	
<b>Mass</b>	Heavy	Moderate	Light	Wood has much lower density compared to concrete. Thus, TCC systems are much lighter compared to an all reinforced concrete system.
<b>Damping system</b>	Highly damped	Highly damped	Poorly damped	TCC have relatively highly damping, about 2% of viscous damping, compared to a timber system.
<b>Sound Insulation</b>	Good	Good	Bad	The air-transmitted noise is improved from the timber structure on account of the increased mass. Impact noise insulation is improved relative to an all concrete system, in terms of the greater damping.
<b>Fire performance</b>	Good	Better	Bad	The upper concrete slab is an efficient barrier against fire propagation that increases fire resistance compared to a timber system. Timber ribs are more fire-resistant than pre-fabricated pre-stressed concrete
<b>Total construction cost</b>	High	Average	Low	These are comparisons to a concrete system based on total cost, owing to factors such as rapid construction, less concrete formwork and less shoring needed during construction. Also reduced foundations because of the low self-weight.

source: (Ceccotti, 1995)

### 2.1.1 Development of TCC

The development of TCC has focused on shear connectors between the timber and concrete topping. Ample research has been done to improve solutions for this connection system. The earliest development of the timber and concrete composite system dates back to the 1920's and 1930's. The systems were initially developed in Europe in 1929 when Mueller patented a system of nails and steel braces that formed the connection between a concrete slab and the timber, and in 1939, Schwab applied for a patent on timber-concrete composite components as mentioned by Seibold (2004) in her literature.

The development of TCC in Europe expanded in 1985 when Sprig introduced a new type of connector made of a doubled-headed screw. Another fastener was invented in 1992 by Provis using a special screw. The screw had a special thread on the lower part to allow for placement in the timber girder without having to drill a pilot hole first and the smooth upper shaft was anchored into the concrete. In 1993, Blaß introduced several types of mechanical fasteners for TCC construction; (a) mechanical fasteners with pin-shaped joints, (b) mechanical fasteners with special connectors and (c) adhesive fasteners to create form closure. A new innovation of timber-concrete composite systems called the HBV-system in 2000 was introduced by Bathon with steel plates as a connector between the timber and concrete as reported by HBV-Systeme (2003).

Lukaszewska et.al (2006) and Lukaszewska (2009) tested different types of connectors to prevent the slip behaviour on the timber-concrete composite floor. The proposed connectors were (1) nail plate, (2) continuous steel mesh, (3) a set of 2 steel tubes with 20 mm diameter screw, (4) bent steel plate with nails, (5) bent steel plate with epoxy glued, (6) a set of steel tube with 20 mm diameter screw and notch in the joist and (7) 20 mm diameter dowels with flanges. The wooden shear anchor-keys with inclined nails were developed by Crocetti et. al (2010) as a connector for timber-concrete composite floors, which attached to the timber joist by glue or screws. Crocetti et al. (2015) added extra screws at both sides of the wooden anchor-keys. The functions of the screws were to get the proper anchorage of the shear anchor-key to the concrete topping and to reduce the risk of the anchor-key splitting as the specimen was loaded.

The development of a composite system using steel connectors was carried out at the University of Oregon, USA in 1930 (Benitez, 2000). Unlike Europe, where the composite systems developed because of renovating historical timber floors, in the USA, they focused more on low to medium rise construction. Work at Colorado State University by Gutkowski et. al. (2000) adopted a connection detail using notched shear keys with anchors in the timber-concrete composite floor system, which was proposed by (Natterer et.al., 1996).

New Zealand introduced a composite system for bridges around 1970 (Nauta, 1970). Glulam was used as beams in conjunction with 150 mm thick concrete slabs for heavy duty traffic loads.

As mentioned previously, mechanical fasteners were used widely to tie together concrete slabs and timber joists. However, alternative products such as adhesives have been produced, which are capable of bonding the concrete both in wet and hardened conditions which create slip-free connections and decrease beam deflections (Brunner et al., 2007).

There is still strong uncertainty on the effectiveness of using a glued interface between the concrete slab and the timber beam, although some research has been carried out and presented (Brunner et al. (2007) and Hehl et al. (2014) ). However there is no research proving that the glued interface will remain effective in the long-term - therefore there is concern about using a pure glued interface between the concrete slab and the timber beam, not only due to thermal strains and stresses, but also due to possible moisture variations in the timber, and drying shrinkage of the concrete slab which may produce problems (e.g. detachment) in the long-term.

The relationship between the mechanical fasteners with their stiffness was summarized in Figure 2-1 which, (Ceccotti, 2002), range from the less stiffness connection (group a) to the stiffest connection (group d). Connections in group (a), (b) and (c) permit relative slip between concrete and timber, i.e cross-sections do not remain planar under load. Only connections in group (d) maintain planarity. Roughly speaking, systems with group (a) connections achieve 50% of the bending stiffness of systems with group (d) connections. The latter corresponds to fully composite action.

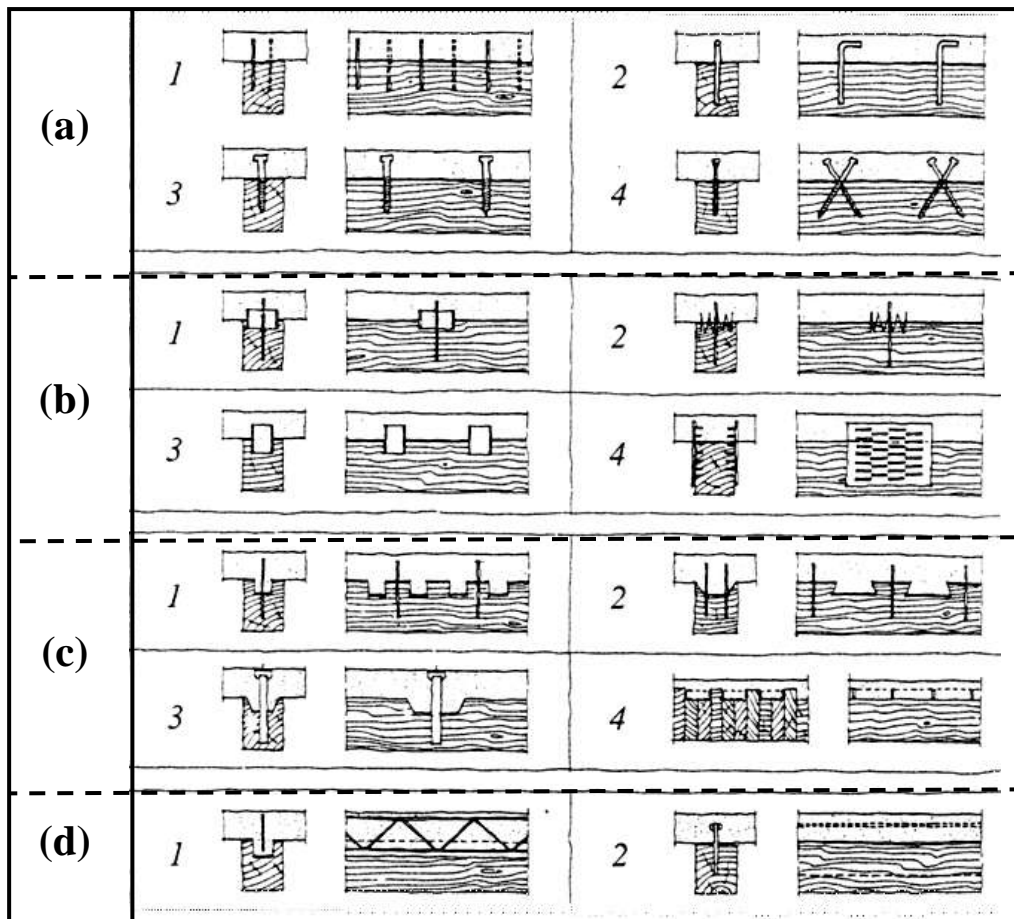


Figure 2-1 Timber-concrete interlayer connections; (a1) nails; (a2) glued reinforced concrete steel bars; (a3/4)screws; (b1/2) connectors (split rings and toothed plates); (b3) steel tubes; (b4) steel punched metal plates; (c1) round indentations in timber, with fasteners preventing uplift; (c2) square indentations, ditto; (c3) cup indentation and prestresses steel bars; (c4) nailed timber planks deck and steel shear plates slotted through the deeper planks; (d1) steel lattice glued to timber; (d2) steel plate glued to timber (Ceccotti, 2002)

### 2.1.2 Design of TCC floors

The TCC system is designed using the gamma method as proposed in Eurocode 5. The flexural stiffness of the composite beam  $(EI)_{com}$  is obtained using Equation 7.8, as recommended by Eurocode 5 (CEN, 2004b), i.e.:

$$(EI)_{com} = (EI)_c + (EI)_t + \gamma_1 E_c A_c a_c^2 + \gamma_2 E_t A_t a_t^2; \quad (2-1)$$

where  $(EI)_c$  is the flexural stiffness of concrete topping ( $Nm^2$ ),  $(EI)_t$  is the flexural stiffness of the LVL joist ( $N/m^2$ ),  $E_c$  is the modulus elasticity of the concrete topping ( $N/m^2$ ),  $E_t$  is the modulus elasticity of the LVL joist ( $N/m^2$ ),  $A_c$  is the concrete topping area ( $m^2$ ), and  $A_t$  is the LVL joist area ( $m^2$ ).

The  $a_c$  and  $a_t$  distances can be determined as below:

$$a_c = \frac{\gamma_t E_t A_t H}{\gamma_c E_c A_c + \gamma_t E_t A_t}, \quad a_t = \frac{\gamma_c E_c A_c H}{\gamma_c E_c A_c + \gamma_t E_t A_t}; \quad (2-2a, 2-2b)$$

Where;

$$H = \frac{t_c}{2} + t_p + \frac{t_{LVL}}{2}; \quad (2-3)$$

$$\gamma_c = \frac{1}{1 + \frac{\pi^2 E_c A_c s_{eff}}{k_s l^2}}, \quad \gamma_t = 1 \quad (2-4a, 2-4b)$$

where  $s_{eff}$  is the effective spacing (mm) of connection,  $k_s$  is the slip modulus of the connection (kN/m),  $t_c$  is the thickness of concrete topping,  $t_{LVL}$  is the thickness of LVL and  $t_p$  is the thickness of permanent formwork. The slip modulus is obtained from the push-out test as discussed in (Yeoh, 2010). The effective spacing of connection can be calculated as below:

$$s_{eff} = 0.75s_{min} + 0.25s_{max} \quad (2-5)$$

where  $s_{min}$  is minimum spacing of connection and  $s_{max}$  is maximum spacing of connection along the beam span.

### 2.1.3 LVL-Concrete Composite Flooring System

The TCC flooring system as mentioned before is a sandwich of concrete (as a slab) and timber (as a joist). The timber joist used is usually solid sawn timber. To improve the system strength, glued laminated (Glulam) timber was used to replace the solid timber (Van der Linden, 1999). However, he found that the engineered wood material, laminated veneer lumber (LVL), was designed to get better strength and material properties compared to Glulam. LVL also used widely in New Zealand and Australia, thus, in this research, LVL was used to replaced traditional solid timber or glued laminated (Glulam) timber joist in an LVL-Concrete Composite (LCC) flooring system.

LVL is made from rotary peeled timber veneers which are glued together using a durable adhesive and laid up with parallel grain orientation to form a continuous billet, up to 12 m long and 1.2 m wide, usually having a thickness of 45, 63 or 90 mm. Solid and Glulam timber have larger coefficients of variation for both strength (modulus of rupture) and stiffness (modulus of elasticity) compared to LVL, which is very strong (almost three times the strength of sawn timber), more reliable and with a higher modulus of elasticity (about 1.5 times the MOE of sawn timber) (Abd Ghafar, 2008).

Researchers at the University of Canterbury in Christchurch, New Zealand have collaborated with Carter Holt Harvey Wood products, local LVL manufacturers and developed an experimental programme aimed at producing a semi-prefabricated LCC floor system for Australasian market demands. The programme started when Seibold (2004) studied the performance of LVL used as joist members in LCC systems, and investigated the best shear connection of the system. Seibold (2004) studied a series of different types of timber concrete composite connectors and found that the best performance in shear was obtained using a specimen with notched joists and coach screws, which resulted in high stiffness connections.

Gross (2004) used LCC beams with the connector suggested by Seibold (2004) to determine the stiffness and strength of the system for use in long-span flooring applications. The beams were built in three different cases; (a) lightweight concrete with a strong shear connection, (b) pre-stressing the composite system beam with a

straight tendon using a strong shear connection, and (c) a pre-stressed beam with a draped tendon and a weaker shear connection. The results showed that the composite beam stiffness was increased sufficiently.

Furthermore, Yeoh (2008, 2010) continued the study to optimise the notch geometry, both in mechanical and economical terms. He found that the best types of connectors for LCC flooring systems were (a) a 300 mm long rectangular notch cut in the LVL-joist and reinforced with a 16 mm diameter coach screw, (b) a triangular notch reinforced with the same coach screw, and (c) two 333 mm long toothed metal plates, pressed into the edges of the LVL joists.

Yeoh (2010) also developed guidelines for their design and proposed a semi-prefabricated panel LCC floor system as shown in Figure 2-2 and Figure 2-3. The 'M' section panel investigated included a single 400 x 63 mm LVL joist on each outer edge and a double LVL joist in the centre, and 17 mm thick plywood as permanent formwork. A series of LCC beams were built to study the static behaviour of the system. 8 m and 10 m long span LVL composite beams with six to eight connectors along the length were tested to failure.

Unfortunately, the long span semi-prefabricated panel has potential serviceability problems, especially vibration issues. Even though the concrete slab will increase the mass and the damping due to the long simply supported spans, an uncomfortable human feeling of vibration and effects from rotating machines may exist. Hence, the investigation on dynamic behaviour was continued using the specimens built by Yeoh (2008). Details of the specimens will be discussed in Chapter 3.

Parallel to this, the University of Technology of Sydney also studied the performance of LCC flooring systems. The study began by testing a series of connectors, with (1) normal screws, (2) SFS screws, (3) bird-mouth notch with coach screw and (4) trapezoidal notch with coach screw (Rijal, 2013). The results showed that both notches in connections (3 and 4) produced higher strength and stiffness compared to a screw only connection. The research continued using LCC beams having a 600 mm x 75 mm concrete topping and 250 mm x 48 mm LVL joists, and 6 m span length, to carry out vibration tests (Rijal, 2013).

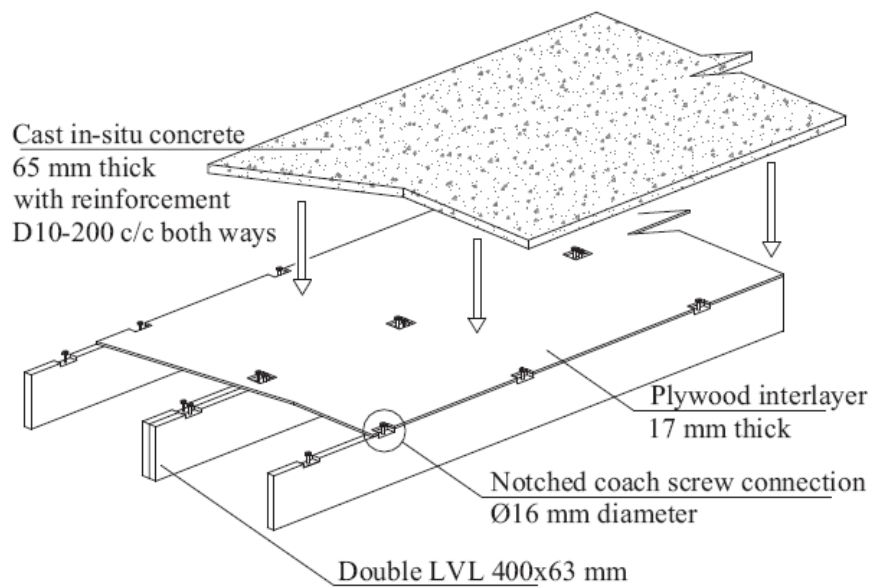


Figure 2-2 Proposed semi-prefabricated TCC floor system (Yeoh, 2008)

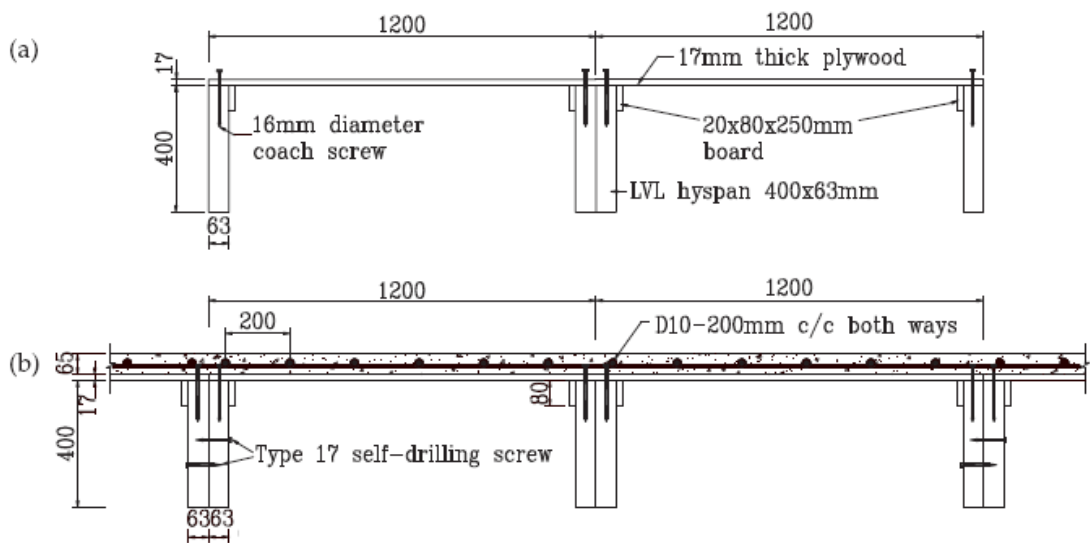


Figure 2-3 Layout details of semi-prefabricated 'M' panel (a) off-site panel, (b) 'M' panel connected to adjacent panels with concrete topping (dimension in mm) (Yeoh, 2008)

## 2.2 Floor Vibration

The vibration serviceability problem of the floor has been a concern since the early 19<sup>th</sup> century when in 1828 Tredgold stated that girders over long spans should be deep to avoid the inconvenience of not being able to move on the floor without shaking everything in the room (Allen and Murray, 1993). Since then, floor vibrations have been studied in order to determine the vibration behaviour due to human-induced loads and methods to prevent uncomfortable vibration on floors.

These days, the vibration serviceability problem of a floor due to decreased floor mass and longer span lengths as demanded in a large variety of construction using long span floors. The vibration on floors happens due to cyclic motion which repeats itself, in particular over a certain interval of time, and affects its occupants during the course of their normal human activities.

The activities that cause the serviceability problem are categorised as those due to continuous vibration or to transient vibrations. Human group activities such as dancing or jumping, or from the use of machinery, produce periodic forces and cause continuous vibration. If a periodic force has similar frequency to the natural frequency of the structure, the amplitude of the resultant motion is increased significantly, leading to the condition known as resonance. Impact force from human activities such as walking can generate transient vibrations. Such motion decays in propagation due to the available damping in the structural system.

A vibration can be translated into six degrees of freedom (DOF), of which three are translations and three are rotations through the centre of gravity in the x, y and z axes. The translational motions produce stresses due to bending, which translate as mode shapes from a vibration point of view. The research in this thesis only focuses on translational vibration behaviour.

### 2.2.1 Floor Vibration Assessment

The vibration serviceability problem can be determined by investigating the vibration behaviour of the floor, such as the natural frequency and damping ratio. To get the vibration behaviour, the floor should be examined by experimental testing or finite element analysis. The earliest experimental work was performed by Tilden (1913) and Fuller (1924). Both studied the dynamic loads due to group activities on the floors. Tilden (1913) also investigated the effect of an individual person on the floor. The transient vibration problem was studied by exposing a group of persons to vertical and horizontal vibrations while standing on a platform as discussed by Reiher and Meister (1931), and Lenzen (1966) to investigate the damping performance of the floor.

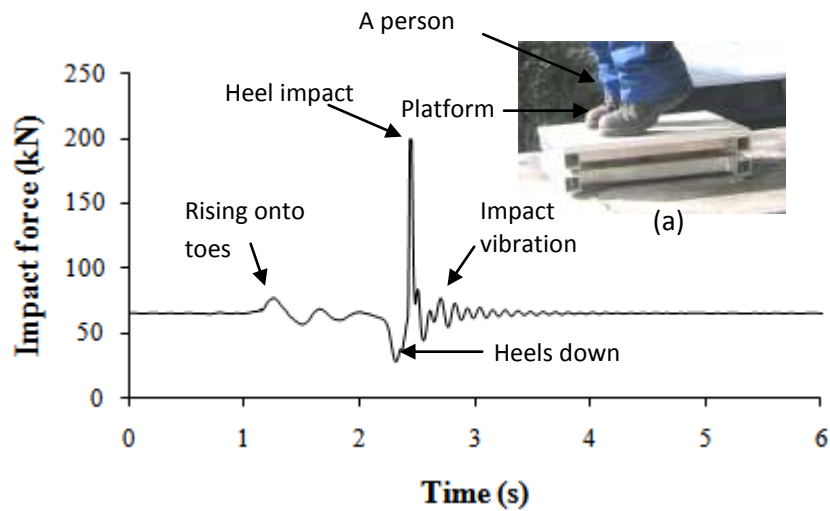
Testing was performed by Wiss and Parmelee (1974) to propose a rating factor as a function of the initial amplitude, the vibration frequency and the damping ratio. For this work, individuals were asked to rate their perceptions while standing and being seated on the floor in order to evaluate the human sensitivity due to transient vibration. Nelson (1974) also recommended using a rating curve, but with a greater damping ratio of the floor compared with the Wiss and Parmelee (1974) rating curve.

Later, the force platform was used to study the effect of human activities in a group. Tuan and Saul (1985) investigated a group of persons in a weight range from 52 kg to 98 kg simulating crowd movement in a stadium and proposed that a narrow-band live load spectrum with rhythmic jumping should be included when designing the serviceability of the floor system under these conditions. Ebrahimpour and Sack (1989 & 1992) and Ebrahimpour et. al (1996) measured the force imposed by individuals and groups of two and four people. A simplified expression for dynamic loads and a footstep frequency for walking tests were suggested of 1.5, 1.75, 2.0 and 2.5 Hz.

The heel-drop test was developed by Lenzen (1966) to simulate a worst case transient event. This method was the simplest of the excitation methods, where a person stood in the middle of the floor, on the load cell platform, rose onto their toes and then dropped down so that their heels struck the floor (Blakeborough and Williams, 2003).

The typical heel drop response is illustrated in Figure 2-4. The moment the person rose to their toes from the normal position, a small fluctuation appears until the initial reduction in vertical force occurs when the heel comes down. The force

dramatically increased at the time of heel impact and was followed by the damped oscillation due to vertical vibration of the human body.



(b) Heel drop time history

Figure 2-4 A person perform the heel drop test and the time history of the test

The heel impact test was performed by Allen and Rainer (1976) to study human-induced walking loads on long-span steel-concrete composite floors with different percentages of critical damping ratios. The results suggested that the criterion for a 5 % damping ratio was in agreement with the Lenzen (1966) criterion.

Rainer (1980) determined that the heel drop test provided the most complete set of vibration characteristics compared to shaker tests and walking tests. Pernica and Allen (1982) tested a shopping centre floor area to determine the dynamic properties from heel impact forces and found that the method to calculate the fundamental natural frequency using the Dunkley approach was reasonable, having less than 10% difference in fundamental natural frequency between measured and calculation values.

Soltis and Hunt (2002) evaluated the vibration properties and response on salvaged individual joists and a salvaged floor system with an impact hammer and a motor with an eccentric rotating mass attached to the floor decking. They found that the impact hammer test was easy to apply and provided both natural frequency and damping ratio data, however the response was sometimes too weak. The force function

gave a stronger response and a more consistent result, but no damping ratio could be obtained.

As the technology has grown with time, the vibration behaviour on floors is no longer solely dependent on dynamic testing, and finite element modelling has been conducted to evaluate experimental data. Pavic and Reynolds (2003) performed vertical force excitation testing using an electrodynamic shaker and calibrated the response with finite element modelling.

The preliminary finite element modelling was developed to predict the vibration characteristics compared to judgement based on experience. El-Dardiry and Ji (2006) created a 3-D model for isotropic and orthotropic flat plates for steel-composite flooring systems and determined that the isotropic flat floor model was more accurate than the orthotropic flat floor model.

### **2.2.2 Vibration Assessment on Timber-Concrete Composite (TCC) Floor**

Bernard (2003) performed a series of dynamic tests on TCC floors. The research concentrated on the influences of concrete thickness, plywood thickness, joist size and spacing and also the specimen length. The impact hammer test and walking test were carried out to determine the vibration behaviour according to the research needs. As a result, Bernard found that the stiffness of the system had a major influence on the natural frequency and damping ratio.

Bernard (2008) continued his research on lightweight Engineered Timber Floors (ETF) and performed 5 series of laboratory tests which concentrated on common design parameters (use of glue, nails and blocking), the effect of the joist spacing, span and lumped mass at the mid-span of the floor, and the effect of the post-tensioning with rubber inserts to improve the floor vibration response. The design features and the proposed remedy to improve floor vibration behaviour were found to be largely ineffective.

ARUP (2012) and Franklin and Hough (2014) performed the impact and footfall induced test on a 3 bay x 5 bay TCC office floor in Nelson Marlborough Institute of Technology (NMIT). The study points out that some local areas of floor

plate close to openings are predicted to exhibit potential vibration levels that exceed the comfort criterion for typical offices. In addition, the damping was estimated from the impact hammer test to be in the range 2.0 % to 3.0 %. The suggestion for modelling was 2.0 % damping.

Rijal (2013) conducted the impact hammer test on 6 m TCC beams and a 6 m and a 8 m timber floor module. The timber floor module was built using hySPAN cross-banded LVL as the top flange and hySPAN PROJECT LVL as the webs and bottom flanges. The natural frequencies for both floors were found to be more than 10 Hz, and influenced by material properties, shear connectors, moisture content, bouncing at the supports and the boundary condition.

Skinner et al. (2013) studied the influences of concrete topping for upgrading a timber floor. The concrete topping increased the stiffness of an existing timber floor whilst minimising the load added to the existing structure and the change to the finished floor to ceiling height. The thickness of concrete topping suggested was between 0 to 100 mm. Skinner (2013) determined the optimum thickness of concrete topping on an TCC floor, suggesting that 20 mm thickness of concrete topping was sufficient to increase the bending stiffness and improve the transient vibration response.

### **2.2.3 Human Perception of Floor Vibration**

The human perception of floor vibration is very complex and difficult to measure due to every person having their own perception. According to Ohlsson (1988), the three most important parameters for human perception of vibration are the duration, the activities on the floor, and the relative locations of the source and the affected human person.

The evaluation of human response can be evaluated using a base curve as shown in Figure 2-5 as recommended by ISO (ISO 2631-2:1989). The sensitivity of human perception on the floor vibration can be evaluated by acceleration or velocity responses to fundamental natural frequency,  $f_n$  as illustrated in Figure 2-5 (a) and Figure 2-5(b), respectively.

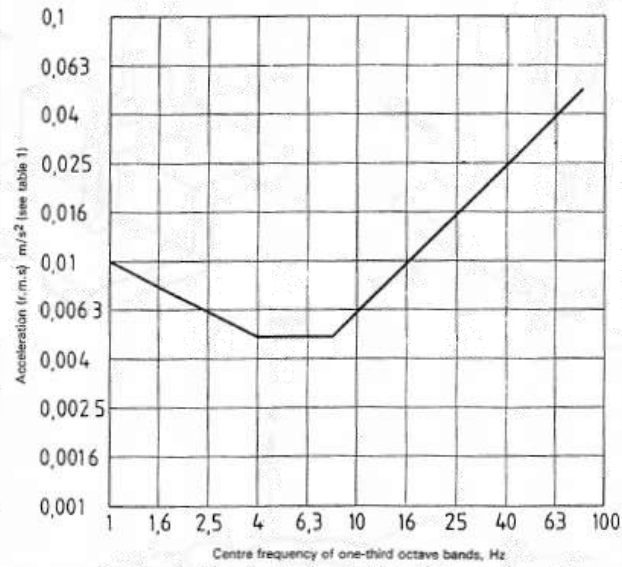


Figure 2a – Building vibration z-axis base curve for acceleration (this represents the foot-to-head vibration base curve, see 4.2.1)

(a) Acceleration versus natural frequency,  $f_n$

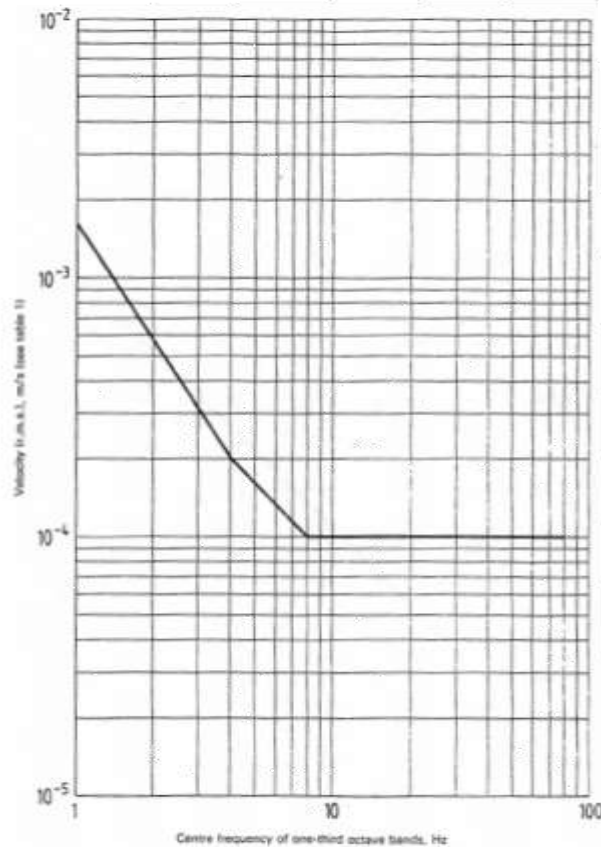


Figure 2b – Building vibration z-axis base curve for velocity (this represents the foot-to-head vibration base curve, see 4.2.1)

(b) Velocity versus natural frequency,  $f_n$

Figure 2-5 Evaluation of human sensitivity by acceleration or velocity response versus natural frequency,  $f_n$

#### 2.2.4 Design Criteria for Floor Vibration

Traditional standards are recommended for evaluating the vibration of floors according to the maximum deflection at the mid-span of the floors, as a span to length ratio of 360. However, vibration design was neglected by only considering the static stiffness, only guaranteeing by proxy that the vibration due to dynamic loads would not be excessive. However, in some cases, this criterion was not satisfied because dynamic loading produced by human or machinery influenced the floor and gave an annoying feeling to the human subjects. Furthermore, the urban trends of buildings require longer span floors to accommodate larger open spaces in residential and light commercial construction. Thus, the design criteria to evaluate the vibrations of the floor have been expanded using the fundamental natural frequency and response acceleration.

The pioneer design criteria was established by Reiher and Meister (1931) based on frequency-dependent human perceptibility and annoyance limits for vibration and developed a first chart as a reference for human perception on vibration based on the group performance on the floor. The chart is based on a displacement range of 0.01 – 10 mm and a frequency range of 1 – 100 Hz as illustrated in Figure 2-6. The chart scaled the human comfort into six categories, which were: (1) not perceptible, (2) slightly perceptible, (3) distinctly perceptible, (4) strongly perceptible, (5) disturbing and (6) very disturbing.

After 36 years, the Reiher-Meister scale was modified by Lenzen (1966) and proposed a new curve based on vibration due to walking impact, with less than 5 % critical damping ratios, that the original scale be applied if the displacement is increased by a factor of ten as depicted in Figure 2-7. Lenzen reduced the scale into four categories only; (1) not perceptible, (2) slightly perceptible, (3) distinctly perceptible and (4) strongly perceptible.

Lenzen (1966) also found that the damping and mass of the system were important parameters to prevent the vibration behaviour of the floor and more critical than the system stiffness. Later, methods for estimating vibration behaviour for steel T-beams, such as frequency and displacement, was proposed as shown in Equations (2-6) and Equation (2-7).

$$\text{Fundamental natural frequency, } f_n = 1.57 \sqrt{\frac{gE_s I_j}{Wl^3}}, \quad (2-6)$$

$$\text{Displacement, } \delta = \frac{Pl^3}{48E_s I_j} \quad (2-7)$$

where  $g = 9.81 \text{ m/s}^2$ ,  $E_s =$  modulus of elasticity for steel,  $I_j =$  sum of transformed moment of inertias for all joists ( $\text{mm}^4$ ),  $W =$  total weight,  $l =$  span length of beam and  $P =$  force (N) for floors that have partitions.

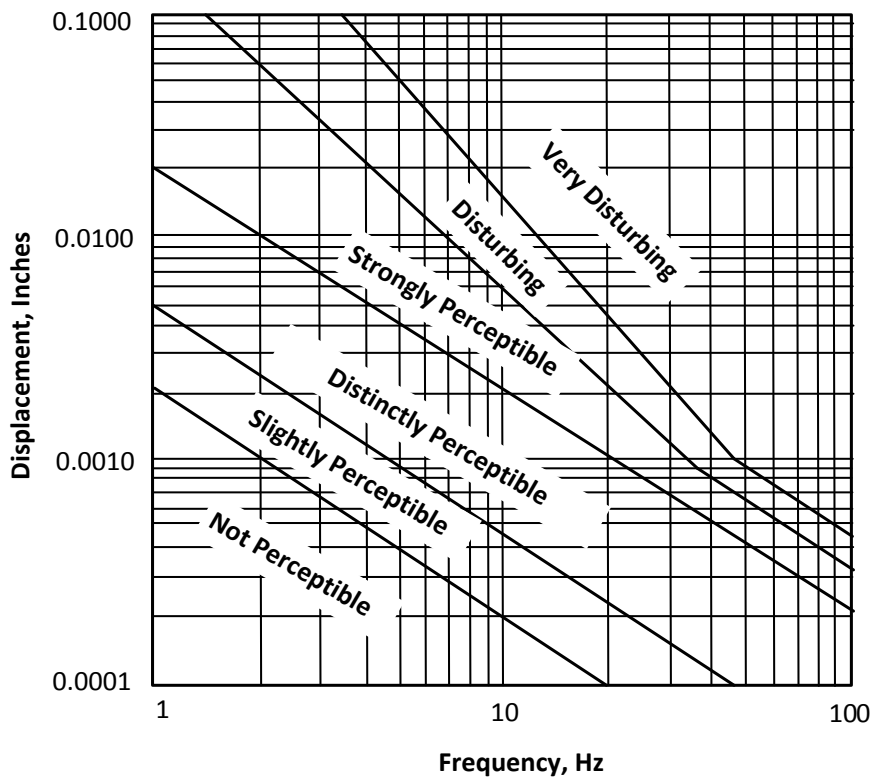


Figure 2-6 Reiher-Meister scale

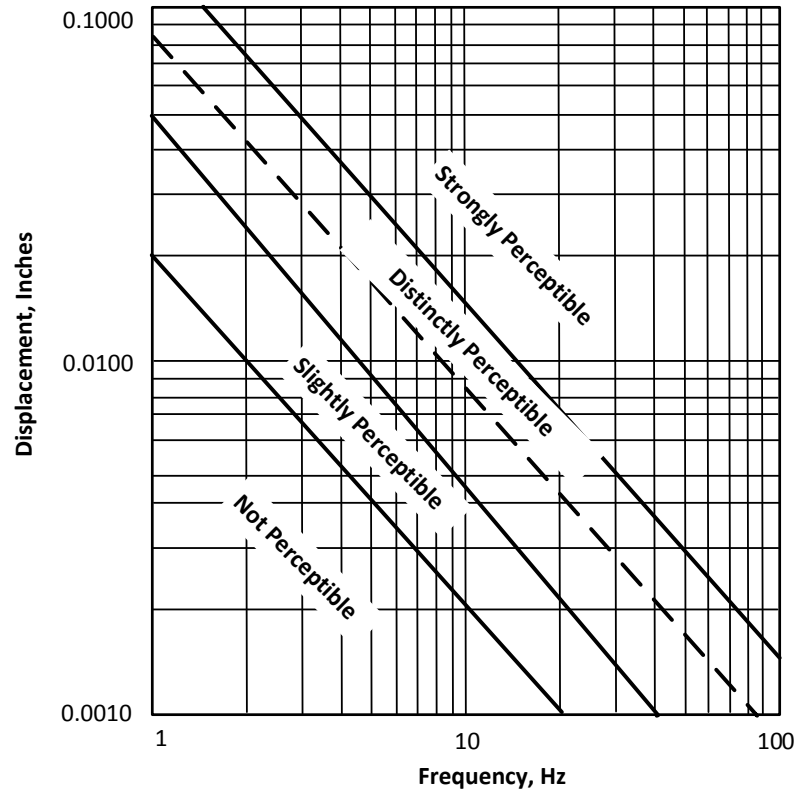


Figure 2-7 Modified Reiher-Meister scale

Ohlsson (1988) created methodology to determine the vibration behaviour for timber floors by limiting the impulse velocity response,  $h'_{max}$  and static deflection. However, this criterion was applicable only for timber floors with 8 Hz fundamental natural frequency, or above. The impulse velocity response,  $h'_{max}$  of simply supported plates can be calculated as

$$h'_{max} = \frac{40(0.4+0.6n_{40})}{gBl+200} \quad (2-8)$$

where  $n_{40}$  is the modal number corresponding to 40 Hz,

Murray et al. (2003) proposed a design criterion to fulfil the human comfort. The criterion states that the floor system is satisfactory if the peak acceleration,  $a_p$ , due to walking excitation as a fraction of the acceleration of gravity,  $g$ , determined from

$$\frac{a_p}{g} = \frac{P_o \exp(-0.35f_n)}{\beta W} < \frac{a_o}{g} \quad (2-9)$$

where  $P_o$  is a constant force representing the excitation,  $f_n$  is the fundamental natural frequency of a joist panel, a beam panel or a combined panel as applicable,  $\beta$  is

the modal damping ratio and  $W$  is the effective weight supported by the beam or joist panel, or combined panel, as applicable. The value of parameters for Equation (2-9) are given in Table 2-2.

Table 2-2 Recommended Values of Parameters,  $P_o$ ,  $\beta$ , and  $a_o/g$  limit

	<b>Constant Force, <math>P_o</math> (kN)</b>	<b>Damping ratio, <math>\beta</math></b>	<b>Acceleration limit, <math>a_o/g \times 100</math> % (%)</b>
Office, residences, churches	0.29	0.02 – 0.05*	0.5
Shopping malls	0.29	0.02	1.5
Footbridges (indoor)	0.41	0.01	1.5
Footbridges (outdoor)	0.41	0.01	5.0
<b>Note :</b>			
0.02 for floors with few non-structural components (ceilings, ducts, partitions, etc) as can occur in open work areas and churches			
0.03 for floors with non-structural and furnishings, but with only small demountable partitions, typical of many modular office areas			
0.05 for full height partitions between floors			

The following design criterion for rhythmic excitation is based on the dynamic loading function for rhythmic activities and the dynamic response of the floor structure:

$$f_n \geq (f_n)_{req} = f \sqrt{1 + \frac{k}{a_o/g} \times \frac{\alpha_i w_p}{w_t}} \quad (2-10)$$

where  $(f_n)_{req}$  is minimum natural frequency required to prevent unacceptable vibrations at each forcing frequency,  $f_n$ ,  $k$  is a constant (1.3 for dancing, 1.7 for lively concert or support event and 2.0 for aerobics),  $\alpha_i$  is a dynamic coefficient (see Table 2-3) and  $a_o/g$  is the limit of ratio of peak acceleration to the acceleration due to gravity (from Figure 2-8) in the frequency range 4 – 8 Hz.

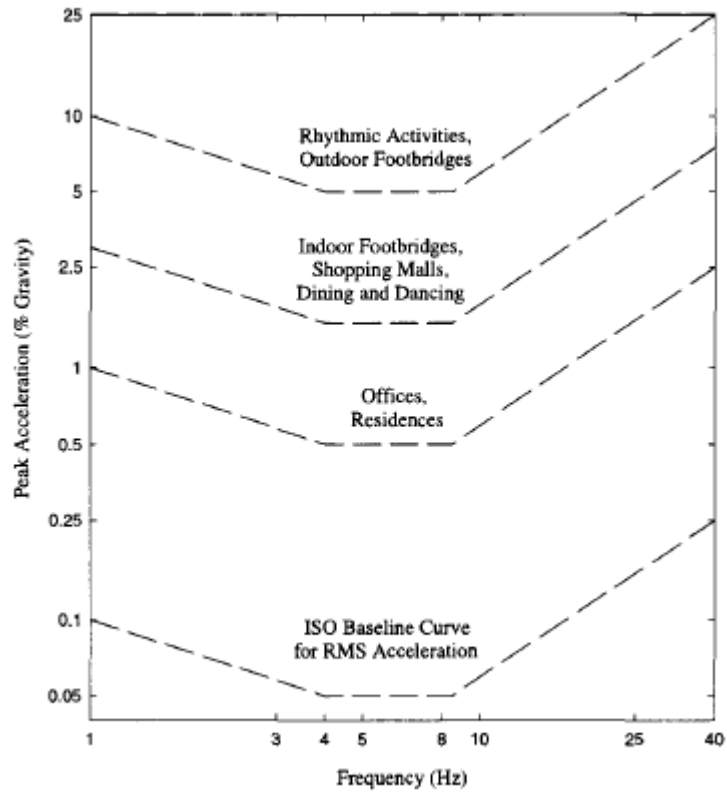


Figure 2-8 Recommended peak acceleration for human comfort for vibration due to human activity (source : Murray et al.,2003)

Table 2-3 Recommended Acceleration Limits for Vibrations Due to Rhythmic Activities (Murray et.al, 2003)

Occupancies Affected by the Vibration	Acceleration Limit, % gravity
Office or residential	0.4 – 0.7
Dining or weightlifting	1.5 – 2.5
Rhythmic activity only	4 - 7

The static deflection recommended by Ohlsson, as published in the Swedish Building Code, was for the deflection at midspan to not exceed 1.5 mm when subjected to a 1 kN point load. For a uniformly distributed load, the limitation of deflection can be calculated as in Equation (2-11).

$$\frac{5Wl^4}{384 D_x} < \frac{l}{600} \quad (2-11)$$

The equation of natural frequencies for rectangular orthotropic floors, simply supported along all four edges, as in Equation (2-12) was adopted from Leissa (1969).

$$f_{1,n} = f_n = \frac{\pi^2}{L^2 \sqrt{\rho}} \sqrt{D_x m^4 + 2D_{xy} m^2 n^2 \left(\frac{l}{B}\right)^2 + D_y n^4 \left(\frac{l}{B}\right)^4} \quad (rad/s) \quad (2-12)$$

Ohlsson proposed a simplified equation to calculate fundamental natural frequency as in Equation (2-13), for the low values of  $D_y/D_x$  ( $\leq 0.01$ ) (Weckendorf, 2009).

$$f_n = \frac{\pi}{2} \sqrt{\frac{D_x}{\rho l^4}} \quad (Hz) \quad (2-13)$$

Hu (2007) proposed a new design criterion based on a 1 kN static deflection and fundamental natural frequency for wood-framed timber floors. If the combination of the calculated fundamental natural frequency,  $f_n$  (Hz) and 1 kN static deflection,  $\delta$  (mm) is larger than 18.7, then the floor is most likely acceptable to occupants in terms of its vibration serviceability and vice versa. The design criterion equation was as below:

$$design\ factor = \frac{f_n}{\delta^{0.44}} > 18.7 \quad (2-14)$$

or the simplified as

$$\delta < \left(\frac{f_n}{18.7}\right)^{2.27} \quad (2-15)$$

where the fundamental natural frequency,  $f_n$  and static deflection,  $\delta$  was following ribbed-plate model as in Equation (2-16) and Equation (2-17).

$$f_n = \frac{\pi}{2\sqrt{\delta}} \sqrt{D_x \left(\frac{1}{a}\right)^4 + 4D_{xy} \left(\frac{1}{ab}\right)^2 + D_y \left(\frac{1}{b}\right)^4} \quad (\text{Hz}) \quad (2-16)$$

$$d = \frac{4P}{ab\pi^4} \sum_{m=1,3,5..} \sum_{n=1,3,5} \frac{1}{\left(\frac{m}{a}\right)^4 D_x + 4\left(\frac{mn}{ab}\right)^2 D_{xy} + \left(\frac{n}{b}\right)^4 D_y} \quad (m) \quad (2-17)$$

where

$$D_x = \frac{EI_{CJ}}{b_1} \quad (\text{Nm}) \quad (\text{system flexural rigidity in x-direction})$$

$$D_y = \frac{\sum_i^k EI_b^i}{L} + \frac{EI_p b_1}{b_1 - t + \alpha^3 t} \quad (\text{Nm}) \quad (\text{system flexural rigidity in y-direction})$$

$$D_{xy} = \frac{G_p h^3}{12} + \frac{C}{2b_1} \quad (\text{Nm}) \quad (\text{Shear rigidity of multi-layered floor deck + torsion rigidity of joist})$$

$$\alpha = \frac{h}{H}$$

$\delta$	=	$m_j/b_1 + \partial_s t_s + \partial_c t_c$ (kg/m <sup>2</sup> )
$m_j$	=	per unit length of joist (kg/m)
$\partial_c$	=	density of topping (kg/m <sup>3</sup> )
$\partial_s$	=	density of sub-floor (kg/m <sup>3</sup> )
$t_c$	=	thickness of topping (m)
$t_s$	=	thickness of sub-floor (m)
$G_p$	=	modulus of multi-layer floor deck (N/m <sup>2</sup> ),
$EI_p$	=	multi-layer floor deck EI (Nm),
$EI_{CJ}$	=	composite EI of joist (Nm <sup>2</sup> ),
$(EI_b)^i$	=	ith lateral bracing member (Nm <sup>2</sup> ),
$k$	=	total number of rows of lateral bracing elements,
$b_1$	=	spacing of joist (m),
$t$	=	width of joist (m),
$l$	=	span of floor (m) and $b$ is width of floor (m),
$h$	=	thickness of multi-layer floor topping (m),
$H$	=	height of floor system (joist depth + floor deck thickness (m))
$C$	=	joist torsional constant

Later, Hu (2015) extended the design criteria by Hu (2007) through the proper combination of floor stiffness and mass to control the vibration floor span can be calculated as below;

$$l \leq \frac{1}{8.22} \times \frac{EI_{com}^{0.284}}{(F_{scl}^{0.14})(m_{com}^{0.15})} \quad (2 - 18)$$

where

- $EI_{com}$  = effective composite bending stiffness
- $m_{com}$  = mass per unit length (kg/m)
- $F_{scl}$  = adjustment factor related to lateral stiffness

Eurocode 5 (CEN, 2008b) proposes the range of timber floors performance based on the relationship of a and b, as illustrated in Figure 2-9. The floors were categorised in two parts, (1) better performance when the value of flexibility coefficient, a (mm/kN) is below 2 and (2) when the value of b is greater than 100, as shown in Figure 2-9 and Equation (2-16) and (2-17).

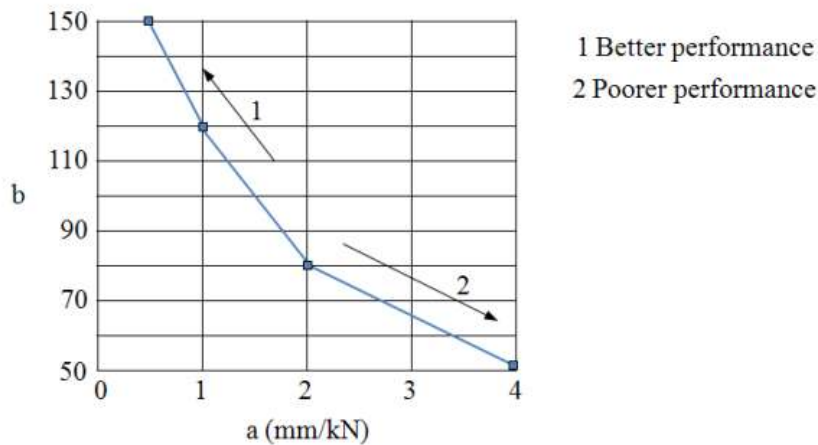


Figure 2-9 Relationship between a and b (CEN, 2008b)

Eurocode 5 (CEN, 2008b) also uses 8 Hz fundamental natural frequency,  $f_n$ , as a serviceability vibration limitation for residential timber floors. For floors with  $f_n$  lower than 8 Hz, special investigation is required. If the floor has  $f_n$  greater than 8 Hz, the following requirements should be as met with  $a = 1.5$  and  $b = 100$ .

$$\frac{w}{F} \leq a \quad (mm/kN) \quad \text{and} \quad v \leq b(f_n \zeta^{-1}) \quad (2-18) \text{ and } (2-19)$$

where  $w$  is the maximum instantaneous vertical deflection caused by a vertical concentrated static force  $F$  applied at any point on the floor,  $v$  is the unit impulse velocity response,  $\zeta$  is damping ratio and  $f_n$  is natural frequency. The value of  $v$  and  $f_n$  can be estimated as from Equation (2-20) to Equation (2-22).

$$v = \frac{4(0.4+0.6n_{40})}{m b l+200} \quad (2-20)$$

$$n_{40} = \left\{ \left( \left( \frac{40}{f_n} \right)^2 - 1 \right) \left( \frac{b_2}{L} \right)^4 \frac{EI_l}{EI_b} \right\}^{0.25} \quad (2-21)$$

$$f_n = \frac{\pi}{2l^2} \sqrt{\frac{(EI_l)}{m}} \quad (2-22)$$

where  $n_{40}$  is the number of first-order modes with natural frequencies up to 40 Hz,  $m$  is the mass per unit area ( $kg/m^2$ ),  $b_2$  is floor width (m),  $L$  is the floor span length and  $(EI)_l$  is the equivalent plate bending stiffness of the floor about an axis perpendicular to the beam direction ( $Nm^2/m$ ) and  $(EI)_b$  is the equivalent plate bending stiffness ( $Nm^2/m$ ) of the floor about an axis parallel to the beams, where  $(EI)_b < (EI)_l$ .

The design criteria based on a point load at midspan was also proposed by Ellingwood and Tallin (1984), Australian/New Zealand Standard (AS/NZS, 2002), American Institute of Steel Construction (AISC), (Murray et al., 2003). Ellingwood and Tallin proposed the deflection of the floor should not exceed 0.5 mm under a 2 kN force. Both AS/NZ Standard and AISC recommend that the deflection under a 1 kN point load should be less than 1 mm to get a better stiffness criterion.

The limitation of natural frequency to control the serviceability problem was suggested to be between 5 Hz to 10 Hz, according to the material of the floor and the dynamic force that applied on the floor. Earlier researchers recommended 5 Hz natural frequency as design criterion where Allen and Rainer (1976) recommended that the minimum natural frequency requirement is between 5 Hz when floors are subjected to rhythmic motion. Later, Ungar and White (1978) proposed a limitation natural frequency of 5 Hz. If the  $f_n$  is less than 5 Hz, the mass of the floor was supposed to be the governing parameter and if the  $f_n$  is greater 5 Hz, the stiffness was believed to govern the response of floor.

The limitation of the natural frequency increased to higher than 5 Hz when Allen (1985) produced a design procedure for rhythmic activities and suggested that the minimum requirement for fundamental natural frequency is higher than 6 Hz. Smith and Chui (1988) proposed the requirement that the fundamental frequency of vibration for the floor is greater than 8 Hz. Wyatt (1989) recommended that the design criterion of requiring the natural frequency to be greater than 7 Hz, but if the frequency is greater than 9 Hz, the criterion becomes overly conservative because it ignores the benefits of decreased decay time. Allen and Murray (1993) studied the effects of human induced vibrations such as walking activities on steel floors and proposed that the natural frequency for offices and residential system must be beyond 9 Hz to control impulse vibration from footsteps based on harmonic resonance.

The Steel Construction Institute (SCI) 2nd Edition (Devine et. al, 2007) classified the floor into two categories; (1) a low frequency floor if the fundamental natural frequency was lower than 10 Hz and can be excited into resonance by walking, and (2) a high frequency floor if the fundamental natural frequency is over 10 Hz for general floors and the response to each individual is assumed to decay before the next footfall.

In the United Kingdom, the traditional approach used to design conventional composite floors for serviceability criteria has been to check the primary and secondary beams independently for a minimum frequency of 4.0 Hz, and assuming that simply-supported boundary conditions exist. Zivanovic and Pavic (2009) proposed a guideline based on randomness in the walking force. The checking procedure is still based on fundamental natural frequency and the cut-off frequency is 10 Hz. The floor was considered to be prone to resonant vibration under walking-induced force if the fundamental frequency is below 10 Hz. The human walking typically causes a transient response to the heel impact each step if the fundamental frequency is over 10 Hz.

Human-imposed walking excitation was performed on four open-plan classroom floors (9 m x 7 m) by Zivanovic and Pavic (2009). The testing protocol followed was the Technical Report 43 (Appendix G), UK Concrete Society, and brought to light a few drawbacks of the procedure. The floor cannot be classified as a low- or high-frequency floor due to the non-negligible frequency content in the measured response time history both below and above 10 Hz.

A summary of guidelines to control the vibration of timber floors is illustrated in Table 2-4, from Hu (2015). The deflection criterion is mentioned in rows 1 to 3. The floor deflection should be calculated under a uniformly distributed load or a 1 kN point load as suggested by CCMC (1997) and NRC (2010). The limitation of natural frequency in row 4,  $f_n$  more than 14 Hz as proposed by Dolan et al. (1999) is very high compared to 8 Hz as mentioned by Ohlsson (1988) Smith and Chui (1988) and many others. Later, Table 2-5 gives a summary of many different standards introduced to give some guidelines to limit the vibration for flooring systems, over the past 80 years

Table 2-4 Summary of design methods to control vibrations in timber floors  
(Hu, 2015)

	Design parameters	Design criteria	Reference
1	$\delta_{UDL}$ where $\delta_{UDL}$ = deflection under uniformly distributed load	$\delta_{UDL} < \text{span}/\text{factor}$  Factor can be 360,480 etc	UDL method: Specifications of engineered wood products, U.S. Building Code
2	$\delta_{1kN}$ where $\delta_{1kN}$ = deflection under a 1 kN load in mm	for span < 3 m, $\delta_{1kN} \leq 2$ mm  for span $\geq 3$ m, $\delta_{1kN} \leq 8/\text{span}^{1.3}$	NBC method: National Building Code of Canada (NBC) (NRC,2010)
3	$\delta_{1kN}$ where $\delta_{1kN}$ = deflection under a 1 kN load in mm	for span < 3 m, $\delta_{1kN} \leq 2$ mm  for $5.5 \text{ m} \geq \text{span} \geq 3 \text{ m}$ , $\delta_{1kN} \leq 8/\text{span}^{1.3}$  for $9.9 \text{ m} \geq \text{span} \geq 5.5 \text{ m}$ , $\delta_{1kN} \leq 2.55/\text{span}^{0.63}$  for span $\geq 9.9 \text{ m}$ , $\delta_{1kN} \leq 0.6$ mm	CCMC method: Canadian Wood Council et al. (1997)
4	$f_n$ where $f_n$ = fundamental natural frequency	$f_n > 14$ Hz	Dolan et al. (1999)
5	$f_n$ , $\delta_{1kN}$ and $V_{\text{peak}}$ where $V_{\text{peak}}$ = peak velocity due to unit impulse	$\delta_{1kN} < 1.5$ mm  $f_n > 8$ Hz  $V_{\text{peak}} < 100^{(f_n \xi - 1)}$  $\xi$ is damping ratio	Eurocode 5 method: Ohlsson (1988)
6	$f_n$ , $a_{\text{rms}}$ where $a_{\text{rms}}$ = root mean square acceleration	$f_n > 8$ Hz  $a_{\text{rms}} = 0.45 \text{ m/s}^2$	Smith and Chui (1988)

Table 2-5 Acceptance criteria over time (Murray et.al, 2003)

<b>Year</b>	<b>Reference</b>	<b>Loading</b>	<b>Application</b>	<b>Comments</b>	<b>Cut-off Frequency (Hz)</b>
1931	Reiher and Meister	Steady State	General	Human response criteria	-
1966	Lenzen	Heel-drop	Office	Design criterion using Reiher and Meister scale	-
1974	International Standard Organization	Various	Various	Human response criteria	-
1974	Wiss and Parlee	Footstep	Office	Human response criteria	-
1975	Murray	Heel-drop	Office	Design criterion using Modified Reiher and Meister scale	9
1976	Allen and Rainer	Heel-drop	Office	Design criterion based on experience	-
1981	Murray	Heel-drop	Office	Design criterion based on experience	-
1984	Ellingwood and Tailin	Walking	Commercial	Design criterion	-
1985	Allen, Rainer and Pernica	Crowds	Auditorium	Design criterion related to ISO scale	-
1986	Ellingwood et al	Walking	Commercial	Design criterion	-
1988	Ohlsson	Walking	Residential/Office	Lightweight Floors	8
1989	International Standard ISO 2231-2	Various	Buildings	Human response criteria	-
1989	Wyatt	Walking	Office/Residential	Design criterion on ISO 2631-2	-
1990	Allen	Rhythmic	Gymnasium	Design criterion for aerobics	-
1993	Allen and Murray	Walking	Office/Commercial	Design criterion ISO 2631-2	-
2003	Murray, Allen and Ungar	Walking	Office/Commercial	Design criterion ISO 2631-2	9
2009	Zivanovic and Pavic	Walking	Office/Commercial	UK Concrete Standard	10

### **2.2.5 Use of Dampers to Control Floor Vibrations**

The floor vibration problem could be improved by improving the stiffness, the mass or the damping of the floor. However, changing the existing stiffness or mass of a floor is not economical and satisfactory especially if it involves major retrofit (Ljunggren, 2006). Another solution is to increase the damping by adding a non-structural element on the floor or adding a mechanical damping device.

Mechanical damping devices (referred to as “dampers”) can reduce the vibration problem and prevent discomfort from the floor vibration. Several methods or types of damper are found, however, tuned mass dampers (TMD), active control, semi-active tuned vibration absorbers and visco-elastic dampers are commonly reported, as discussed by Ljunggren (2006). The earlier TMD had been developed by Lenzen (1966), using a simple system of mass-spring-dashpot to synchronize the floor’s natural frequency with the TMD’s natural frequency and hence dissipate the vibration energy. The used of TMDs continued especially for lightweight floors (Bachmann & Ammann, 1987), gymnasiums (Thornton et. al, 1990), long-span floors (Webster and Vaicajtis, 1992)\_and long-span balconies of auditoriums (Setareh and Hanson, 1992).

Later, a new TMD system introduced by Nguyen et al. (2012 and 2014) used viscoelastic materials to control the vibration issues of real office floors. 12 TMDs were applied on one bay of the office floor and walking and shaker tests were conducted to study the vibration behaviour. The results show that the peak response was reduced 40% and the floor became acceptable from a human comfort perspective.

## **2.3 Summary**

This chapter has reviewed the development of the timber-concrete composite (TCC) floors and the previous studies on floor vibration, especially on assessment of floors subjected to dynamic loads, and design guides to control the serviceability vibration problem of floors.

The development of TCC concentrated on upgrading the stiffness of TCC's connectors. The connectors suggested ranged from nails only to notches with screws. The stiffness of the connector is important to prevent slip behaviour between the

concrete and timber. Furthermore, the traditional timber joist was replaced by LVL to increase the strength of the floor since LVL has a higher strength compared to other types of timber. However, the flexibility of the LVL was a concern when subjected to dynamic loads.

The previous research showed that the natural frequency was one of the important parameters that influenced the sensitivity of humans to dynamic floor responses. The limitation of natural frequency was suggested to be from 5 Hz to 10 Hz, according to the types of dynamic loads, and flooring material. However, in this research, the limitation of natural frequency was focused on 8 Hz only after considering the flexibility of LVL and the LCC flooring as designed for long-spans.

## **CHAPTER 3            FULL-SCALE LCC T-JOIST SPECIMENS**

This chapter presents a comprehensive study on the dynamic performance of full-scale LCC T-joist specimens including both experimental and finite element simulation. Initially, the LCC T-joist specimen system is described together with past experimental work by various researchers on LCC systems. The chapter follows with a detailed investigation of the dynamic performance of the LCC flooring systems. This preliminary investigation provides guidance for the subsequent investigation of reduced-scale LCC T-joist specimens and floor as described in Chapters 4 and 5.

The investigation of the dynamic behaviour of LCC T-joist specimens was carried out using an electrodynamic shaker. The shaker was placed on the top of the specimens to conduct a vertical vibration test to determine the modal parameters of the specimens, including natural frequencies, damping ratios and mode shapes. A signal generator was connected to the electrodynamic shaker to generate the harmonic signal and excite the specimens. Due to limited equipment, only a single harmonic signal was applied, from 0 Hz to a maximum frequency, at 0.1 intervals, depending on resonance of the specimens. Later, when a digital signal generator was available, a sweep signal, from 2 Hz to 25 Hz, was used to verify the results from the single harmonic signal.

To process the experimental data, a signal processing software package known as ME'scope was used. The data was processed using Fast Fourier Transform (FFT) method and curve fitting method to determine the modal parameters (natural frequency, damping ratio and mode shape).

A post-test numerical analysis was carried out using the Sap 2000 finite element software package to compare with the experimental modal analysis (EMA) results. The modelling was important because the similar modelling was expending to analysis the full-scale LCC floor as discussed in Chapter 6.

### 3.1 LCC T-joist Specimen Details

The investigation of LCC flooring systems were continued using the same specimens that been used to determine the static behaviour by Yeoh (2008). The specimens were built with a 400 mm x 63 mm LVL joist, with a 65 mm thick concrete topping. The concrete was reinforced with 12 mm reinforcement bars and poured on 17 mm thick plywood sheathing, which provided permanent formwork, as shown in Figure 3-1 (a). Composite action was provided by the rectangular notches cut from the top surfaces of the LVL joist, including a cutout in the plywood sheathing at the area of notches, which were reinforced with 16 mm diameter coach screws, refer Figure 3-1 (b) and Figures 3-2(b) to 3-4 (b). The advantages of this type of connection were reported by Seibold (2004), Deam et al. (2008) and Yeoh (2008, 2010) Further construction details were given by Yeoh et al. (2008, 2010).

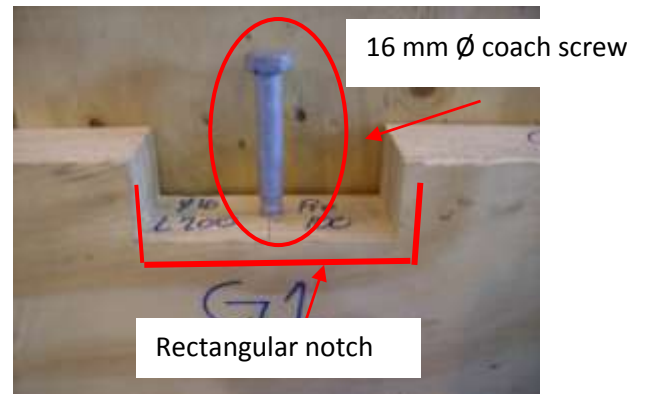
However, the length of span and concrete topping width, including the length of the notches were design variations to help understand more about the specimen's behaviour. The details of each specimen are described in Table 3-1 and illustrated in Figures 3-2 to 3-4. Timber block supports were relocated one (1) metre toward midspan of the specimen at both ends, to reduce the 8 m specimen to 6 m for the vibration test on the short beam, as described in Figure 3-5 for both specimens D and E. The 8 m specimen was not cut to reduce the span in order to allow for re-use of the specimen for other tests.

Table 3-1 Detail of LCC T-joist specimens

<b>Specimen</b>	<b>Span (m)</b>	<b>Breadth of concrete topping (m)</b>	<b>Dimension of notches (mm)</b>	<b>Cantilever arm (each end) (m)</b>
<b>A</b> (see Figure 3-2)	8	0.6	150 x 25	-
<b>B</b> (see Figure 3-3)	8	1.2	150 x 25	-
<b>C</b> (see Figure 3-4)	10	0.6	300 x 25	-
<b>D</b>	6	0.6	150 x 25	1
<b>E</b>	6	1.2	150 x 25	1

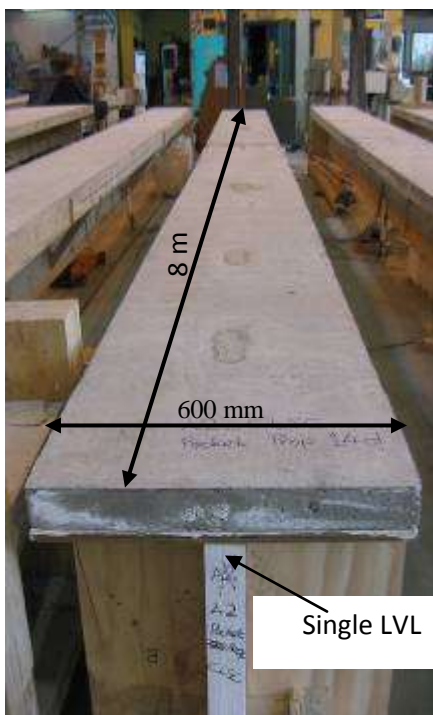


(a)

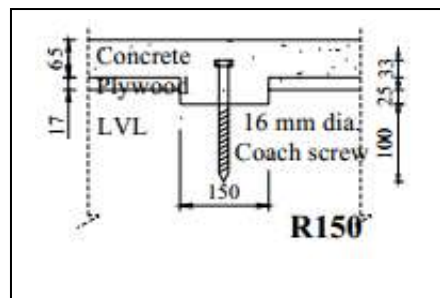


(b)

Figure 3-1 (a) LVL-concrete composite specimen detail and (b) Notched connection detail

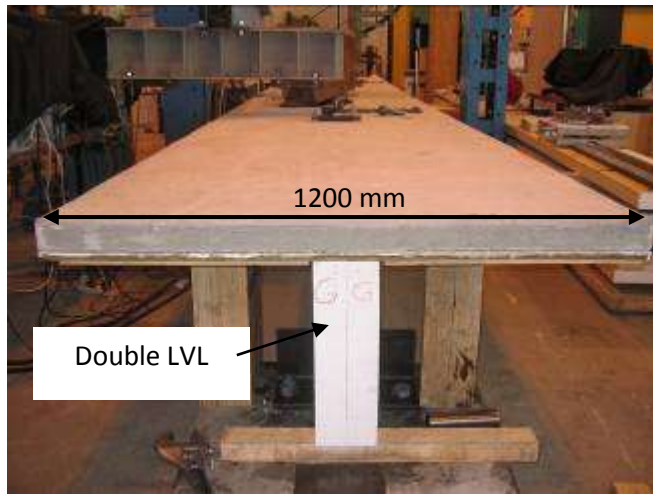


(a)

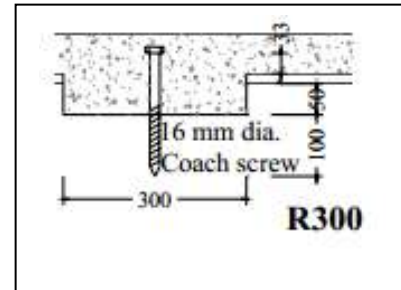


(b)

Figure 3-2 (a) 8 m LVL-concrete composite specimen with single LVL and (b) 150 mm x 25 mm rectangular notches (Yeoh, 2010)

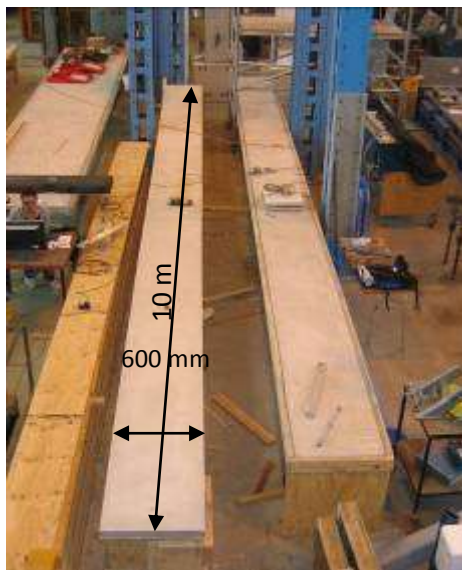


(a)

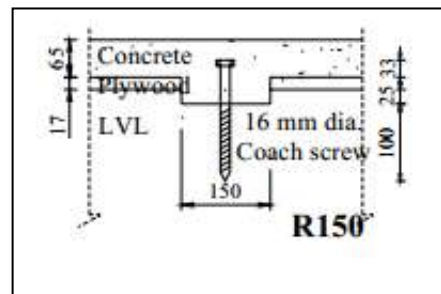


(b)

Figure 3-3 (a) 8 m LVL-concrete composite specimen with double LVL and (b) 150 mm x 25 mm rectangular notches (Yeoh,2010)



(a)



(b)

Figure 3-4 (a) 10 m LVL-concrete composite specimen and (b) 150 mm x 25 mm rectangular notches (Yeoh,2010)

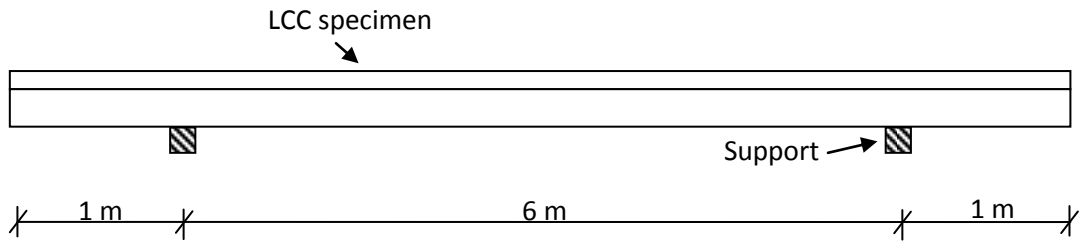
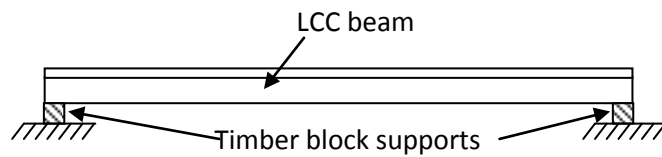
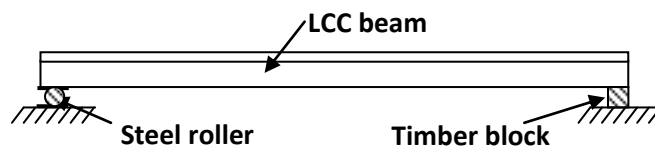


Figure 3-5 Layout of 6 m beam

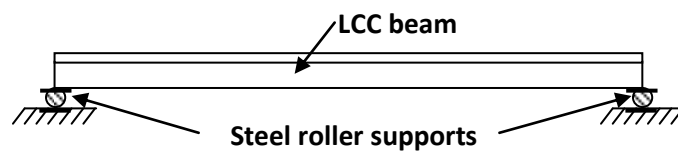
Boundary conditions were expected to affect the dynamic behaviour. Thus, three types of boundaries were considered. In the first type of boundary condition, solid timber blocks were used as a support at both ends of the beam. In the second type, a steel roller at one end of the beam replaced one of the timber blocks. In the last type, steel rollers supported both ends of the beam. The sketches of the different end conditions are shown in Figure 3-6. In all of these tests, the ends of the beam were free to rotate on the supports and there was no clamping to restrict this rotation.



(a) solid timber block at both ends of the beam



(b) solid timber block at the one end and solid steel roller at the other end of the beam



(c) solid steel roller at both ends of the beam

Figure 3-6 Different types of support condition

### 3.2 Experiment Modal Testing Method

The procedure for modal testing of a building had been proposed by Reynolds and Pavic (2000), and Raebel et. al (2001), on an existing floor and a lightweight steel-framed floor, respectively. Their experimental modal testing and analysis procedure was adopted for this research project, using available equipment and facilities in University of Canterbury's structural laboratory, such as;

1. Specimens set up on the lab strong floor,
2. 4 no's of accelerometers, and
3. APS Dynamic electrodynamic shaker.

The vibration test for this research consisted of a single input and multi outputs (SIMO) that measured acceleration (g) simultaneously at several points, but all under the same single-point excitation.

Grid lines were drawn along the LVL-joist to locate important node points, as illustrated in Figure 3-7. The sensors were attached at these node points to measure the vibration response from the specimens and were connected to a data recorder that was connected to the computer. Only the important points or nodes that are pointed out were attached with sensors to record the specimens response with the strongest response being detected at the point of maximum displacement, which was generally at the mid-span of the specimens. To get the complete mode behaviour of the specimen, the sensors were placed along the specimens.

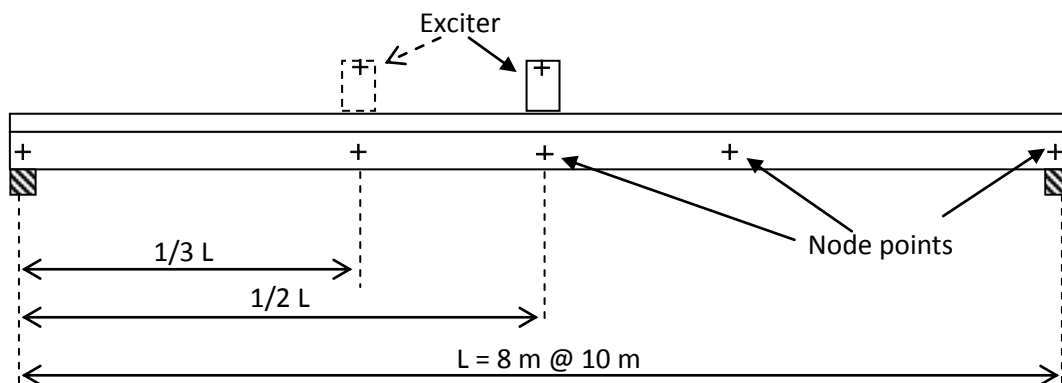


Figure 3-7 Location of exciter and node points along the LVL joist

At the beginning, only four (4) roving sensors were available for this research to measure the vibration response on specimen A. At a later stage, four (4) additional sensors were supplied for the rest of vibration tests on specimens B, C and D, hence a total of eight (8) sensors were used. One sensor was placed on the shaker armature to record the input responses. The place of the sensor should be careful, either at node points (no displacement) or antinode points (maximum displacement) to get better mode shapes.

The vertical force excitation was produced by an APS Dynamic electrodynamic shaker, which was placed on top of the specimens, as illustrated in Figure 3-7. The shaker was placed at two different locations, (a) at mid-span of the specimen (1<sup>st</sup> test) and (b) at one-third length of the specimen (2<sup>nd</sup> test). The second location was to ensure that higher modes (2<sup>nd</sup> and 3<sup>rd</sup> mode) were also excited, which were probably missed during the 1<sup>st</sup> test (shaker at mid-span), as it was suggested by Reynolds and Pavic (2000) that the location of the exciter should be far away from the maximum point of deflection or antinodes of any of the important modes.

The shaker excited the specimens with the excitation signals generated by the signal generator. A stepped sine signal was used to generate the excitation signal for all vibration tests as it was not possible to use broadband excitation signals in the structures laboratory. There were two main reasons for performing step sine testing. Firstly, a step sine excitation signal gives a signal to the shaker/amplifier system with a finite power output. This is important if there is a requirement to test a structure, which cannot be excited sufficiently using broadband excitation. Secondly, the sinusoidal excitation is the best form of excitation for quantifying any non-linearity in a test structure (Reynolds and Pavic, 2000).

In this research, the signal frequency applied went from 0 Hz up to a maximum to find the maximum amplitude of the specimen, known as a pre-test. The range of the input frequency applied to the exciter was then decided based on the pre-test results and changed depending on the specimen stiffness and the cross section. Then, the frequencies selected were based on the resonance of the specimen. If the specimen had a resonance at input frequency of 10 Hz, then the frequency applied was from 1 Hz to 20 Hz, in 0.1 Hz increments. This was done in order to plot the graph to determine the natural frequency and critical damping ratio for the specimens.

### 3.3 Modal Parameter Extraction Method

The experimental modal parameters were estimated by a curve-fitting routine that was available in the ME'scope (ME'scope,2008) data processing software package. Initially, the single sinusoidal responses were combined manually using MATLAB to acquire the complete sinusoidal responses from a low frequency (i.e. 5 Hz) to a high frequency (i.e. 23 Hz). Before the test was conducted, a few trial and error measurements were performed to determine the optimum data acquisition parameters, as illustrated in Table 3-2, where the fundamental relationships are follows ;

- i. Time window length (s), T =  $RL / 2.56 (BW)$
- ii. Sample rate (Hz), SR =  $RL/T$   
=  $2.56 (BW)$
- iii. Frequency resolution, FR =  $1 / T$   
=  $BW / 2.56$

where;

BW = usable frequency bandwidth (Hz);

RL = record length using the number of the discrete points in the time history, often a fixed quantity on an FFT based analyzer;

FR = frequency resolution which is the frequency step between data points

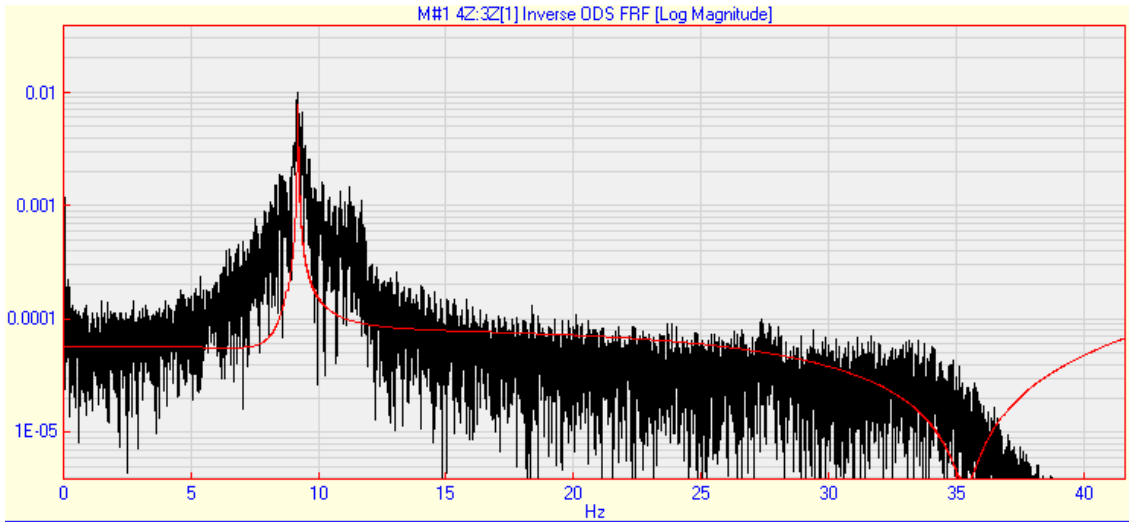
Table 3-2 Main digital data acquisition parameters adopted for FRF measurements

<b>Parameter description</b>	<b>Parameter value</b>
Data acquisition time	197 s
Excitation frequency limits	5 – 25 Hz
Frequency span	20 Hz
Number of frequency lines, RL	6400
Frequency resolution, FR	0.03 Hz
Total number of samples	16384
Sampling frequency	83.3 Hz
Number of averages	21
Window	Exponential ( $\lambda = 0.01$ )

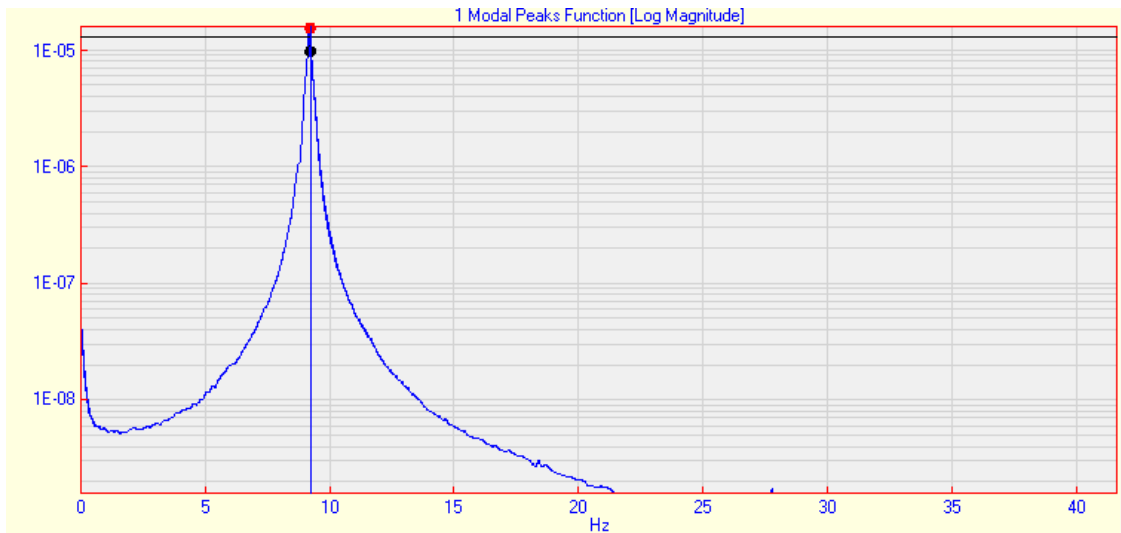
Later, the measurement responses, which are in the time-domain, were converted to a Frequency Response Function (FRF) before the modal parameters for each specimen were derived. The analysis process was performed using the ME'scope software (ME'scope,2008 ).

The ME'scope software includes single-degree-of freedom (SDOF) and multi-degree-of-freedom (MDOF) curve-fitting methods to estimate the modal parameters. The SDOF method was divided into two methods, (1) a Co-Quad method and (2) a Peak method, which both approximated the modal parameters one mode at a time and no damping ratio is estimated with these methods. On the other hand, MDOF methods simultaneously estimate the modal parameters of two or more modes from the set of FRF measurements, using a polynomial method. The polynomial methods perform a least square error curve fit and obtain the global frequency and damping ratio for each mode from the curve fitting data.

To begin with, the experimental measurement data was analysed using both the SDOF and MDOF curve-fitting methods. Both methods show similar results for the frequencies and mode shapes but the damping ratios were only obtained from the MDOF method. For the rest of the experimental data, only the MDOF curved-fitting method was used to estimate the modal parameters, as illustrated in Figure 3-8.



(a) frequency spectrum and curve-fit graph



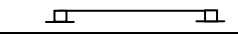
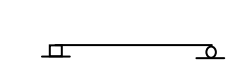
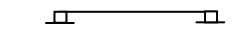
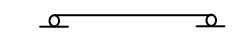
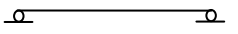
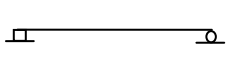
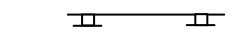
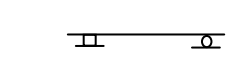
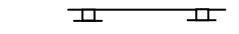
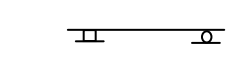
(b) Modal peak function

Figure 3-8 Response of Specimen A

### 3.4 Dynamic performance of LCC T-joist specimens

The investigation and observations were carried out on the LCC specimens to understand their vibration behaviour and to obtain the vibration parameters, especially the natural frequency or fundamental frequency of the systems. Some of the preliminary results have been published in Abd Ghafar (2008). The natural frequencies and damping ratios of each specimen are summarised in Table 3-3 Also, since the vibration test results are numerous, comparison results are presented in Table 3-4 to Table 3-7.

Table 3-3 Results of vibration tests on LCC simply supported specimens

Specimen	Support system	Location of shaker											
		S <sub>1</sub> (mid-span)						S <sub>2</sub> (one-third span length)					
		f <sub>1</sub> (Hz)	ξ <sub>1</sub> (%)	f <sub>2</sub> (Hz)	ξ <sub>2</sub> (%)	f <sub>3</sub> (Hz)	ξ <sub>3</sub> (%)	f <sub>1</sub> (Hz)	ξ <sub>1</sub> (%)	f <sub>2</sub> (Hz)	ξ <sub>2</sub> (%)	f <sub>3</sub> (Hz)	ξ <sub>3</sub> (%)
<b>A</b>	<b>8 m x 0.6 m</b>												
	Block	9.2	0.8	27.8	0.5	50.1	0.1	9.2	0.5	27.2	0.6	50.5	0.1
	Roller	8.7	0.6	25.4	0.4	50.1	0.1	8.0	0.4	25.6	0.5	49.5	0.1
	Block & Roller	9.1	0.8	26.3	0.5	50.0	0.1	9.0	0.62	26.0	0.5	50.0	0.1
<b>B</b>	<b>8 m x 1.2 m</b>												
	Block	9.2	0.4	29.4	0.3	50.2	0.1	9.2	0.5	31.0	0.3	50.1	0.1
	Roller	8.8	0.6	25.3	0.2	50.0	0.1	8.6	0.5	26.7	0.3	50.0	0.1
	Block & Roller	9.2	0.6	27.2	0.3	50.0	0.1	8.9	0.5	28.0	0.3	50.0	0.1
<b>C</b>	<b>10 m x 0.6 m</b>												
	Block	6.4	1.3	22.2	0.2	50.6	0.1	6.3	1.4	23.0	0.6	50.6	0.
	Roller	6.4	1.4	20.3	0.2	50.0	0.1	6.3	1.4	20.5	0.5	40.6	0.1
	Block & Roller	6.3	0.6	21.2	0.2	50.5	0.1	6.4	1.4	21.1	0.5	50.3	0.1
<b>D</b>	<b>6 x 0.6</b>												
	Block	12.8	1.4	25.5	0.4	50.0	0.1	13.1	1.6	25.8	0.5	50.3	-
	Roller	11.0	0.7	23.4	0.2	50.0	0.1	12.9	1.0	23.8	0.2	50.0	0.1
	Block & Roller	12.5	0.7	22.5	0.3	50.0	0.1	12.4	0.4	22.0	0.3	50.0	0.1
<b>E</b>	<b>6 x 1.2</b>												
	Block	12.3	1.7	21.1	0.2	50.1	0.1	12.4	1.3	20.7	0.3	50.1	0.1
	Roller	10.0	1.4	19.6	0.2	50.0	0.1	10.3	1.1	18.4	0.1	50.1	0.1
	Block & Roller	11.0	1.2	20.3	0.2	50.1	0.1	11.1	1.4	19.5	0.3	50.1	0.1

The results in Table 3-3 show that natural frequencies are more consistent compared to damping, where the damping for mode 1 varies from 0.4 % to 1.4 %. However, the damping in real buildings are more often in a range 2 % to 3 % depending on material, furniture in the room and attachments to the underside of the floor such as ceilings and services (ARUP, 2012).

As mentioned before, two series of modal testing were conducted with different locations of the shaker (refer section 3.3) and the best results from these tests were selected to determine the first three modes of the specimens. The higher modes were not determined in this research, as the sensitivity of a human can feel a maximum frequency between 4 and 8 Hz for vibration in the vertical direction and 0 to 2 Hz horizontally, and the vertical vibration frequencies are the most important in design (Chapter 2, ISO, 1989).

The modal parameters that are presented in these results were selected from the distinguished mode shape. The modal behaviour of the specimens should be similar, or almost similar, with the theory. Figure 3-9 shows the theoretical mode shape behaviour while Figure 3-10 shows the LCC specimen's mode shape behaviour from the vibration test.

The identified mode shapes of the specimens are shown in Figure 3-10, where the shape was a half sine wave, up or down if not a node, as only first order effects were considered. Weckendorf, (2009) mentions that, the location of an anti-node and node of the specimens were important to identify, as the antinode was always in the mid-span of the specimens for an odd mode number (1 and 3) frequency while for even mode (2), the node was located at a similar location. Thus, to get better results for the mode shape, a smaller grid line should be used.

Additional modes or coupled modes sometimes occurred during the test, which was due to movement from the supporting system, external vibration forces, or background noise, as well as a movement from the shaker itself during the resonant period. The modes that could not be fully identified were not included in the analysis, especially for second and third mode behaviours.

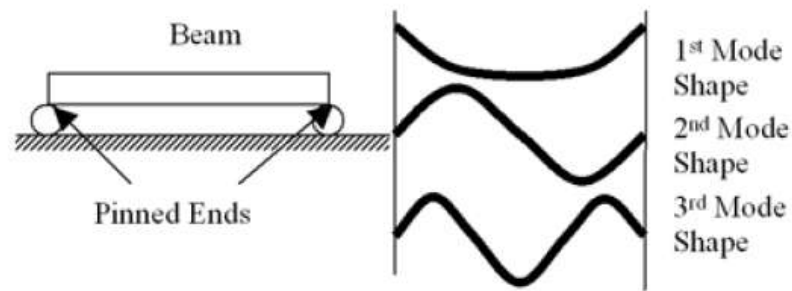


Figure 3-9 Theoretical mode shape for simply supported beam

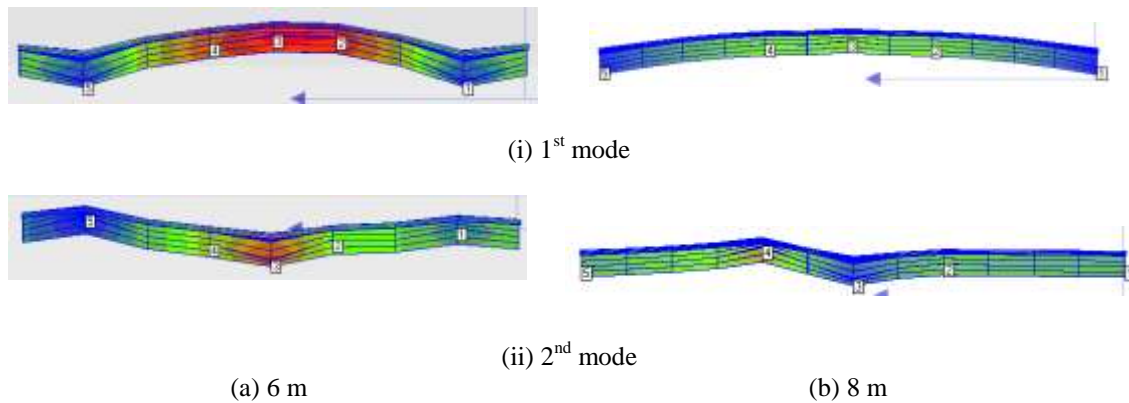


Figure 3-10 The first three mode shape of 6 m and 8 m specimens from vibration tests

During the tests, a couple of issues were discovered relating to: (1) the input signal frequency, and (2) movement on the supports. As mentioned before, the signal generator that was used in the early part of this research can only supply a single sinusoidal input frequency, and later using established software (Me'scope), the experimental data were combined from the lowest frequency to the highest frequency to obtain the modal parameters of the specimens (refer to section 3.3). Some important data was probably missed during this lengthy process, and could affect the results. Consequently, the vibration test on an 8 m x 0.6 m specimen was repeated using a sweep sinusoidal input frequency, as the equipment was only available in the final stages of this study. Hence, the test was repeated to validate the previous experimental data.

The methodology of this later testing and data analysis was similar to that mentioned in Section 3.2 and 3.3. Again, the shaker was located at two different places: (1) at the mid-span of the specimen, and (2) at one-third of span length specimen. Both cases provided a natural frequency of about 9 Hz and 27 - 28 Hz for first (1<sup>st</sup>) and second (2<sup>nd</sup>) modes, respectively.

The comparison of the natural frequencies and damping ratios of the two different input signal vibrations are illustrated in Table 3-4. The percentage errors between these two experiments are between 1.5 % to 5.0 %. Small differences between the natural frequencies for both cases prove that the experimental results from a single signal sinusoidal frequency were accurate and the method can be used to determine the modal parameters of a specimen.

Table 3-4 Comparison of modal properties between a single and a sweep sinusoidal vibration test on 8 m specimen

Input signal frequency	Location of shaker			
	S <sub>1</sub> (mid-span)		S <sub>2</sub> (one-third span length)	
	$f_1$ (Hz)	$f_2$ (Hz)	$f_1$ (Hz)	$f_2$ (Hz)
Single sinusoidal	9.68	-	9.22	27.2
Sweep sinusoidal	9.18	28.2	9.38	27.6
<b>Different (abs)</b>	<b>0.50</b>	-	<b>0.16</b>	<b>0.40</b>
<b>Error (%)</b>	<b>5.17</b>	-	<b>1.74</b>	<b>1.47</b>

The second issue that had been noticed was the movement of the support system during the vibration experiments. As described in section 3.2, the support system at both ends of the specimens were stand alone without any extra support to make sure the support was perfectly rigid. Hence, the test on an 8 m x 0.6 m specimen was repeated with the timber block that supported the LCC specimen screwed to the ground, as shown in Figure 3-11, to compare the vibration behaviour before and after the supports were fixed. The same sweep signal frequency was applied to vibrate the specimen.



(a) before being fixed



(b) after being fixed

Figure 3-11 End support condition before and after being fixed to the ground

The natural frequencies for the 8 m specimen before and after fixing the support system are as illustrated in Table 3-5 shows the differences between these two cases were small at about 0.4 to 2.5 % and are considered negligible. Thus, the movement of the support system during the vibration experimental for all specimens was neglected.

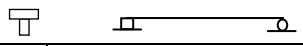
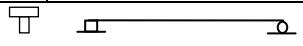
Table 3-5 Comparison of modal properties between a non-fixed and a fixed support

Input signal frequency	S <sub>1</sub> (mid-span)		S <sub>2</sub> (one-third span length)	
	$f_1$ (Hz)	$f_2$ (Hz)	$f_1$ (Hz)	$f_2$ (Hz)
	Non-fixed support	9.18	28.2	9.38
Fixed support	9.12	28.3	9.18	28.3
<b>Difference (abs)</b>	<b>0.06</b>	<b>0.10</b>	<b>0.20</b>	<b>0.70</b>
<b>Error (%)</b>	<b>0.65</b>	<b>0.35</b>	<b>2.13</b>	<b>2.54</b>

### 3.5 Effect of span length

The relationship between the span and the vibration properties of the specimens are illustrated in Table 3-6. The span length was increased from 6 m to 10 m, with 2 m intervals and as expected, the shorter specimen gave the highest value of natural frequency since this is related to the structural stiffness, but only applies to the first mode natural frequency. As shown, the longer specimens had more flexibility and slenderness compared to the shorter specimens. However, the third mode frequency was roughly similar for all the specimens, and the second mode frequency was difficult to analyse as more than one additional mode appeared.

Table 3-6 Comparison of modal properties between different span lengths

Specimen (m <sup>2</sup> )		$f_1$ (Hz)	$\xi_1$ (%)	$f_2$ (Hz)	$\xi_3$ (%)	$f_3$ (Hz)	$\xi_3$ (%)
<b>A</b>	<b>8 x 0.6</b>	9.1	0.8	26.3	0.5	50.0	0.1
							
<b>C</b>	<b>10 x 0.6</b>	6.3	0.6	21.2	0.2	50.0	0.1
							
<b>D</b>	<b>6 x 0.6</b>	12.5	0.7	22.5	0.3	50.0	0.1
							

### 3.6 Effect of topping width

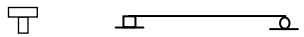
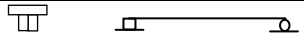
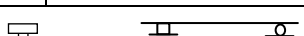
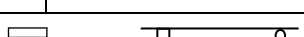
The modal parameters of LCC specimens with a single joist were compared with LCC specimens with double joists, as illustrated in Table 3-7. Even though both specimens had different cross-section properties, their stiffnesses were similar for both specimens. The ratio of stiffness and mass of the LCC with a single joist to an LCC with double joists is 2:1. From the fundamental natural frequency equation, the natural

frequency for a LCC with a single joist is  $f_{1-LCC} = \frac{\pi}{2l^2} \sqrt{\frac{EI_{com}}{m_{com}}}$  and the natural

frequency for a LCC with double joists is  $f_{2-LCC} = \frac{\pi}{2l^2} \sqrt{\frac{2EI_{com}}{2m_{com}}}$ , thus

$f_{1-LCC} = f_{2-LCC}$ . The experimental results agreed with the theory with differences in the fundamental natural frequency of the 6 m x 0.6 m and 6 m x 1.2 m specimens being only 1.80 %. The reason for this comparison was to check the vibration behaviour of the specimens when the scale is larger. In a the real life scenario, double LVL joists will used on LCC flooring systems as will be discussed later in a subsequent chapter.

Table 3-7 Comparison of modal properties between different topping widths

Specimen (m <sup>2</sup> )		$f_1$ (Hz)	$\xi_1$ (%)	$f_2$ (Hz)	$\xi_2$ (%)	$f_3$ (Hz)	$\xi_3$ (%)
<b>A</b>	<b>8 x 0.6</b>	9.1	0.8	26.3	0.5	50.0	0.1
							
<b>B</b>	<b>8 x 1.2</b>	9.2	0.6	27.2	0.3	50.0	0.1
							
<b>D</b>	<b>6 x 0.6</b>	12.5	0.7	22.5	0.3	50.0	0.1
							
<b>E</b>	<b>6 x 1.2</b>	11.0	1.2	20.3	0.2	50.1	0.1
							

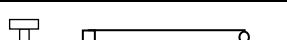
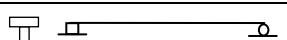
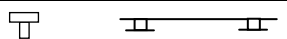
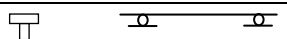
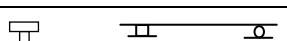
### 3.7 Effect of support stiffness

Initially, the specimens were placed on timber blocks with no additional support to create a rigid support. Thus, small gaps or friction may have allowed small deflections and movements to occur at the ends. Placing a steel roller between the beam and timber block gave more flexibility to the boundary conditions of the system.

Table 3-8 shows the natural frequencies and damping ratios of three different support systems used with the LCC specimens. The comparisons only focus on the first (1st) natural frequency, as the higher natural frequencies were not very different as discussed previously. The specimens with a timber block at both end supports were used as a reference for the other types of supports, since this support system had a higher stiffness compared to the other two support systems, and gave the highest value for the first natural frequency.

Using roller supports at each end gives an unstable support system compared with the use of blocks, and block and roller support systems. Theoretically, this boundary system will provide the lowest natural frequency compared to the other support systems. The results in Table 3-8 show that for spans of 6 m and 8 m the roller supports had lower natural frequencies than for the block supports, but there was little difference for the 10 m span. The experimental error including disturbances from outside sources and problems with the data analysis, as mentioned, before probably caused the unexpected results for the 10 m span.

Table 3-8 Comparison of natural frequencies between different support conditions

Specimen (m <sup>2</sup> )	Support types	$f_1$ (Hz)	$f_2$ (Hz)	$f_3$ (Hz)
<b>A 8 x 0.6</b>				
	Blocks	9.2	27.8	50.1
	Roller	8.7	25.4	50.1
	Block and roller	9.1	26.3	50.0
<b>C 10 x 0.6</b>				
	Blocks	6.4	22.2	50.6
	Roller	6.4	20.3	50.0
	Block and roller	6.3	21.2	50.5
<b>D 6 x 0.6</b>				
	Blocks	12.8	25.5	50.0
	Roller	11.0	23.4	50.0
	Block and roller	12.5	22.5	50.0

This research found that the boundary conditions have a big influences on the vibration of the systems with the relationship between the fundamental natural frequencies being linear with the boundary rigidity stiffness and the flexibility of the LVL blocks used as the support system affected the results of the vibration tests. Thus, to get a better understanding, the interaction between the support surface and LVL joist was modelled in SAP 2000, as illustrated in Figure 3-12. The LVL-concrete composite

beam was modelled as a block mesh and the rigid support was applied underneath. The force (point load) was applied on five nodes at the end of the block and the outer force is half of the force applied to the central three nodes of the specimen.

The results from the support modelling are shown in Figure 3-13, where the deflection occurred over the loaded area and a length of the beam near the support. The deflection represented the movement and indentation of the timber support. The effective support length could be obtained as the length of the timber support, as illustrated in Figure 3-14. The effective length was found to be approximately 80% of the loaded area, based on the finite element modelling results. The remaining support systems will not be discussed in detail here, but there was approximately a 10% difference in deflection between the timber block support and the other types of support system. Thus, it shows that the timber block support is flexible and will affect the vibration behaviour of the system.

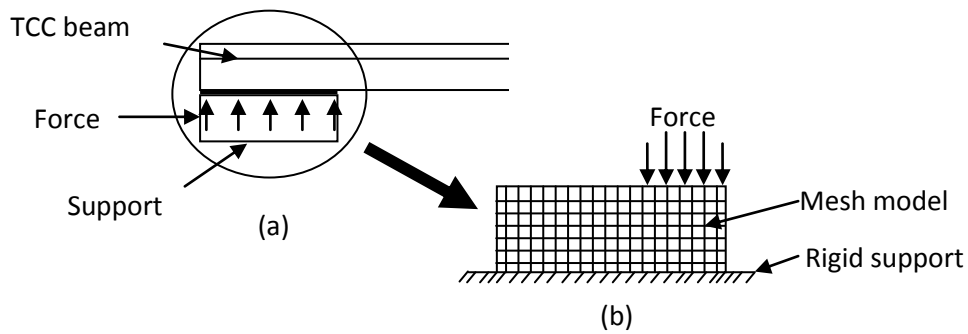


Figure 3-12 (a) Boundary stiffness a timber block as support and (b) mesh model

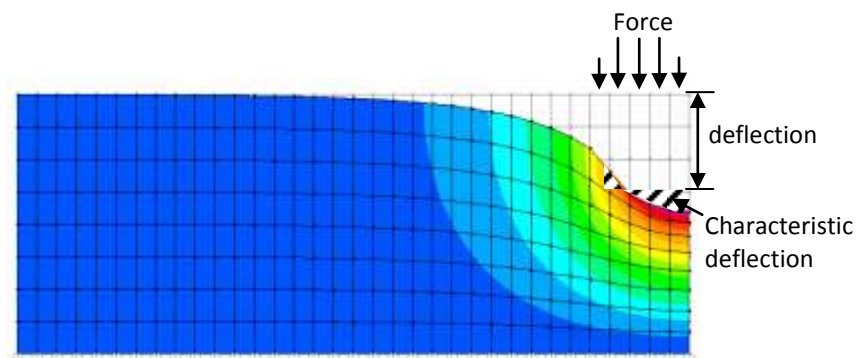


Figure 3-13 Finite element model

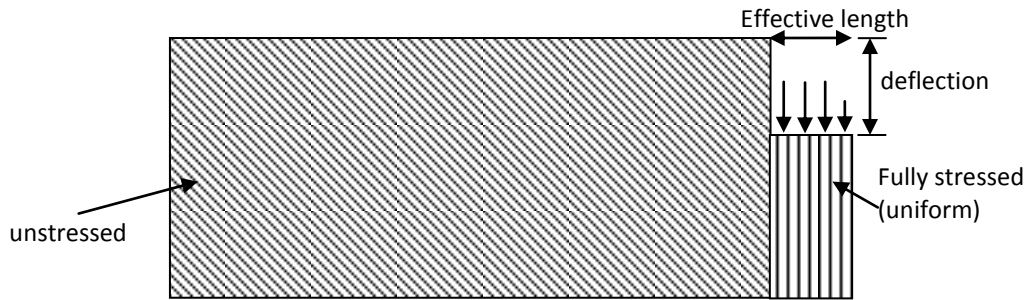


Figure 3-14 Support effective width

### 3.8 Finite Element Modelling of LCC T-joist specimens

Finite element analysis (FEA) has become commonly used as a tool to solve complicated stress problems using a system of points called nodes which make a grid called a mesh. Material and structural properties were assigned to the elements of the mesh, such as beam or shell elements to define how the structure will react to certain loading conditions.

The finite element package, SAP 2000 v.14 (SAP2000, 1997) was used to model the LCC beams to evaluate the experimental modal analysis results using the same material properties and cross-section, with a modulus of elasticity for concrete of  $E_c = 30$  MPa and for timber,  $E_t = 12.7$  MPa. The same procedure as described in section 3.2 was applied in this analysis. Additionally, all elements were assumed to have isotropic material characteristics, including LVL, even though LVL is an orthotropic material, to get the optimum dynamic behaviour of the system. The complete properties of concrete and LVL are reported in Appendix A.

The lumped mass system illustrated in Figure 3-15 was modelled in a preliminary study to find the dynamic behaviour of the TCC beam using the same configuration as discussed in section 3.2. A more refined finite element (FE) mesh is outlined in Figure 3-16. Nodes, corresponding to the lumped masses were modelled at 200 mm centres. The connectors were modelled as spring elements with stiffness,  $k$ , as provided by Yeoh (2010). The spring elements were connected between the nodes of the two elements, while beam elements represented the LVL joist, and shell elements represented the concrete topping as illustrated in Figure 3-16. The serviceability slip

modulus,  $k$ , was calculated by taking the tangent of the force and deflection relationship (refer to Figure 3-17). Only 6 to 10 connectors were modelled for each beam (depending on the beam design). The remainder of the nodes were connected with spring elements (as link elements), but with very high stiffness. The purpose of this is to transfer the load from the concrete beam element to the LVL joist beam element as depicted in Figure 3-16.

Descriptions of the elements used are given below and the FEA SAP 2000 model as illustrated in Figure 3-16 was used to assemble models of each of experimental assemblies described in the following chapters.

**Beam element** – A 2-noded linear elastic beam element representing the orthotropic LVL joist with 6 DOFs.

**Shell element** – A 4-noded shell element with bending and membrane capacity was used to model the concrete topping on this system.

**Link element** – A 2-node link element was chosen to act as a spring element between the beam elements and the shell elements. This link element transferred loads from the shell to the beam elements, as a shear connector to the whole system.

**Joint mass** – These represented the shaker and steel masses that could be lumped at the selected joint.

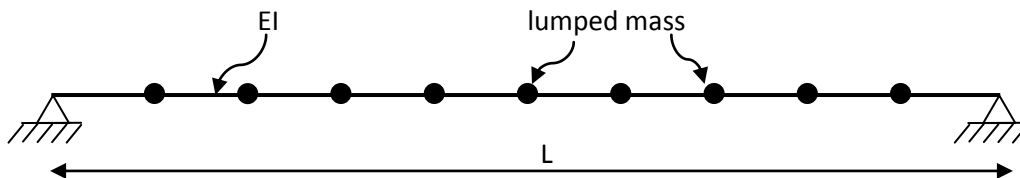


Figure 3-15 Lumped mass system

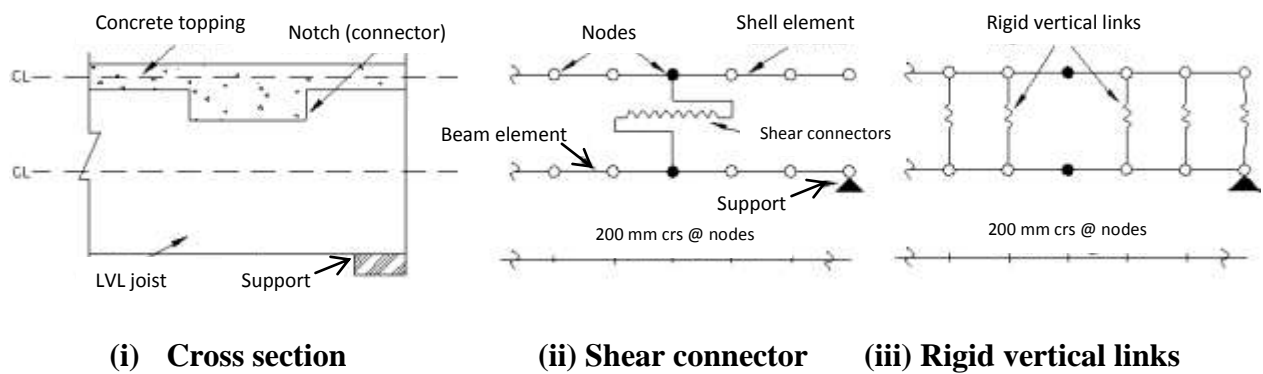


Figure 3-16 LCC finite element models

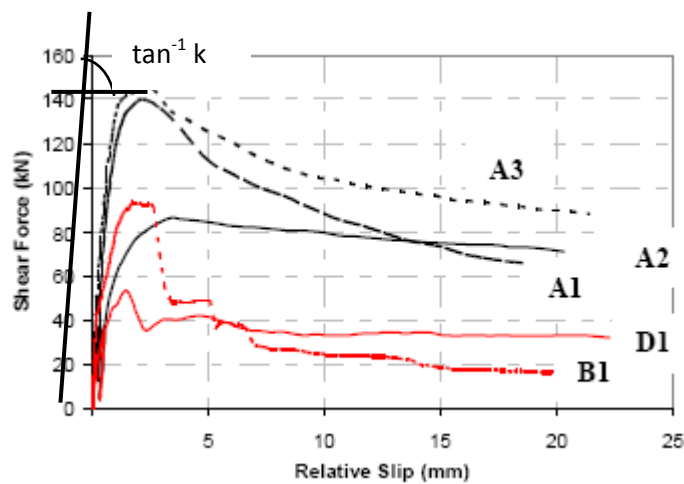


Figure 3-17 Connection experimental load-slip curve (source: Yeoh (2010))

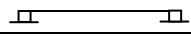
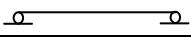
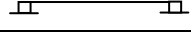
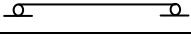
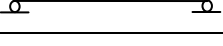
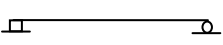
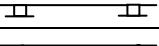
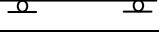
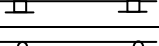
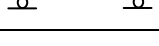
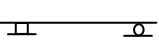
The finite element investigations of the effect of span length, topping width, and support stiffness on the LCC vibration behaviour followed the vibration testing. A summary of the first five modes from the full-scale LCC finite element results are presented in Table 3-9. Detailed discussions of the finite element results will be explained in Section 3.7, including the comparison between the vibration test and the analytical model results.

The mode shapes from the finite element analyses are depicted in

Figure 3-18. Only the mode shapes for specimen A (8 m x 0.6 m) and specimen D (6 m x 0.6 m) are presented because the modal behaviours of the 8 m and

10 m specimens were similar, as both specimens were simply-supported specimens. There was a difference with specimen D, which was simply supported with a 1 m cantilever arm at both ends. To verify the results for specimen D, a simply supported LCC specimen with a 6 m span length was modelled, as shown Figure 3-19. The differences between the 6 m specimens with and without a cantilever arm was negligible at 0.86 % . Thus, the one-meter cantilever arm did not have a big affect on the vibration behaviour.

Table 3-9 Summary of results from the finite element modelling

Specimen	Support system	$f_1$ (Hz)	$f_2$ (Hz)	$f_3$ (Hz)	$f_4$ (Hz)	$f_5$ (Hz)
<b>A</b>	<b>8 m x 0.6 m</b> 					
	Block	10.0	20.7	39.6	57.8	81.1
	Roller	9.4	19.5	37.9	55.8	80.0
	Block and Roller	9.7	20.1	38.8	56.7	80.2
<b>B</b>	<b>8 m x 1.2 m</b> 					
	Block	9.7	19.5	37.2	54.3	76.1
	Roller	9.1	18.4	35.6	52.4	74.1
	Block and Roller	9.4	19.0	36.4	53.3	75.3
<b>C</b>	<b>10 m x 0.6 m</b> 					
	Block	6.8	14.6	26.6	38.7	54.8
	Roller	5.9	12.9	24.1	35.9	52.0
	Block and Roller	6.3	13.8	25.3	37.4	53.4
<b>D</b>	<b>6 m x 0.6 m</b> 					
	Block	15.6	33.0	59.6	92.9	121.8
	Roller	14.2	30.4	52.0	92.2	122.9
	Block and Roller	14.8	31.6	54.2	92.5	124.1
<b>E</b>	<b>6 m x 1.2 m</b> 					
	Block	15.1	31.6	57.6	88.3	118.7
	Roller	13.1	29.0	49.1	87.6	116.7
	Block and Roller	14.4	30.0	51.2	87.9	118.0

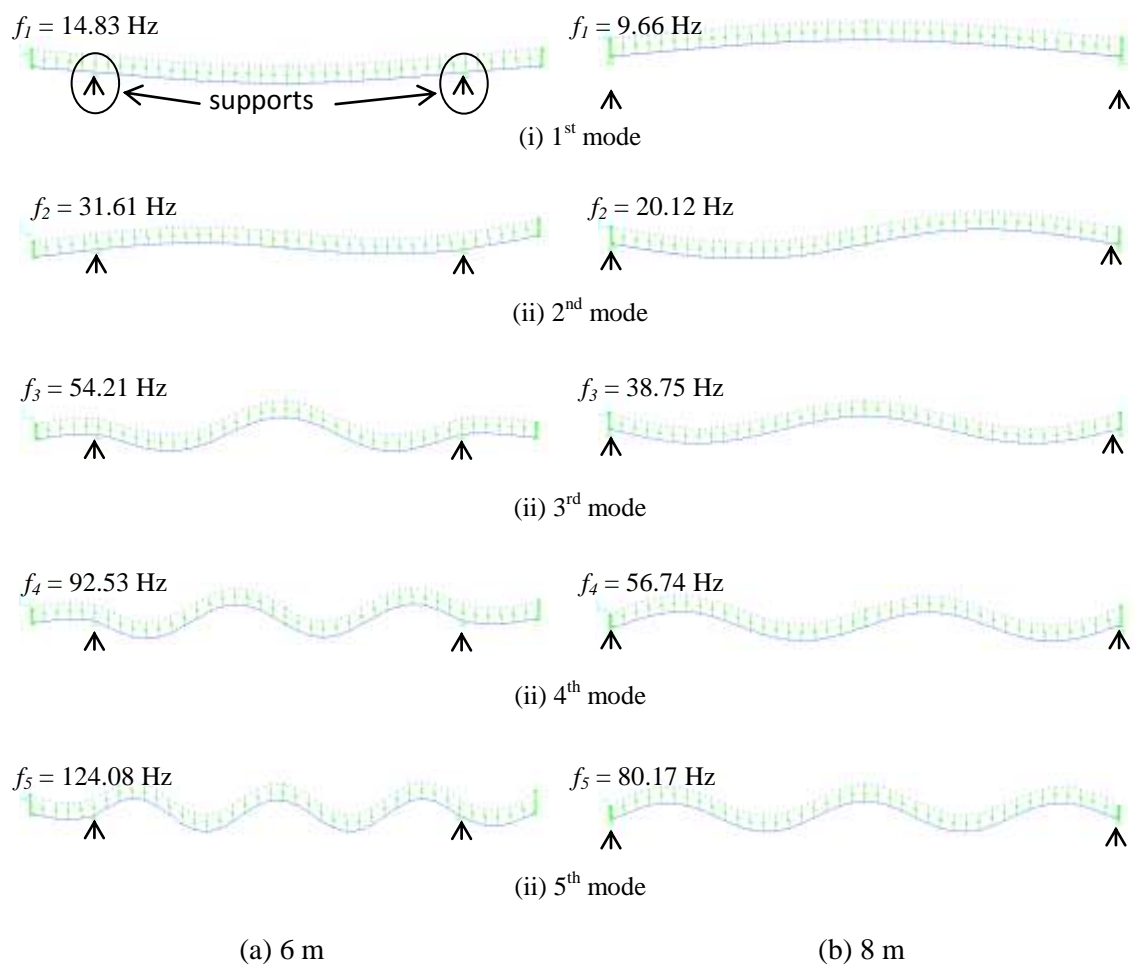


Figure 3-18 Mode shapes from finite element modelling for 6 m and 8 m specimens

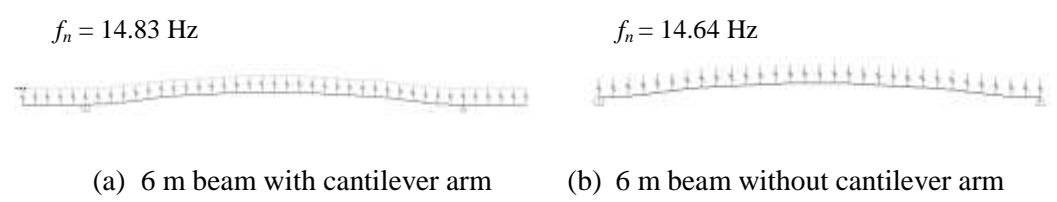


Figure 3-19 Comparison of 6 m specimens with and without cantilever arm

### **3.9 Comparison between the modal test (EMA) and finite element modelling (FEA)**

The discussion of the comparison between the EMA and FEA only focuses on the fundamental frequency, since some of the higher modes from the EMA could not be obtained for some specimens. In addition, the fundamental natural frequency is the most important frequency for serviceability in a structural design compared to the higher frequencies.

Table 3-10 shows the differences in fundamental natural frequency between analytical modelling and vibration test results, together with the percentage errors, based on the support systems of the specimens. The differences in the fundamental natural frequencies predicted from the FEA and EMA was moderately high with the average errors for specimens on blocks, rollers, and block and roller support systems being about 11.5 %, 13.0 % and 9.5 %, or 1.8 Hz, 1.1 Hz or 0.8 Hz, respectively. The flexibility of the support systems in the tests probably caused the big differences. As discussed before (see section 3.2), the specimens were placed on a LVL block which acted as the support system. The flexibility of the LVL block may have affected the overall vibration behaviour of the specimens. Meanwhile, the support systems in FEA modelling were more rigid than the real situation.

Table 3-10 Comparison between FEA and EMA for different support stiffnesses

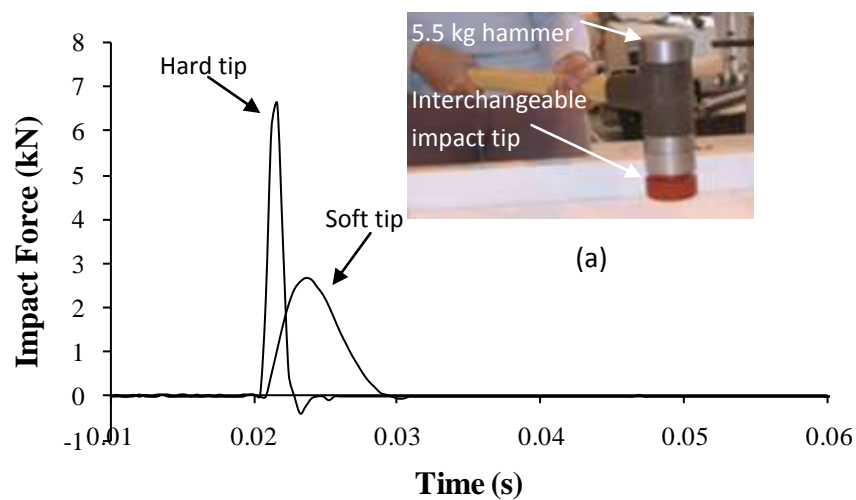
Specimen		Support system		
		Block ( $f_1$ , Hz)	Roller ( $f_1$ , Hz)	Block and Roller ( $f_1$ , Hz)
<b>A</b>	FEA	10.0	9.4	9.7
	EMA	9.2	8.7	9.1
	<b>Difference (abs)</b>	<b>0.8</b>	<b>0.7</b>	<b>0.6</b>
	<b>Error %</b>	<b>10.0</b>	<b>7.4</b>	<b>6.2</b>
<b>B</b>	FEA	9.7	9.1	9.4
	EMA	9.2	8.8	9.2
	<b>Difference (abs)</b>	<b>0.5</b>	<b>0.3</b>	<b>0.2</b>
	<b>Error %</b>	<b>5.2</b>	<b>3.3</b>	<b>2.1</b>
<b>C</b>	FEA	6.8	5.9	6.3
	EMA	6.4	6.4	6.3
	<b>Difference (abs)</b>	<b>0.4</b>	<b>0.5</b>	<b>0</b>
	<b>Error %</b>	<b>5.9</b>	<b>8.5</b>	<b>0</b>
<b>D</b>	FEA	15.6	14.2	14.8
	EMA	12.8	11.0	12.5
	<b>Difference (abs)</b>	<b>2.8</b>	<b>3.2</b>	<b>2.3</b>
	<b>Error %</b>	<b>18.0</b>	<b>22.5</b>	<b>15.5</b>
<b>E</b>	FEA	15.1	13.1	14.4
	EMA	12.3	10.0	11.0
	<b>Difference (abs)</b>	<b>2.8</b>	<b>3.1</b>	<b>3.4</b>
	<b>Error %</b>	<b>18.5</b>	<b>23.7</b>	<b>23.6</b>
<b>Mean</b>	<b>Difference (abs)</b>	<b>1.5</b>	<b>1.1</b>	<b>0.8</b>
	<b>Error %</b>	<b>11.5</b>	<b>13.0</b>	<b>9.5</b>

### 3.10 Damping from Impact Hammer Test

The other method that has been used in this research was the impact hammer test, to determine the natural period and equivalent viscous damping. The Dytran model 5803A instrumented impact hammer illustrated in Figure 3-20 (a) was used to provide an impulse point load. The 5.4 kg hammer head had a 22.2 kN piezoelectric transducer to directly measure the force applied to the specimen. On the other hand, the specimen responses were recorded by accelerometers attached on the beam.

The beam specimens were excited on the upper surface as demonstrated in Figure 4.7 (a). The person using the hammer stood alongside the specimen. The hammer tip controls the excitation frequencies. Four types of hammer tip (soft, medium, tough and hard) were provided with the hammer. The softer tip provides mostly low frequency response due the longer duration of the impact. The soft and hard tips were used to investigate the different behaviour of the lower and higher frequencies. Ten impacts were applied at one point and the readings were averaged due to uneven force applied during the test.

Striking the hammer on the specimen created a half-sine input curve as shown in Figure 3-20 (b), with two kinds of force pulse based on the hammer tip. Figure 3-21 illustrates the specimen's response. The duration of the pulse related to the stiffness of the contacting surface. The stiffer tip provided a short pulse duration of higher frequency. Vice versa, the softer tip contributed to longer periods.



(b) impact hammer time history

Figure 3-20 A person striking the specimen and the time history of the impact force

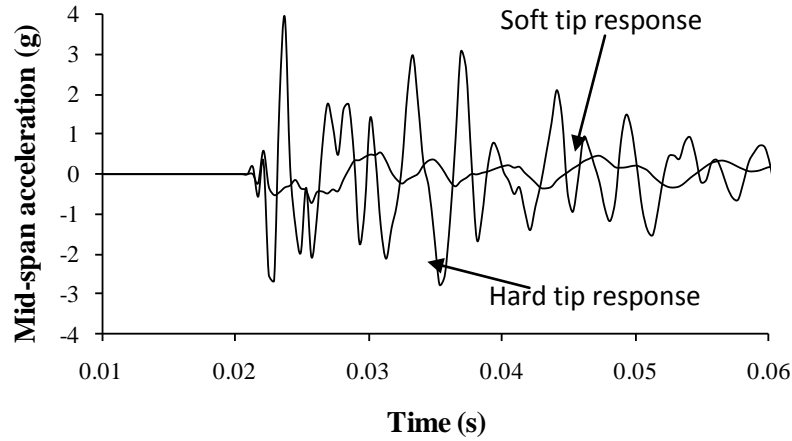


Figure 3-21 Beam responses from impact hammer test

The data processing began by calculating the natural frequency and critical damping ratio for each reading. Each hammer test was carried out ten times at one point. Then, the average of ten natural frequencies and damping ratios was calculated and the natural frequency and damping ratio for each specimen were obtained. The repeat of testing at one point was necessary due to higher modes interfering with the desired fundamental mode early in the response. Once higher modes are attenuated sufficiently, the fundamental response has only a data acquisition sampling error. The logarithmic decrement method was applied to obtain the natural frequencies and critical damping ratio of the specimen according to the following equations (see also Figure 3-22);

$$\text{Period, } T = \frac{t_{i+n} - t_1}{n} \quad (3-1)$$

$$\text{Damping, } \xi = \frac{1}{2\pi j} \ln \frac{u_i}{u_{i+n}} \quad (3-2)$$

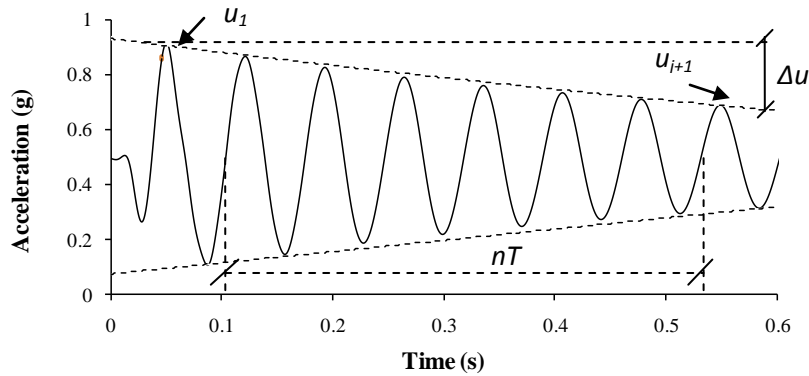


Figure 3-22 Decay of motion

The hardness of the surface does not affect the critical damping ratio of the specimens. However, the hardness of the surface influenced the acceleration amplitude and length of period. The peak acceleration was calculated based on the decay motion of the impulse vibration. This calculation was based on the assumption that the beam vibrates in fundamental mode only. Damping ratios of 2.3 % and 1.5 %, were obtained respectively, as shown in Figure 3-23 . These damping ratios are similar to the of 1 % to 4.5 % as recommended in the AISC design guide (Murray et. al, 2003) for unfurnished floors (1%) to floors with a partitions (4.5 %)

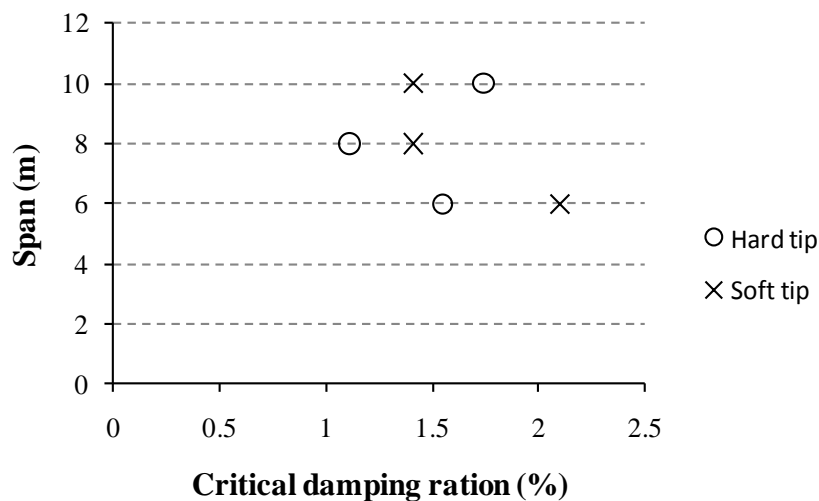


Figure 3-23 Critical damping ratio

### **3.11 Conclusion and Summary**

The LCC flooring system was introduced in the University of Canterbury as an alternative to existing flooring systems (Yeoh, 2010). A series of tests were carried out including electrodynamic shaker tests to understand the vibration behaviour of the system, including obtaining the vibration parameters for serviceability design purposes. As there were limitations on space and time, only full-scale LVL-concrete composite specimens or beams were constructed, as preliminary studies for this research.

The studies included the influences of span length, width length and the support system. Vibration testing and finite element modelling were conducted to obtain the vibration parameters, natural frequencies, damping ratios and mode shapes. Results from both methods were closed with the error percentage not more than 30 %. Thus, it can be concluded that the finite element modelling was suitable to use for further research.

As expected, the rigidity of the boundary condition has an influence on the vibration behaviour and properties of the system. The flexibility of the LVL timber block gave more influence on the vibration behaviour and reduced the natural frequency. Hence, a two-way flooring system is stiffer than a simply supported system and therefore is expected to have a greater natural frequency (Abd Ghafar et. al, 2008) and this will be discussed later in the following chapters.

Two parameters that have been discussed in this chapter are the span length and topping width of the specimens. Both of these parameters changed the natural frequencies of the system as they are affect the stiffness of the system. As is known, the stiffness is inversely proportional to the natural frequency. The reason for both parameters being studied was to understand the basic behaviour of floor systems and whether these systems have a low frequency or high frequency response.

Referring to Figure 3-24, the natural frequency for the 6 m and 8 m beams were more than 8 Hz, however the natural frequency for the 10 m beam was less than 8 Hz. Thus, the 8 m long span was reasonable to construct and further study was discussed in Chapter 6. The detailed design of an LCC floor, including the design guide, will be discussed in Chapter 7.

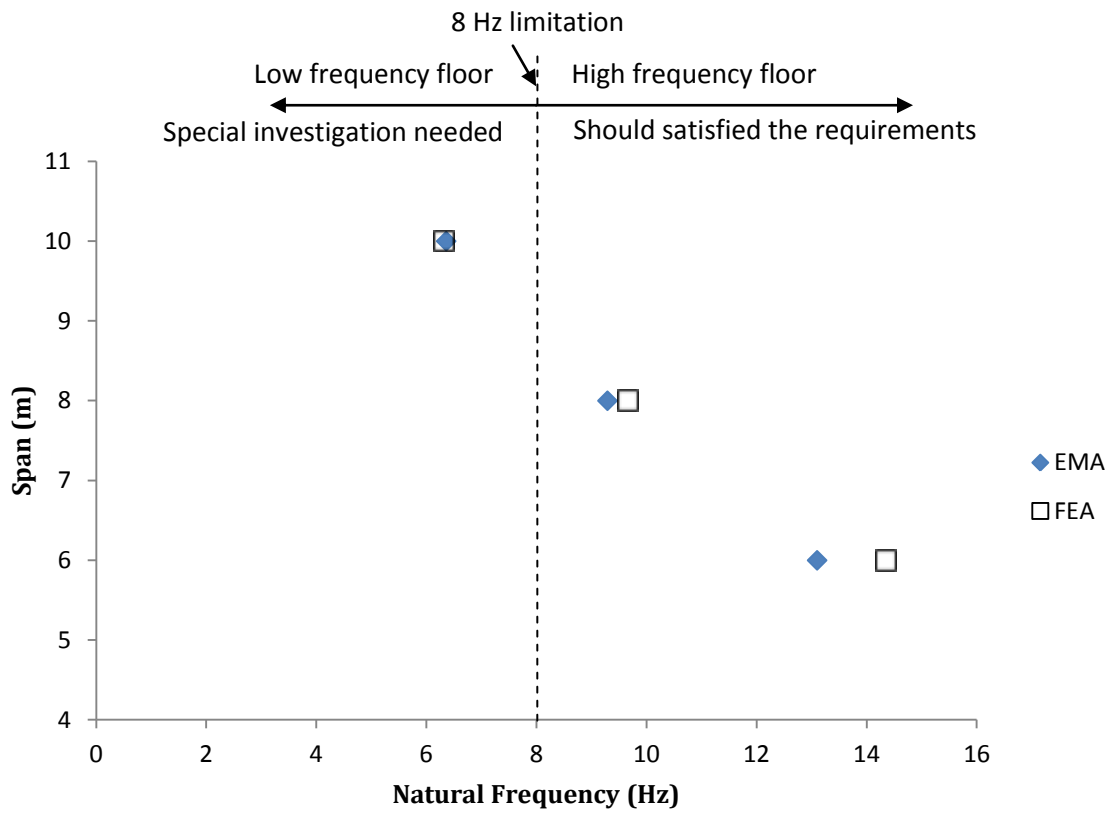


Figure 3-24 Natural frequency limitation for a LCC flooring system

## CHAPTER 4      **EXPERIMENTAL MODAL ANALYSIS (EMA) ON REDUCED SCALE LVL-CONCRETE COMPOSITE (LCC) T-JOIST SPECIMENS**

In this chapter, details of Experimental Modal Analysis (EMA) and Finite Element (FE) modelling of reduced-scale LCC T-joist specimens and floor are presented. The details were implemented from the full-scale LCC specimens discussed in Chapter 3. The reduced-scale LCC specimens that were built and tested were:

- i. ***Multi-span specimens***: Four (4) spans of LCC T-joist specimens built with 2.8 m span length for each T-joist specimen. The T-joists specimens were connected to each other with timber blocks (which simulate a supporting beam) and the concrete was poured on the top as a continuous slab. After each test, the concrete slab was then cut to reduce the number of spans from 4- to 3-, 2- and one.
- ii. ***Multi-storey specimens***: The single span specimens (which were cut from the multi-span specimen) were stacked on top of each other to simulate a multi-storey system, of 2-, 3-, 4-storeys, and a 2-storey 2-bay system.
- iii. ***Single-bay T-joist floor***: A 3 m x 3 m simply supported floor was built using 150 mm x 45 mm joists at 500m spacing and 250 mm x 45 mm supporting lateral beams.

Vibration shaker tests were conducted to determine the modal parameters. The EMA was adopted from Chapter 3 (refer section 3.3), only the location of the electrodynamic shaker was different, based on the number of spans. The test setup for each specimen will be explained later in this chapter.

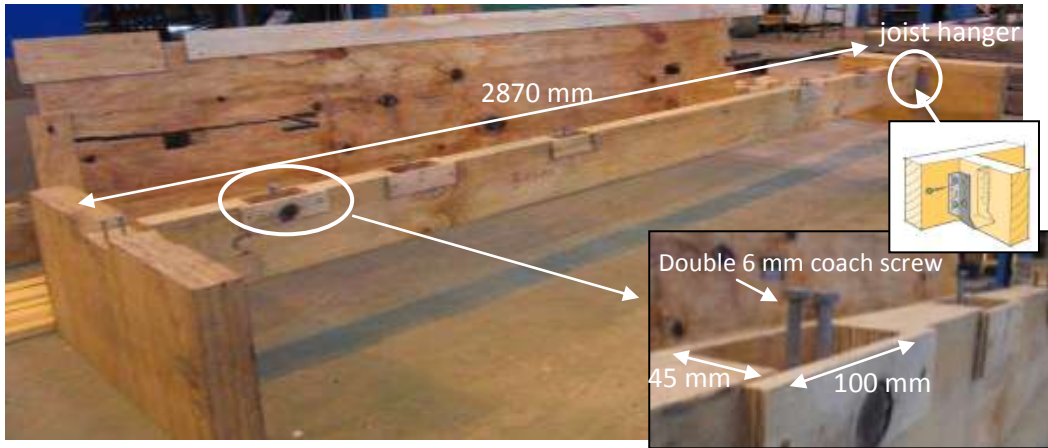
## **4.1 Construction Detail of Reduced Scale specimens**

The multi-span specimens were built in order to understand the vibration behaviour between spans and the influences of the boundary conditions. However, due to limited space in the laboratory, the multi-span specimens were constructed to approximately one-third scale of the full scale specimens, The construction details were similar to the single bay, simply supported, floor described later in section 4.1.3. There was no attempt to apply the principles of similitude to the reduced scale tests, as the reduced scale specimens were separately modelled using FEM (refer to Chapter 5).

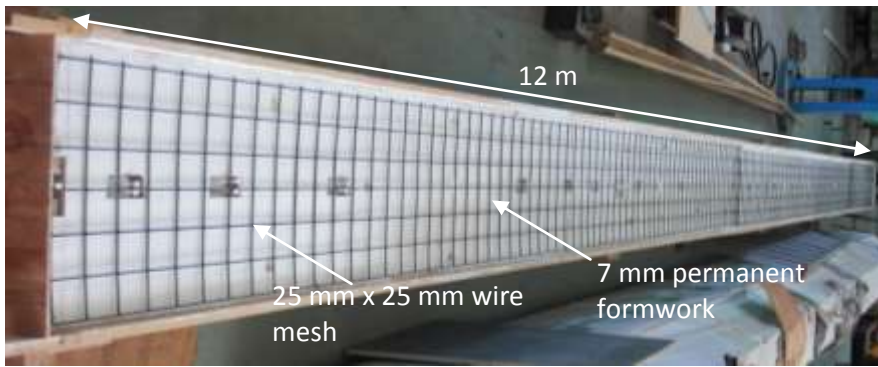
### **4.1.1 Multi-span specimen detail**

Each of the four spans making up the reduced scale, simply supported beam was built as illustrated in Figure 4-1 (a). The joist was 2870 mm long with a cross section of 250 x 45 mm connected to 300 x 65 mm timber blocks at each end using standard joist hangers. Six rectangular 100 x 45 mm notches were cut the top surface of the LVL beam to create the shear connector between the LVL joist and the concrete topping. Two 6 mm diameter coach screws were installed in the centre of the notch to improve the performance of the connection system. The four beams were connected together by screwing the timber blocks together to simulate a supporting beam and 7 mm plywood sheathing was nailed to the LVL joists as permanent formwork for the 500 mm wide x 25 mm thick concrete topping. The concrete was reinforced with 25 mm x 25 mm wire mesh as shown in Figure 4-1(b).

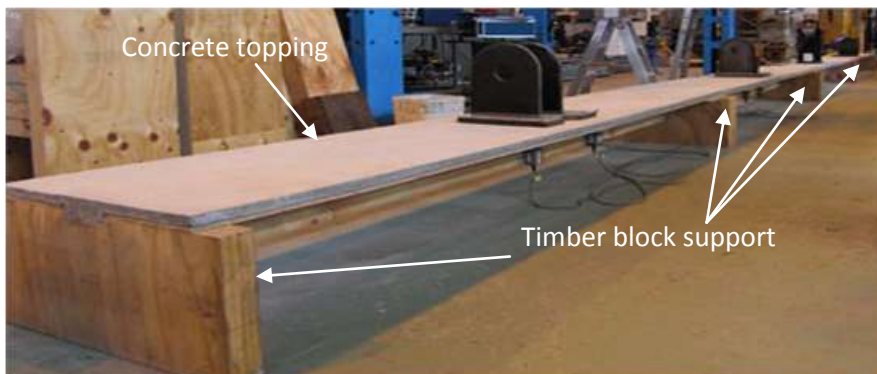
The concrete topping was poured continuously across the tops of the simply-supported LVL-joists as shown in Figure 4-1(c). The concrete topping was continuous over the supports for all of the multi-span tests. The concrete slab was then subsequently cut, as shown in Figure 4-2, in order to reduce the number of spans from 4- to 3-, 2- and eventually, one.



(a) Simply supported LVL beam



(b) Top view of the 4-span LVL beam before the continuous concrete topping was poured



(c) 4-span LVL beam with continuous concrete topping

Figure 4-1 Photographs of the multi-span system

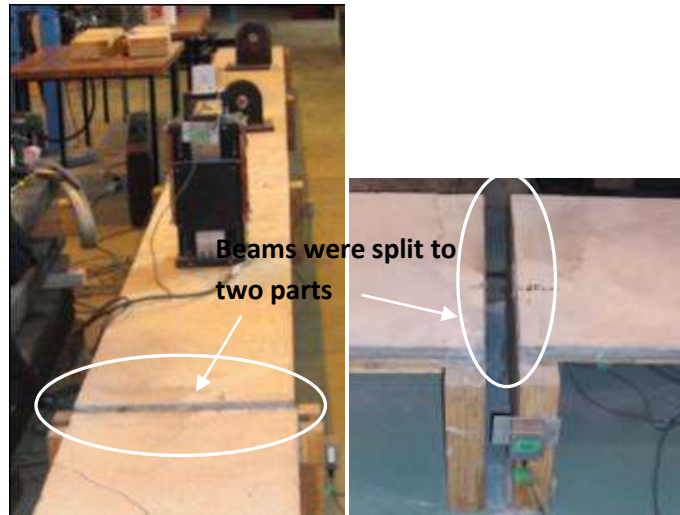


Figure 4-2 Concrete topping being cut to split the beams

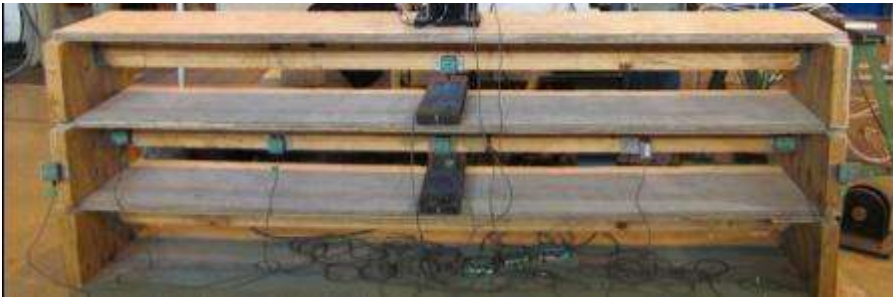
#### 4.1.2 Multi-storey specimen detail

The effect of vibration on one floor to another floor (either underneath or above) was investigated by placing the single-span specimens one above the other in a stacked configuration, without any mechanical connection between the beams (refer Figure 4-3). In this way, 2-storey, 3-storey and 4-storey systems were tested.

Furthermore, a 2-storey, 2-bay system was re-constructed by re-screwing the timber block supports and pouring a cement grout to re-connect the concrete topping as depicted in Figure 4-4 to study more details on multi-span flooring systems.



(a) 2-storey system



(b) 3-storey system

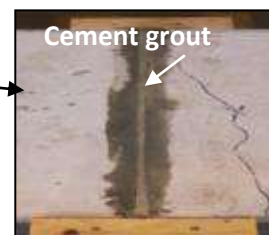


(c) 4-storey system

Figure 4-3 Multi-storey single-bay systems



(a) 2-storey 2-bay system



(b) re-connected beam

Figure 4-4 2-storey, 2-bay T-joint beams

### 4.1.3 Single-bay T-joist floor details

A single 3 m x 3 m floor was built from 150 mm x 45 mm joists at 500 mm spacing and 250 mm x 45 mm lateral supporting beams with 2694mm joist length. A 25 mm concrete topping was poured on 7 mm plywood sheathing which provided a permanent formwork. Shear resistance between the concrete topping and the timber joist was provided the notch connectors in cut in the LVL joists and reinforced with 6 mm diameter coach screws. The joists were connected to the 250 mm x 45 mm primary beams with joist hangers. The floor plan layout and the detail cross section are illustrated in Figure 4-5 and Figure 4-6, respectively. Thus the floor was a one-third reduced-scale specimen of a house floor.

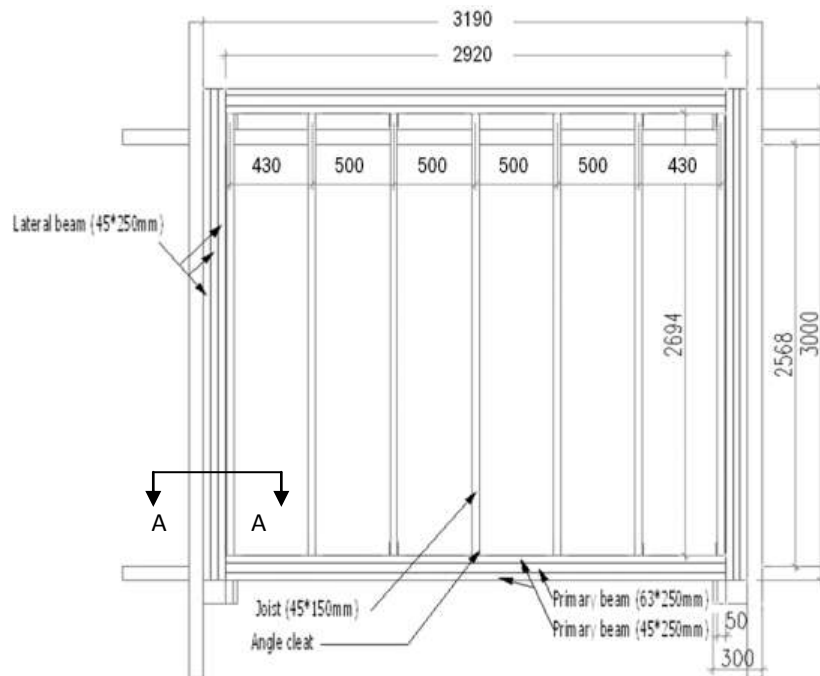


Figure 4-5 Floor plan layout (dimension in mm)

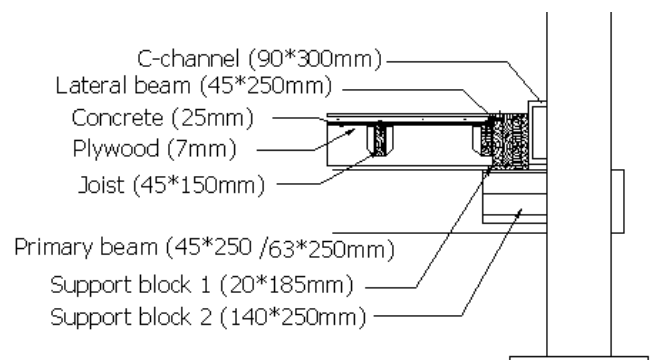


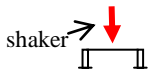
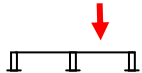
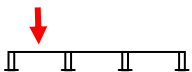
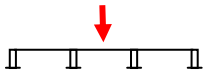
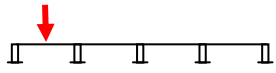
Figure 4-6 Cross-section A - A

## 4.2 Dynamic performance of multi-span specimens

Forced vibration tests were carried out on each multi-span specimen to determine the vibration behaviour of the multi-span flooring system. The excitation signal applied went from 5 Hz to 25 Hz, with a 0.1 Hz interval. The test setup for each multi-span specimen is depicted in Table 4-1. The shaker was located at the midspan of the outer span of the specimens, with accelerometers attached along the LVL joist. The shaker was then relocated to another span, for the 3-span and 4-span specimens, to understand the transmissibility of the vibration wave between entire spans.

Table 4-1 shows the results of the vibration test multi-span specimens. The fundamental natural frequency of the first (1<sup>st</sup>) mode was easy to determine due to the location of the shaker at mid-span, as this is the anti-node location for odd mode numbers (1, 3) as discussed before in Chapter 3.

Table 4-1 Results of vibration test on LCC multi-span specimens

Specimen	$f_1$ (Hz)	$\xi_1$ (%)	$f_2$ (Hz)	$\xi_2$ (%)	$f_3$ (Hz)	$\xi_3$ (%)
1- span 	24.2	1.0	47.3	0.34	57.6	0.1
2-span 	21.1	0.1	42.4	0.1	61.4	0.1
3-span (Setup 1) 	21.7	1.3	43.1	0.2	64.0	0.3
3-span (Setup 2) 	23.3	0.7	46.4	0.8	69.6	0.2
4-span 	22.2	1.9	43.8	0.1	72.1	0.3

The mode shapes for the multi-span specimens are illustrated in Figure 4-7. The mode shape for the 1-span specimen was obvious for both the first (1<sup>st</sup>) and (2<sup>nd</sup>) second modes. However, when the number of spans increased, the mode shapes were difficult to recognise, especially for the second (2<sup>nd</sup>) mode and higher, probably due to the wave propagation between spans, arising from close mode behaviour. Pavic et. al (2002) states that having two identical floors with the modes of the two adjacent floor levels having very close natural frequencies there is the potential to enhance the vibration transmitted between the floors.

Figure 4-7(iii) and (iv) show the mode shape of the 3-span specimen with two test setups, where the shaker is located at one of the outer beams (as setup 1), and at an inner beam (as setup 2). When the span was excited at one of the outer beams, the other end beam gained about one-quarter of the excitation energy, transmitted through the inner beam. The wave reduced due to the material damping, energy dissipated to the ground, and probably due to the boundary conditions of the system. When the shaker was relocated to the inner beam, the tests showed that the energy split to the left and right spans produced different amplitude deflections at these spans.

The transmissibility of the vibration energy between end spans through the inner spans obtained during the force vibration test on the 4-span specimen is illustrated in Figure 4-7 (v) to Figure 4-7 (vii). The shaker was located at three (3) different places: at the mid-span of the outer span (setup 1), and at the mid-span of both inner spans (setups 2). When the shaker excited the outer span, the vibration energy transmitted to the other end span through the inner spans, produced an amplitude that was about half the amplitude produced at the span with the shaker. The wave propagation was also found for the second (2<sup>nd</sup>) mode behaviour. However, the vibration behaviour for the multi-span specimens were difficult to interpret on account of the vibration transmissibility, distraction from outside noise, and the movement at the edges of the specimen. Thus, analytical modelling was performed to provide clearer insight as discussed in detail in the following chapter.

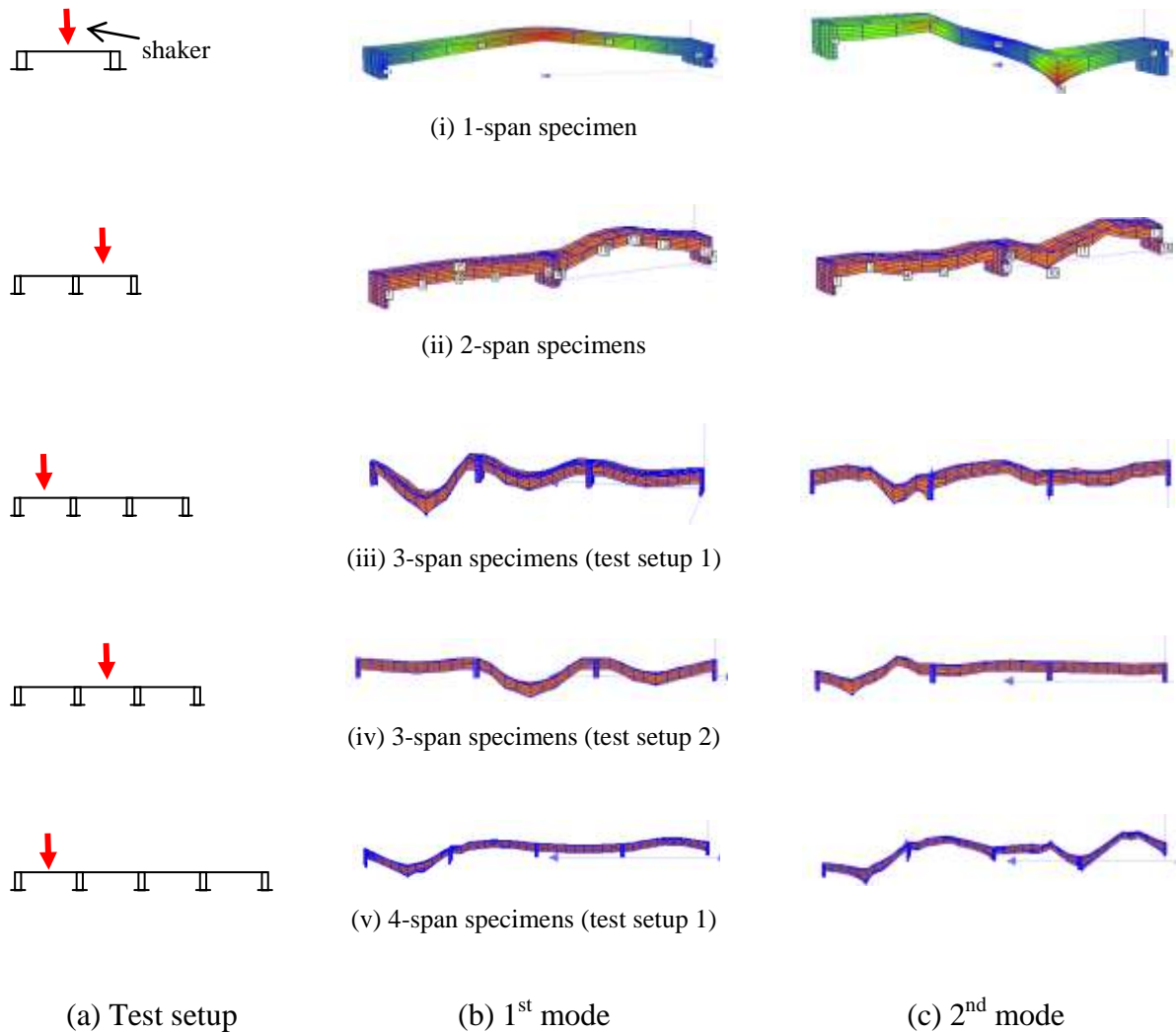
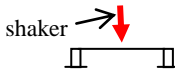
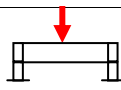
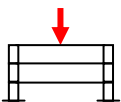
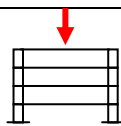


Figure 4-7 Multi-span mode shape

### 4.3 Dynamic performance of multi-storey specimens

The multi-span specimens were cut and stacked together to perform the multi-storey specimens, as explained in section 4.2. The shaker was located on the top span and accelerometers were attached along the span at each storey. The same signal frequency was applied as on the multi-span specimen tests, i.e. ranging from 5 Hz to 25 Hz, with a 0.1 Hz interval. The test method was adopted from section 3.3 (see Chapter 3). The test setup for multi-storey specimens as illustrated in Table 4-2.

Table 4-2 Result summary of multi-storey specimens

Specimen	$f_1$ (Hz)	$\xi_1$ (%)	$f_2$ (Hz)	$\xi_2$ (%)	$f_3$ (Hz)	$\xi_3$ (%)
1- storey 	24.2	0.1	47.3	0.35	57.6	0.1
2-storey 	20.0	1.0	39.1	0.21	53.5	0.1
3-storey 	18.2	0.1	35.7	0.10	53.5	0.1
4-storey 	21.1	0.9	35.0	0.10	47.7	0.2

The mode shapes of the multi-storey specimens are illustrated in Figure 4-8. Because the specimens were stacked on top of each other without additional support caused movement at the edge of the specimens. The movement on the upper specimen introduced an additional coupled mode and may have affected the vibration behaviour of the system.

The modal shape for the lower span became flatter compared to that of the upper span for the first, second and third modes of the 2-span specimen as presented in Figure 4-8 (i). However, the middle span of the 3-storey specimen (refer Figure 4-8 (ii)) had a modal shape with a similar amplitude to that of the top span displacement amplitude, but the shape was in the opposite direction. The lower span mode shape was less curved compared to the two (2) spans above. The mode shapes for the 4-storey specimen were different to the other storey specimens. The top storey, where the shaker was located, was less curved than the lower storey, and both middle storeys showed a higher curvature in the second mode. Meanwhile, the lower span showed a half sine curve for the third mode. It shows that the vibration energy travelled between storeys. Unfortunately, a coupled mode appeared and the real behaviour of the multi-storey system could not be understood sufficiently from these vibration tests. The multi-storey specimens were also modelled in a finite element software package to get more understanding of how the vibration energy dissipated, is discussed in subsequent chapter.

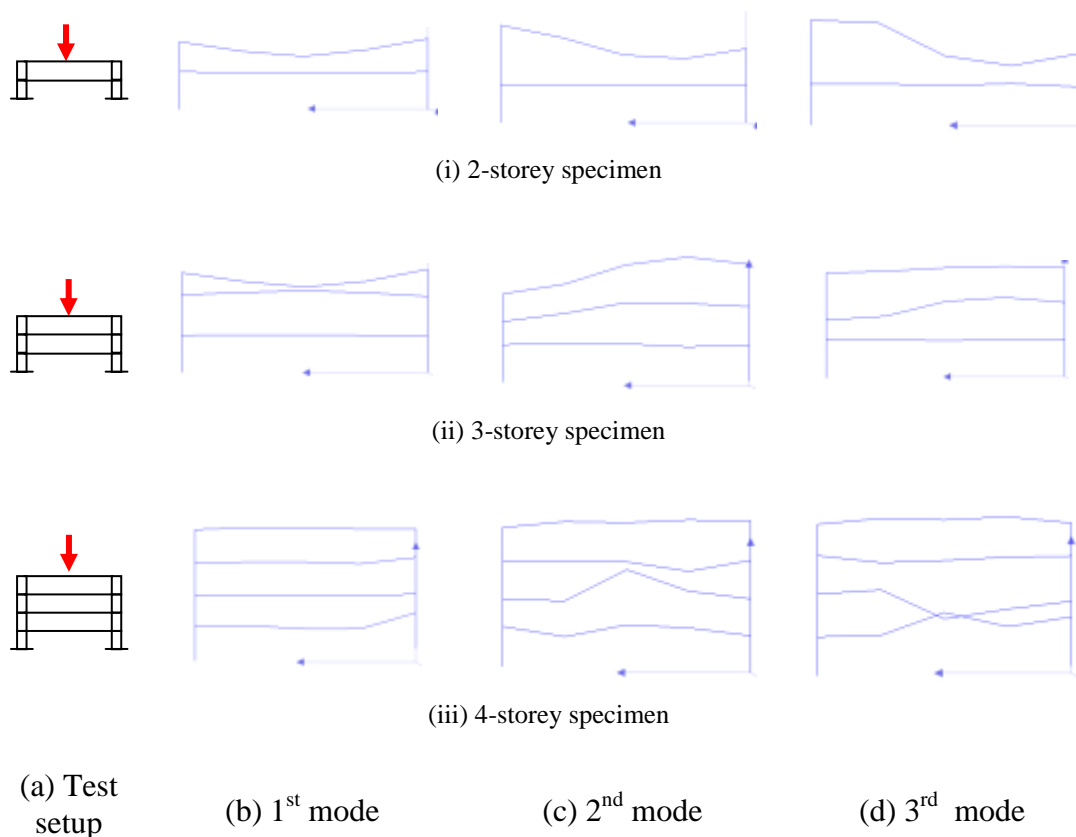


Figure 4-8 Multi-storey mode shape

#### 4.4 Dynamic performance of a single-bay floor

A larger scale specimen was built to investigate the vibration behaviour of an LCC flooring system. A reduced-scale 3 m x 3 m LCC floor was built and tested by electrodynamic shaker to obtain the natural frequencies and mode shapes of the specimen. Details of the specimens is explained in section 4.1.3. In a similar method to that for the full-scale LCC specimen (refer Chapter 3), the accelerometers were placed at the mid-span of the each joist across the floor as illustrated in Figure 4-9. The shaker was first located at the middle point on the floor and later relocated to one-third of the floor length, in order to determine the asymmetric and symmetric modes.

Masses were selected that matched the shaker mass and placed on the floor over each joist at mid span. The natural frequency of the system noticeably decreased. The addition of masses is shown in Figure 6.10 to decrease the resonance frequency of

the specimen from 17.3 Hz to 14.7 Hz. Extra masses provided better performance of vibration behaviour, with only one peak resonance found in the floor's response.

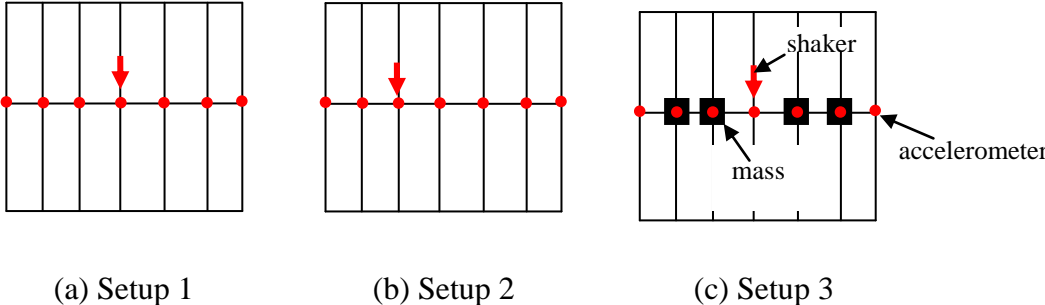


Figure 4-9 Vibration test layout for single-bay floor

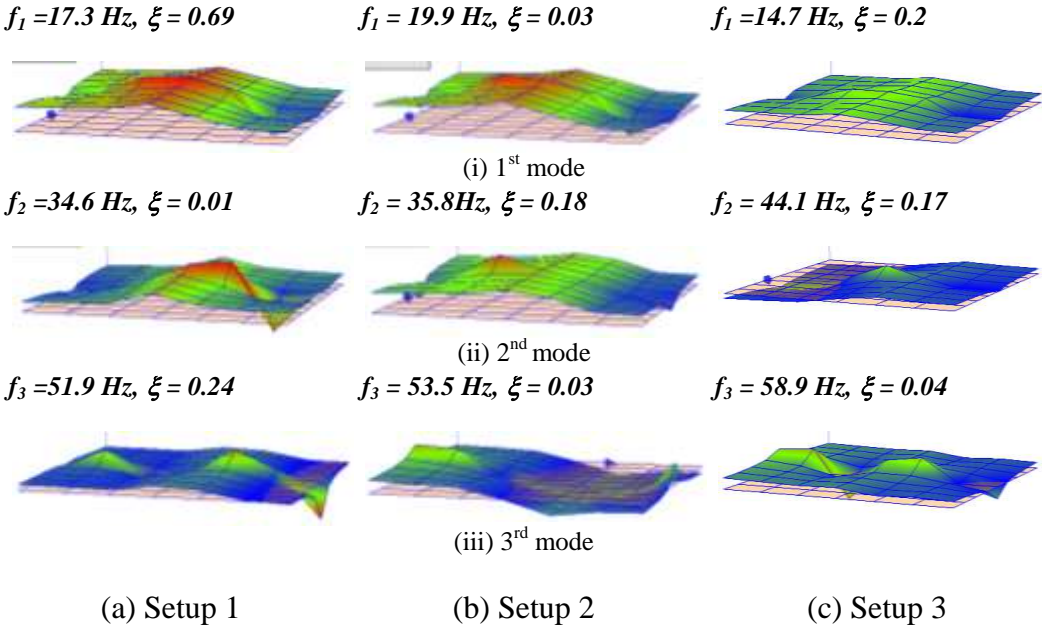


Figure 4-10 Mode shape for single-bay floor

The natural frequencies and mode shapes for the single-bay floor are depicted in Figure 4-10. The mode shapes with additional masses provided a clear curve shape compared to other setup tests. While the additional masses probably influence the results, however without additional mass the acceleration responses had coupling mode issues and extraneous noises. The issues occurred due to the vibration that occurred at

the centre of the floor and the shaker weight probably was more heavy compared to the concrete topping.

Peak accelerations for both experiments, with and without extra masses, were plotted as illustrated in Figure 4-11 and show that the floor without extra masses gave higher peak acceleration compared to the floor with extra masses. End moments issued also discovered on this flooring system, for both test configurations, due to the joist-beam connection.

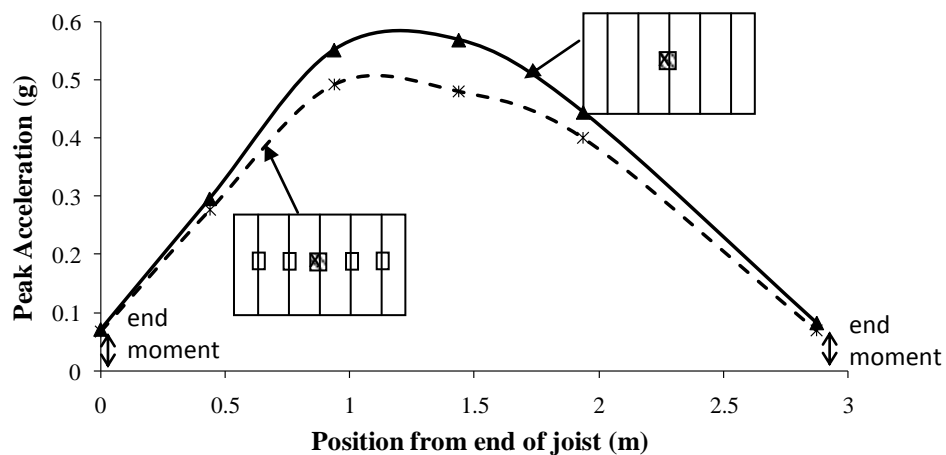


Figure 4-11 Mode shapes curve to the perpendicular of the joist span

#### 4.5 Conclusion and Summary

The forced vibration tests were conducted on reduced-scale, multi-span, multi-storey specimens, as well as reduced-scale single-bay and 2-bay 2-storey flooring systems. The forced vibration tests were carried out to determine the vibration behaviour including the natural frequencies, damping ratios and mode shapes of the specimens and floors. An electrodynamic shaker was used to excite the specimens and floors, along with accelerometers were attached on the specimens and floor to record the acceleration response.

The experiment found that vibration energy was transmitted between spans, and an end span obtained more vibration energy if the other end span was excited, compared to the inner spans, with the vibration energy being transmitted through the

inner spans. The transmitted vibration energy provided close modes between spans or storeys, with the mode shapes difficult to identify, especially for 2<sup>nd</sup> and 3<sup>rd</sup> modes, however the global mode shapes could be recognised. This situation applied for both multi-span and multi-storey flooring systems. Detailed investigation on the vibration transmissibility is discussed in the next chapter where the results of finite element modelling are presented.

## CHAPTER 5 ANALYTICAL MODELLING OF REDUCED SCALE LCC T-JOIST SPECIMENS AND FLOORS

This chapter discusses the results of analytical modelling of reduced-scale T-joist specimens and floors. The vibration parameters, natural frequencies and mode shapes were determined using the eigenvalue analysis in the finite element software package, SAP 2000. The FE results were compared with the experimental investigation results (refer Chapter 4) to understand better the vibration behaviour of LCC T-joist flooring system.

The model description follows the analytical model as explained before in section 3.5 (refer Chapter 3). Three major elements were used in these models as shown in Figure 5-1. The concrete topping and timber blocks were modelled by shell elements, while the LVL joists were modelled as beam elements, and the shear connectors and joist hangers were represented by link elements.

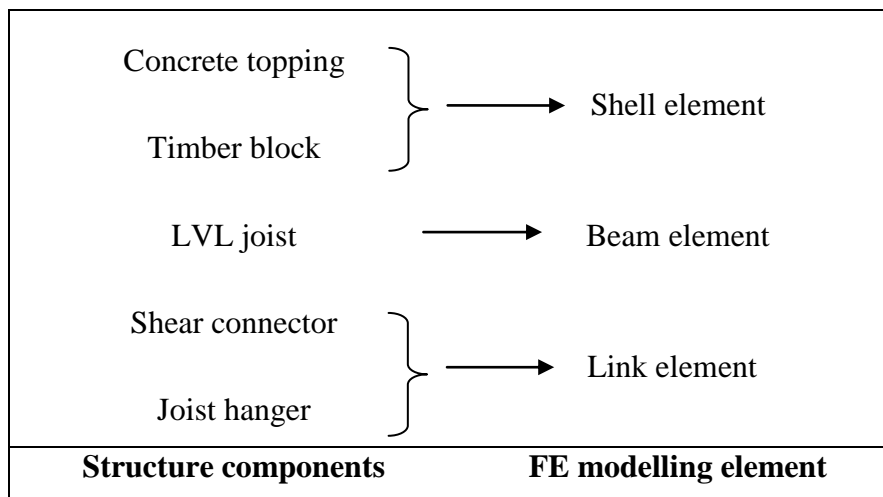
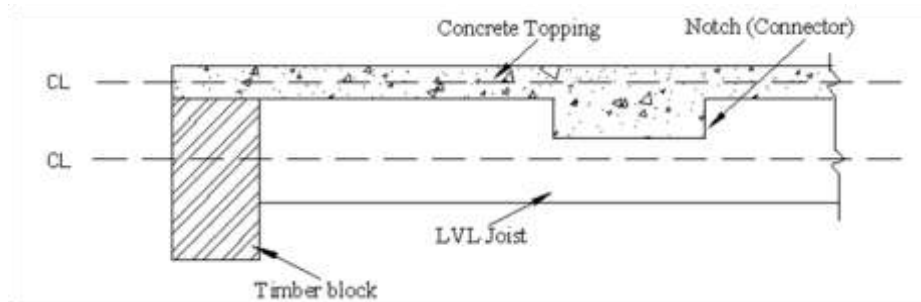


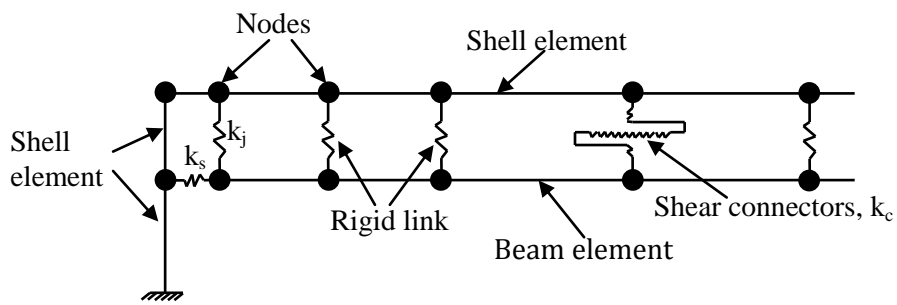
Figure 5-1 FE modelling elements representing structure components

The properties of the concrete and LVL joists are given in Appendix A. The cross section and the simplified elastic model are illustrated in Figure 5-2. As explained previously, the shear connectors were assigned as link elements in the x-axis direction, to model the slip modulus behaviour. However, to transfer loads from the concrete

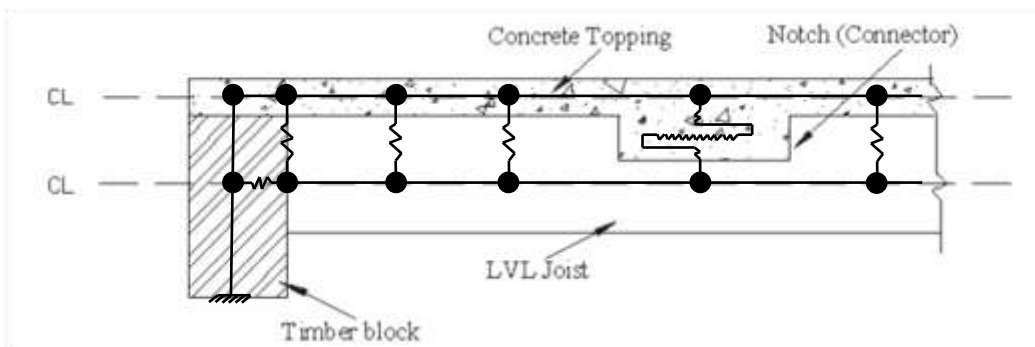
topping to the LVL joists, rigid links were used to connect these two elements as shown in Figure 5-2 (b).



(a) Elevation view of the real structure



(b) Finite element model



(c) The superimposed position of the FE model on the real structure

Figure 5-2 FE model for continuous T-joist specimen

Figure 5-3 shows the details of timber blocks, joists and joist hangers, which later were transformed to three springs whose stiffnesses were considered during the analysis in the same way as shown in Figure 5-2. The descriptions and the stiffness value are shown in

Table 5-1, which also applies to the spring shown in Figure 5-2.

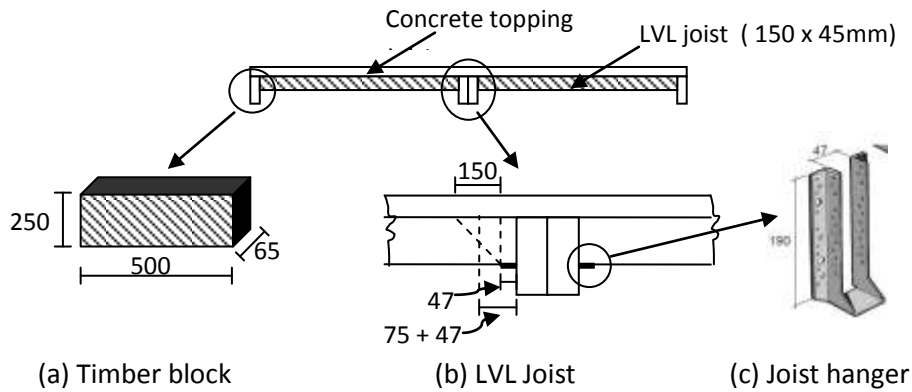


Figure 5-3 Details of timber block, joist and joist hanger (unit in mm)

Table 5-1 Stiffness properties of the springs

Description	Stiffness, k (N/m)
Stiffness of the joist perpendicular to the grain, $k_j$	$2.3 \times 10^7$
The shear stiffness of the screwed connection between the notch hanger and the timber block, $k_s$	$1.86 \times 10^7$
Stiffness of shear connector, $k_c$	Refer to Appendix A

The dimensions of the timber block area and the effective area for the joist hanger are illustrated in Figure 5-3 and were used to calculate the stiffness properties as shown in

Table 5-1. The calculation procedures are described below:

(i) Joist stiffness,  $k_j$

$$k_j = \frac{E_{j\perp} A_j}{\frac{2}{3} h} ; \quad (5-1)$$

$$= \frac{\frac{12700}{30} \times ((75 + 47) \times 45)}{\frac{2}{3(150)}}$$

$$= 23 \text{ N/mm};$$

(ii) Joist hanger (screws) stiffness,  $k_s$

$$k_s = \frac{nP}{\delta}; \quad (5-2)$$

from NZS 3603:1993 clause 4.2 and 4.3, the slip deflection could be calculated from Equation 5.

$$\delta = \frac{k_{37}(0.8)P^2}{Q_n^2} \quad (5-3)$$

where;

$k_{37}$  = 1 (from Table E1)

P = applied nail load

= 500 N

$Q_n^2$  = nominal strength for a single nail with short term loading

= 860.3 N

Thus,

$$\delta = \frac{1(0.8)(500)^2}{(860.3)^2}$$

$$= 0.043$$

and

$$k_s = \frac{500/4}{0.043};$$

= 4.7 kN/mm (for one screw)

= 4.7 x 4 = 18.8 kN/mm (for four screws)

Based on these modelling properties and elements, the FE modelling of the reduced-scale specimens, namely: (1) multi-span specimens, (2) multi-storey specimens, (3) single-bay T-joist floor and (4) 2-storey, 2-bay T-joist floor, was carried out.

## 5.1 Multi-span specimens

The predicted natural frequencies of the multi-span specimens are given in Table 5-2. The natural frequencies for each specimen were determined over the range from the first mode natural frequency (i.e 18 Hz) to a maximum natural frequency of about 90 Hz, depending on the mode behaviour of each specimen. The natural frequencies for a 1-span LCC specimen are shown up to the third mode behaviour. However, for the 2-, 3- and 4-span LCC specimens, the natural frequencies were determined up to the 6<sup>th</sup>, 9<sup>th</sup> and 12<sup>th</sup> modes as depicted in Table 5-2.

Table 5-2 Prediction of natural frequency for multi-span specimens

Specimen	Mode 1, $f_1$ (Hz)	Mode 2, $f_2$ (Hz)	Mode 3, $f_3$ (Hz)	Mode 4, $f_4$ (Hz)	Mode 5, $f_5$ (Hz)	Mode 6, $f_6$ (Hz)	Mode 7, $f_7$ (Hz)	Mode 8, $f_8$ (Hz)	Mode 9, $f_9$ (Hz)	Mode 10, $f_{10}$ (Hz)	Mode 11, $f_{11}$ (Hz)	Mode 12, $f_{12}$ (Hz)
1- span	18.9	40.99	80.5	-	-	-	-	-	-	-	-	-
2- span	18.9	20.4	40.8	44.8	80.1	87.4	-	-	-	-	-	-
3- span	18.9	19.6	21.2	40.8	42.8	46.8	80.0	83.7	91.1	-	-	-
4- span	18.9	19.3	20.4	21.6	40.7	41.6	45.0	47.7	79.9	82.1	87.2	92.8

The fundamental natural frequencies from each specimen were 18.9 Hz for all specimens, as shown in Table 5-2. However, as the number of spans was increased, closer natural frequencies were obtained. This is because, for the multi-span flooring system that had identical properties for each span, the local mode frequencies of each span were very close (Pavic et.al, 2002). For a 2-span LCC specimen, two close local mode behaviours occurred at modes 1 and 2, modes 3 and 4, and modes 5 and 6.

Comparable behaviour occurred for 3- and 4-span LCC specimens. However, for a 3-span LCC specimen, three close local modes were determined and for the 4-span LCC specimen, four close local modes were predicted. Thus, the number of close local modes was proportional to the number of spans.

The mode shape behaviour of the multi-span specimens is illustrated from Figure 5-4 to Figure 5-9. Theoretically, the first mode behaviour shows a half-sine curve and the second mode shows a full-sine curve. The third and fourth modes have the shape of one and half sine curves and two full-sine curves, respectively. These particular shapes were also shown by the 1-span LCC specimen (refer to Figure 5-4).

The mode shape behaviours changed when the 1-span LCC specimens had an adjacent span. The local mode behaviour of each span dominated the global mode behaviour of the system for each mode. For a 2-span LCC specimen, the mode shape behaviour was a half-sine curve for modes 1 and 2, for each span. However, the position of the curves were different. For the first mode, span 1 showed a hogging shape while span 2 was sagging, and both spans had a hogging shape for the second mode. The full-sine curve appeared at the third and fourth modes. Both spans had similar properties, thus the mode shape behaviour was also comparable.

On the other hand, the 3- and 4-span LCC specimens showed different behaviour for the mode shapes. The fundamental natural frequencies of both specimens show that the mode shapes were almost similar for each span (refer to Figure 5-6 and Figure 5-8). However, at some points, either the inner span(s) or the outer spans dominated the global mode of the system. Figure 5-6 and Figure 5-7 show that the inner span for a 3-span LCC specimen governed the global mode at modes 3, 6 and 9 and the rest of the modes were dominated by the outer spans, except for mode 1. Referring to Figure 5-8 and Figure 5-9, the even numbered global modes were governed either by the inner spans or by the outer spans. The odd numbered global mode shapes show an almost similar curve deflection for each span, but in opposite deformation.

Mode	Span 1	Span 2	Span 3	Span 4
1	$f_1 = 18.9 \text{ Hz}$ 	-	-	-
2	$f_2 = 40.9 \text{ Hz}$ 	-	-	-
3	$f_3 = 80.5 \text{ Hz}$ 	-	-	-
4	$f_4 = 130.2 \text{ Hz}$ 	-	-	-

Figure 5-4 Natural frequency and mode shape for 1-span specimen

Mode	Span 1	Span 2	Span 3	Span 4
1	$f_1 = 18.9$ Hz 		-	-
2	$f_2 = 20.4$ Hz 		-	-
3	$f_3 = 40.8$ Hz 		-	-
4	$f_4 = 44.8$ Hz 		-	-
5	$f_5 = 80.1$ Hz 		-	-
6	$f_6 = 87.4$ Hz 		-	-

Figure 5-5 Natural frequency and mode shape for 2-span specimen

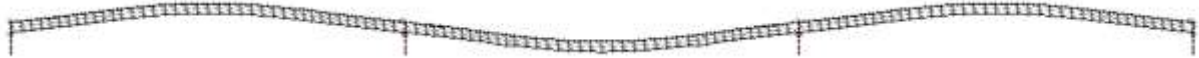
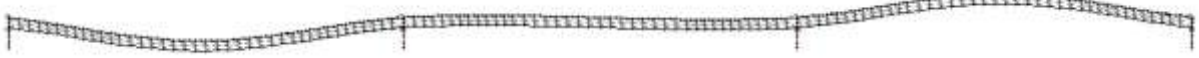
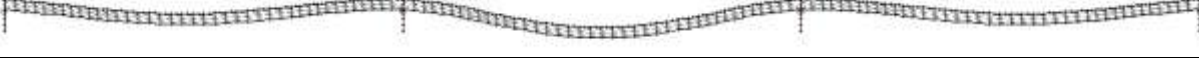
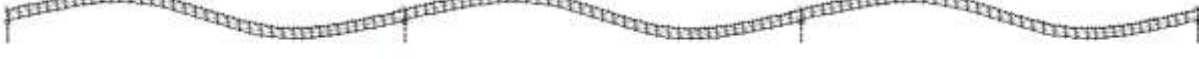
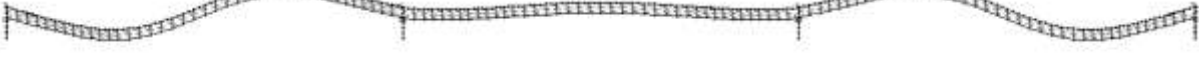
Mode	Span 1	Span 2	Span 3	Span 4
1	$f_1 = 18.8 \text{ Hz}$ 			-
2	$f_2 = 19.6 \text{ Hz}$ 			-
3	$f_3 = 21.2 \text{ Hz}$ 			-
4	$f_4 = 40.8 \text{ Hz}$ 			-
5	$f_5 = 42.8 \text{ Hz}$ 			-
6	$f_6 = 46.8 \text{ Hz}$ 			-

Figure 5-6 Natural frequency and mode shape for 3-span specimen

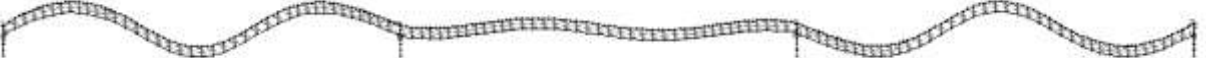
Mode	Span 1	Span 2	Span 3	Span 4
7	$f_7 = 79.9 \text{ Hz}$ 			-
8	$f_8 = 83.7 \text{ Hz}$ 			-
9	$f_9 = 91.1 \text{ Hz}$ 			-

Figure 5-7 Natural frequency and mode shape for 3-span specimen (cont.)

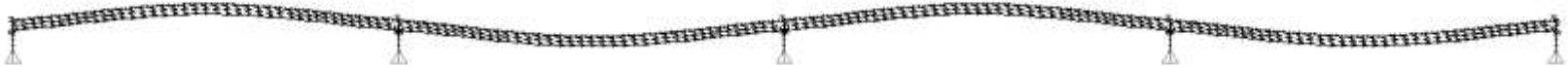
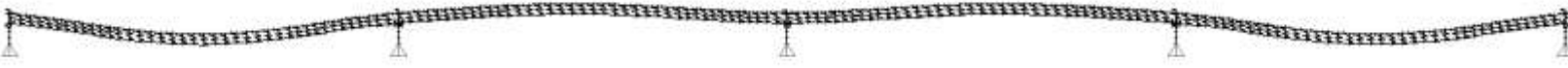
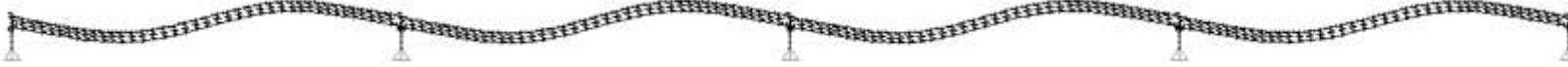
Mode	Span 1	Span 2	Span 3	Span 4
1	$f_1 = 18.9 \text{ Hz}$ 			
2	$f_2 = 18.3 \text{ Hz}$ 			
3	$f_3 = 20.4 \text{ Hz}$ 			
4	$f_4 = 21.6 \text{ Hz}$ 			
5	$f_5 = 40.7 \text{ Hz}$ 			
6	$f_6 = 42.0 \text{ Hz}$ 			

Figure 5-8 Natural frequency and mode shape for 4-span specimen

Mode	Span 1	Span 2	Span 3	Span 4
7	$f_7 = 45.0 \text{ Hz}$			
8	$f_8 = 47.7 \text{ Hz}$			
9	$f_9 = 79.9 \text{ Hz}$			
10	$f_{10} = 82.1 \text{ Hz}$			
11	$f_{11} = 87.2 \text{ Hz}$			
12	$f_{12} = 92.8 \text{ Hz}$			

Figure 5-9 Natural frequency and mode shape for 4-span specimen (cont')

## 5.2 Multi-storey specimens

The first six mode shapes and natural frequencies of a 2-storey specimen are depicted in Figure 5-10. The odd numbered global modes were dominated by the second storey behaviour, while the even numbered global modes were dominated by the first storey behaviour. The natural frequencies of the first two global modes were very close, due to identical members, as discussed previously.

Figure 5-11 shows the first nine modes of the 3-storey specimen. The first three mode natural frequencies were very close, namely 19.1 Hz, 22.0 Hz and 23.4 Hz for global modes 1, 2 and 3, respectively. The third storey behaviour dominated the local modes 1, 4 and 7. The remaining modes showed predominant first and second storey behaviour.

When the number of storey increased to 4 (see Figure 5-12), the behaviour of the specimens was different. The first five global modes were closely spaced at 19.2 Hz, 22.9 Hz, 23.0 Hz, 23.0 Hz and 24.2 Hz. The natural frequencies for the second five global modes were 41.9 Hz, 51.1 Hz, 51.3 Hz, 51.7 Hz and 56.0 Hz. Then, the third five global mode natural frequencies were determined as 82.7 Hz, 99.6 Hz, 99.6 Hz, 101.0 Hz and 110.0 Hz. The top storey dominated the local modes for modes 1, 6 and 11.

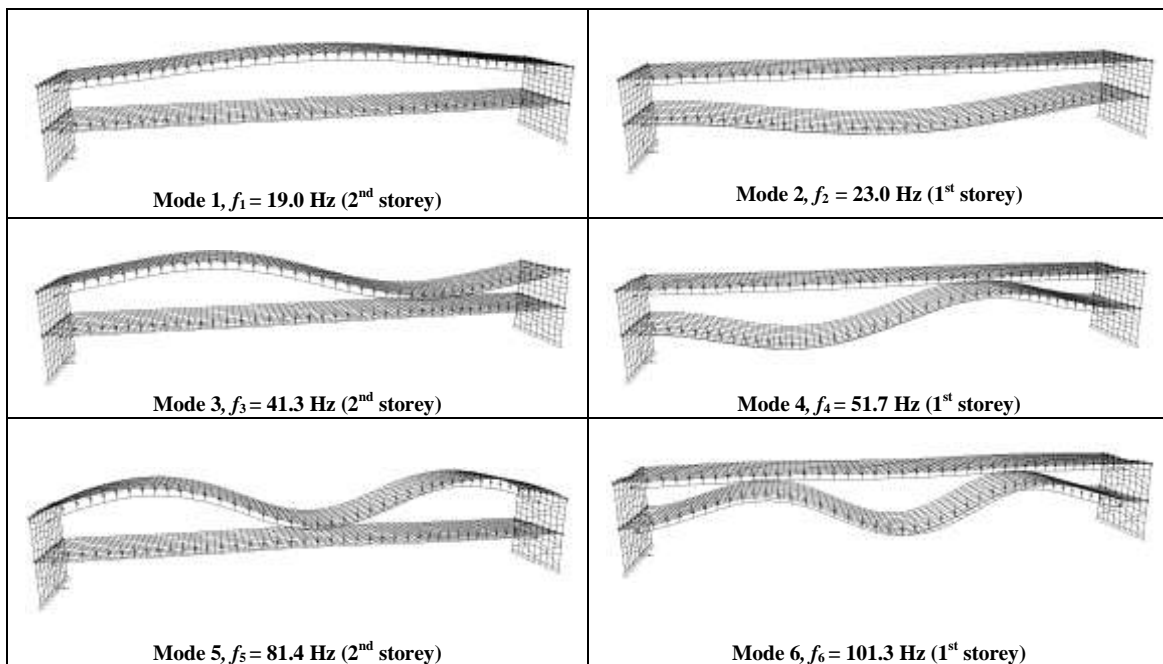


Figure 5-10 Natural frequencies and mode shapes for a 2-storey specimen

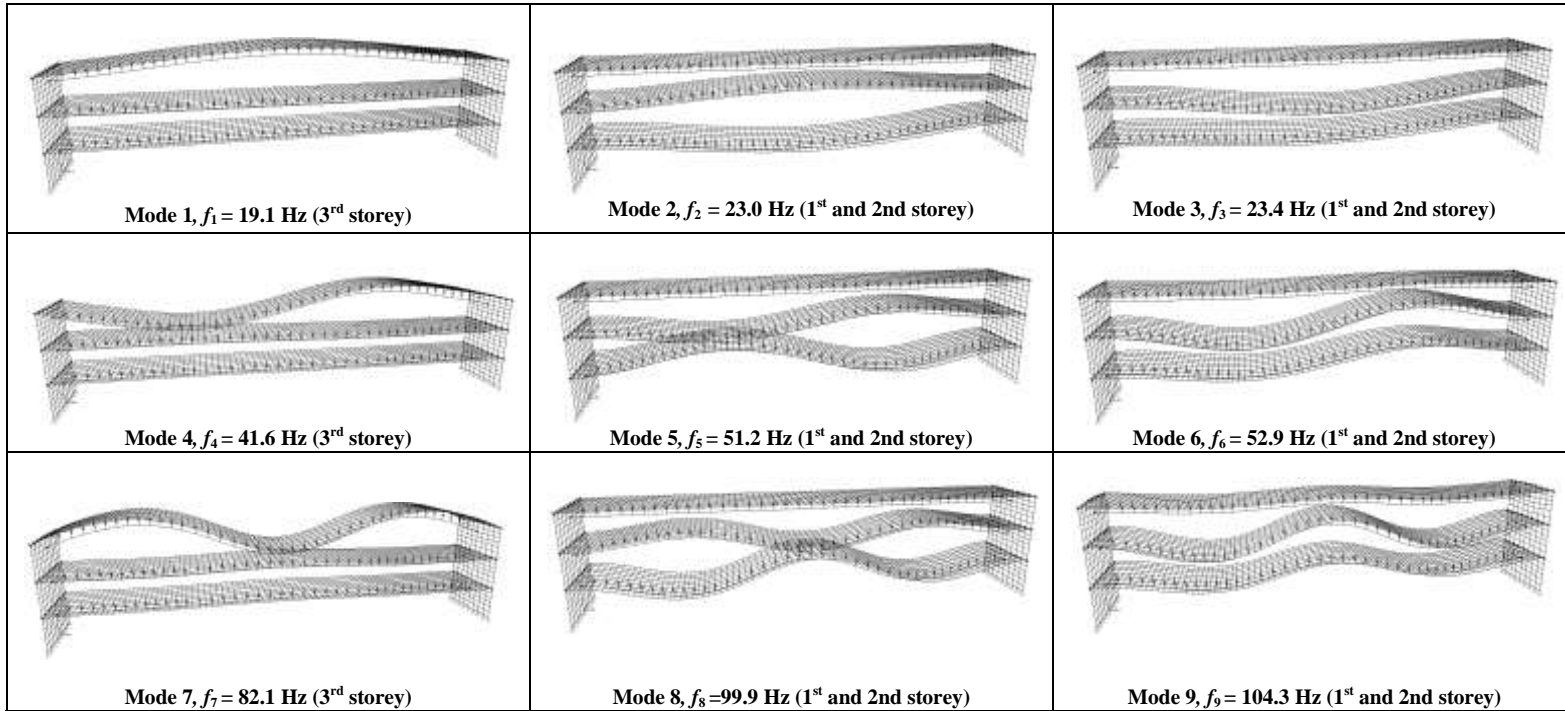


Figure 5-11 Natural frequencies and mode shapes for a 3-storey specimen

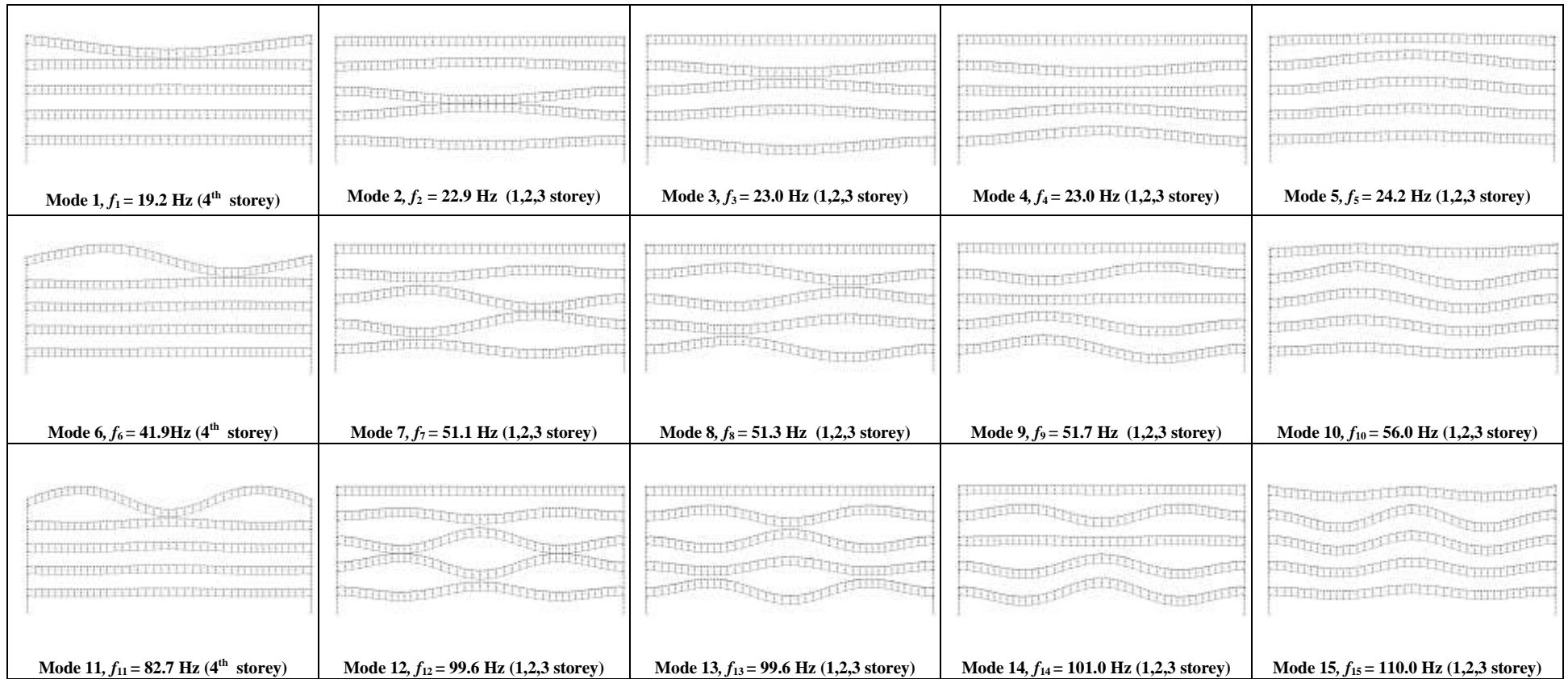


Figure 5-12 Natural frequencies and mode shapes for a 4-storey specimen

The investigation of the vibration behaviour of multi-span and multi-storey specimens continued using a reduced-scale 2-bay and 2-storey LCC specimen with the results illustrated in Figure 5-13. Figure 5-13 shows the first four mode shapes and natural frequencies of the specimen. The top floor behaviour dominates the first two modes and the first storey dominates the third and fourth mode behaviour.

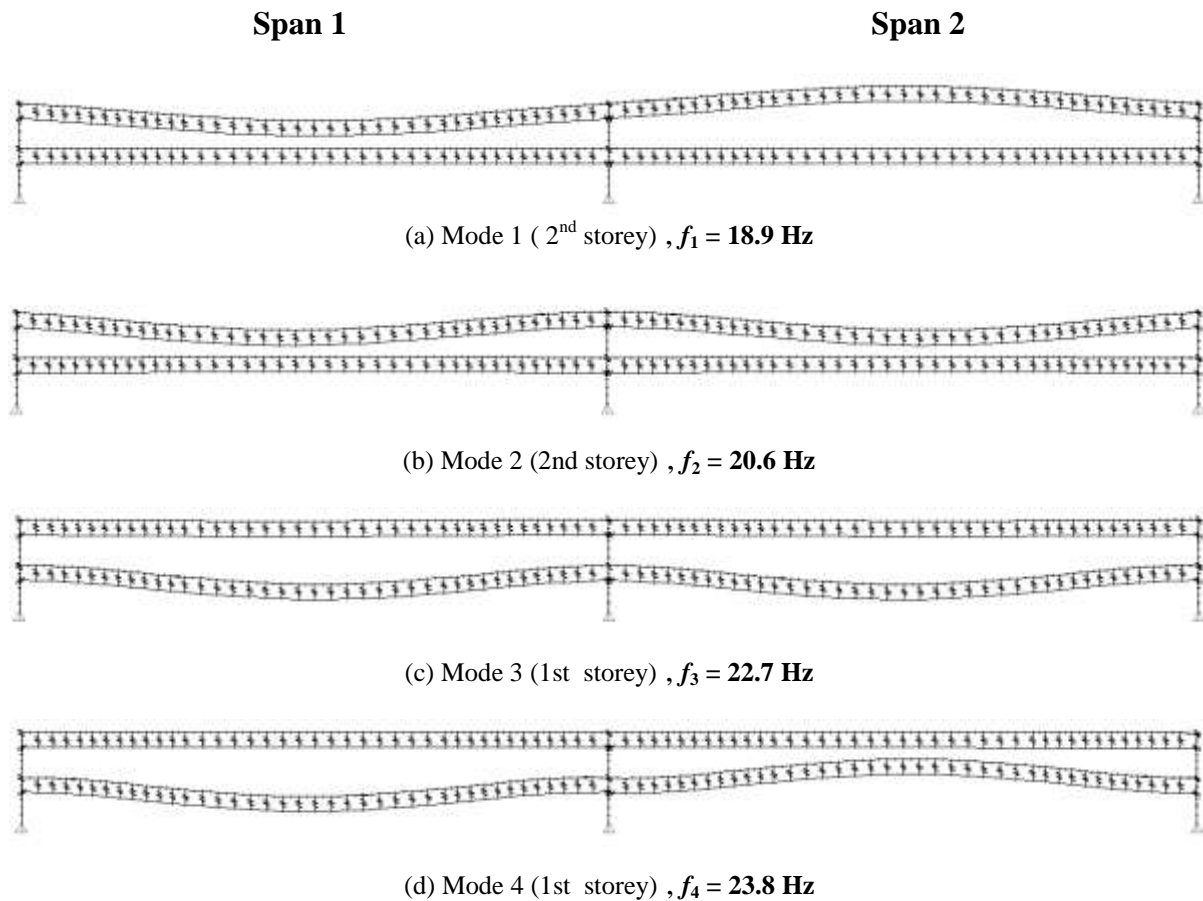


Figure 5-13 Mode shape behaviour for a 2-bay, 2-storey specimen

### 5.3 Single-bay T-joist floor

The mode shapes of a single-bay T-joist floor and the corresponding natural frequencies from mode 1 to mode 6 obtained by FEA, are shown in Figure 5-14. The associated mode shapes for the first natural frequency was the simple bending mode (refer to Figure 5-14 (a)) at 14.33 Hz. While the second and third natural frequencies are associated with full-sine mode shapes, which were transverse to the joists and the main beams, respectively, as illustrated in Figure 5-14 (b) and (c).

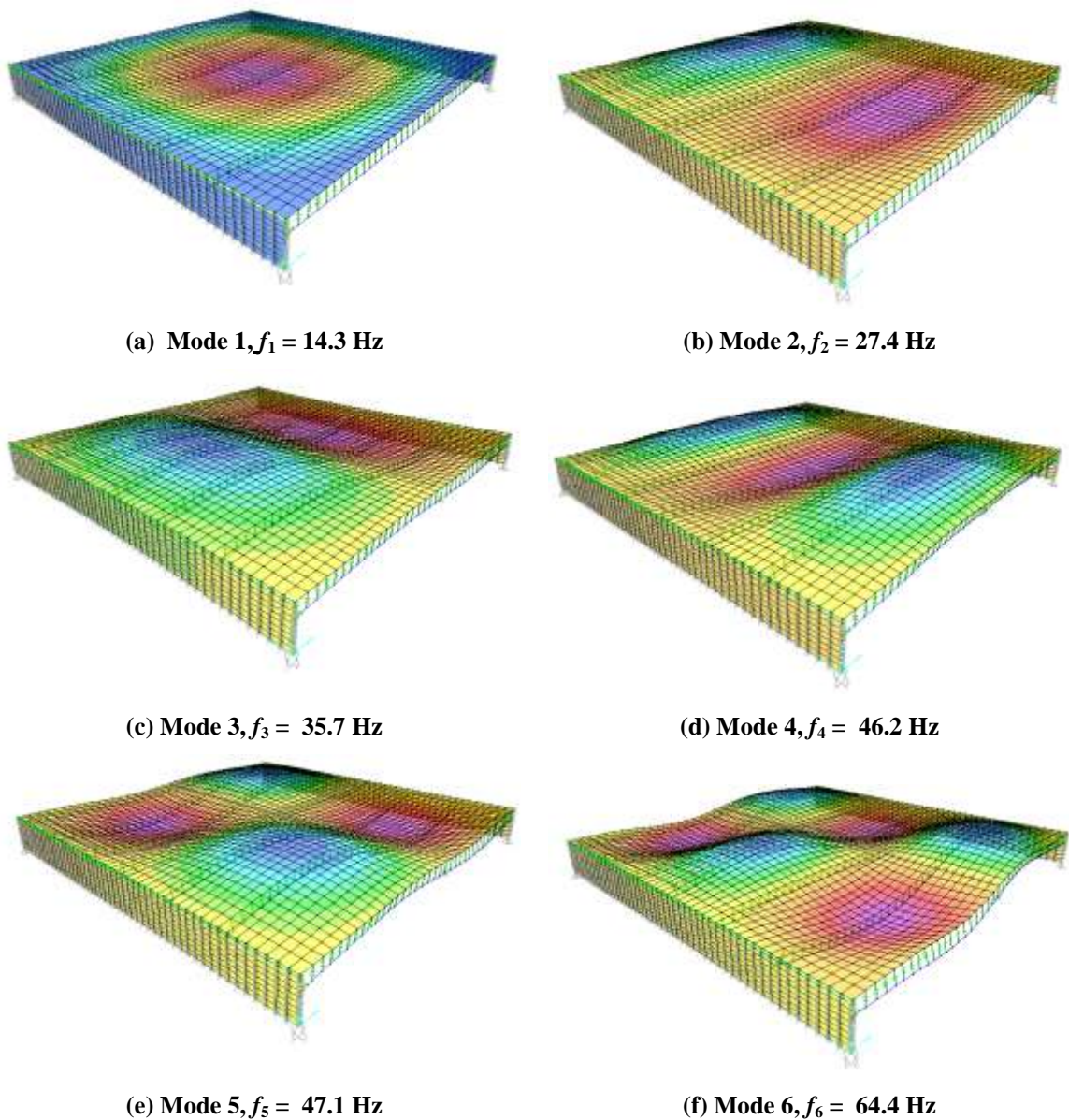


Figure 5-14 Natural frequencies and mode shapes for a single-bay 3 m x 3 m floor

## 5.4 Discussion

A series of EMA tests and FEA modelling were conducted to determine the modal parameters of reduced-scale LCC specimens and a floor, as discussed earlier in this chapter and chapter 4, including the vibration behaviour of the system. Here, the comparison between these two methods of investigation are elaborated.

The comparison of the fundamental natural frequencies from FEA and EMA results for reduced-scale specimens are illustrated in Table 5-3 for multi-span and multi-storey LCC specimens. The differences between the modelling and measured fundamental frequencies were not negligible with an error of about 11.7% to 27.9%, for the multi-span specimens. However, for the multi-storey specimens, the differences were close being 4.2% to 9.9% or 0.8 Hz to 1.9 Hz.

Table 5-3 Comparison of fundamental natural frequency,  $f_1$

Specimens	Fundamental natural frequency, $f_1$ (Hz)						
	1-span	2-span	3-span	4-span	2-storey	3-storey	4-storey
FEA	18.92	18.89	18.88	18.88	19.02	19.10	19.20
EMA	24.20	21.10	21.70	22.20	20.00	18.20	21.10
<b>Different (abs)</b>	<b>5.28</b>	<b>2.21</b>	<b>2.80</b>	<b>3.32</b>	<b>0.80</b>	<b>0.90</b>	<b>1.90</b>
<b>Error %</b>	<b>27.91</b>	<b>11.70</b>	<b>14.83</b>	<b>17.58</b>	<b>4.20</b>	<b>4.71</b>	<b>9.89</b>

Table 5-4 shows that the differences between the FEA and EMA fundamental natural frequencies for a single-bay LCC floor were very close with an error of only 0.37 Hz or 2.6 %. The frequency for mode 2 was under predicted by 1.94 Hz or 7.1 % and mode 3 was over-predicted by 1.75 Hz or 3.8 %.

Table 5-4 Comparison of the natural frequencies of a single-bay LCC floor

Specimen		$(f_1, \text{Hz})$	$(f_2, \text{Hz})$	$(f_3, \text{Hz})$
Single-bay T-joist floor	FEA	14.33	27.36	46.15
	EMA	14.70	29.30	44.40
	<b>Different (abs)</b>	<b>0.37</b>	<b>1.94</b>	<b>1.75</b>
	<b>Error %</b>	<b>2.6</b>	<b>7.1</b>	<b>3.8</b>

When analysing the acceleration responses from the EMA, there were difficulties in determining the correct mode shape of the specimens, except for a 1-span LCC specimen. Close mode frequencies occurred that were difficult to recognise. The location of the shaker affected the vibration behaviour of the specimens. During the testing, the shaker was located only at the mid-span, thus some important data was probably missed, especially for the higher modes. Hence, only the fundamental natural frequencies of all specimens were determined easily. Additionally, there was noise from the machines and other instruments operating in the laboratory, as well as vehicle movements outside of the building that disturbed some readings.

On the other hand, the FEA modelling provided all the natural frequencies of the specimens. The close mode frequencies were determined and the vibration behaviour of the multi-span and multi-storey specimens was easily understood. The vibration energy transmitted between spans and storeys was significant.

The mode shapes calculate using by the FEA were compared with experimental measurements. The modal shapes of the reduced-scale specimens are illustrated in Figure 5-15 to Figure 5-17. The mode shapes of the specimens were very similar, but the amplitudes were different, depending on where the shaker was located. The FEA modelling shows more accurate shapes, which contain more detail than the vibration patterns obtained from EMA. The mode shapes of the EMA were generated from the acceleration response along the joist, whilst 3D modelling was used in FEA.

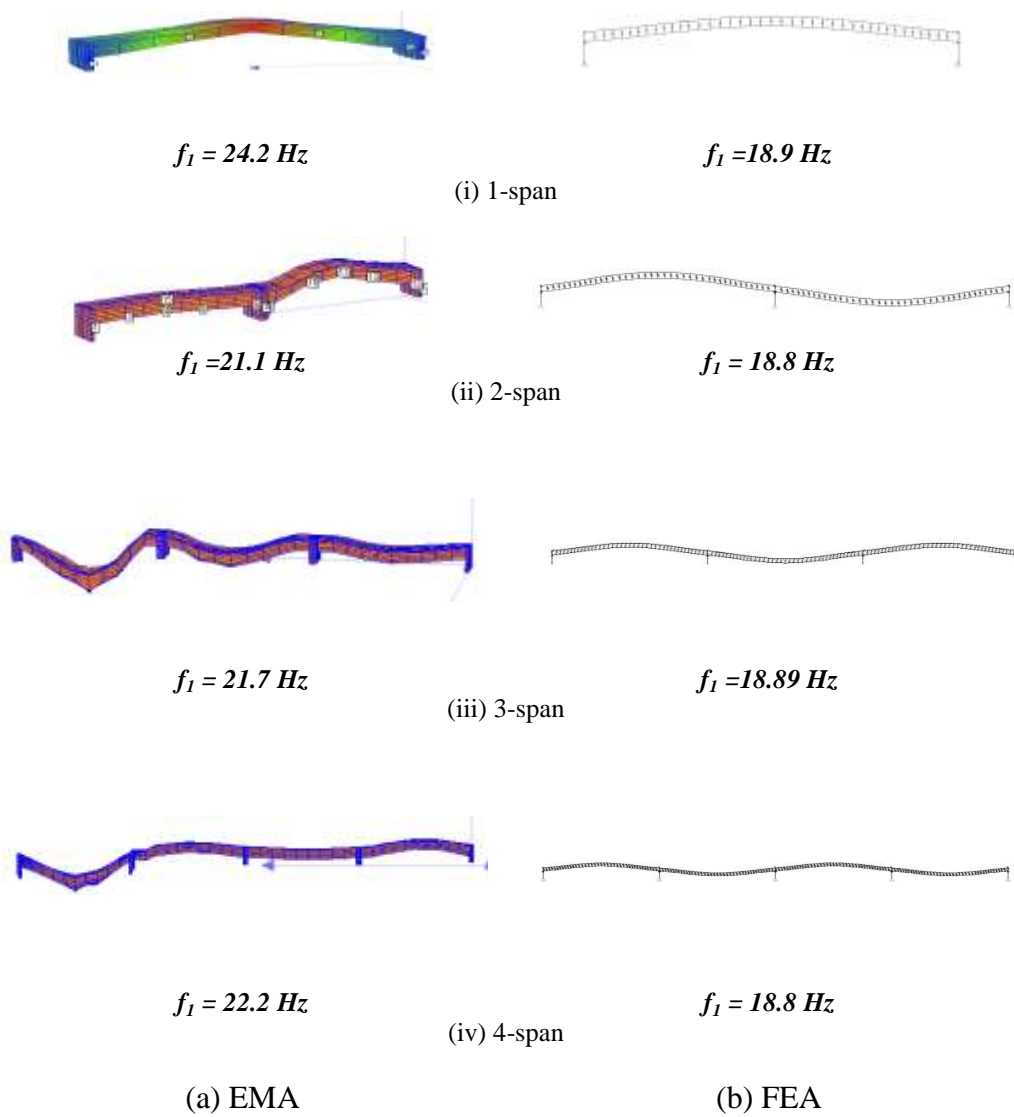


Figure 5-15 Comparative mode shapes for multi-span LCC specimens



$f_1 = 24.2 \text{ Hz}$



$f_1 = 18.9 \text{ Hz}$

(i) 1-storey



$f_1 = 21.1 \text{ Hz}$



$f_1 = 19.0 \text{ Hz}$

(ii) 2-storey



$f_1 = 21.7 \text{ Hz}$

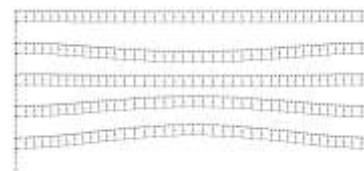


$f_1 = 19.1 \text{ Hz}$

(iii) 3-storey



$f_1 = 22.2 \text{ Hz}$



$f_1 = 23.0 \text{ Hz}$

(iv) 4-storey

(a) EMA

(b) FEA

Figure 5-16 Comparative mode shapes for multi-storey LCC specimens

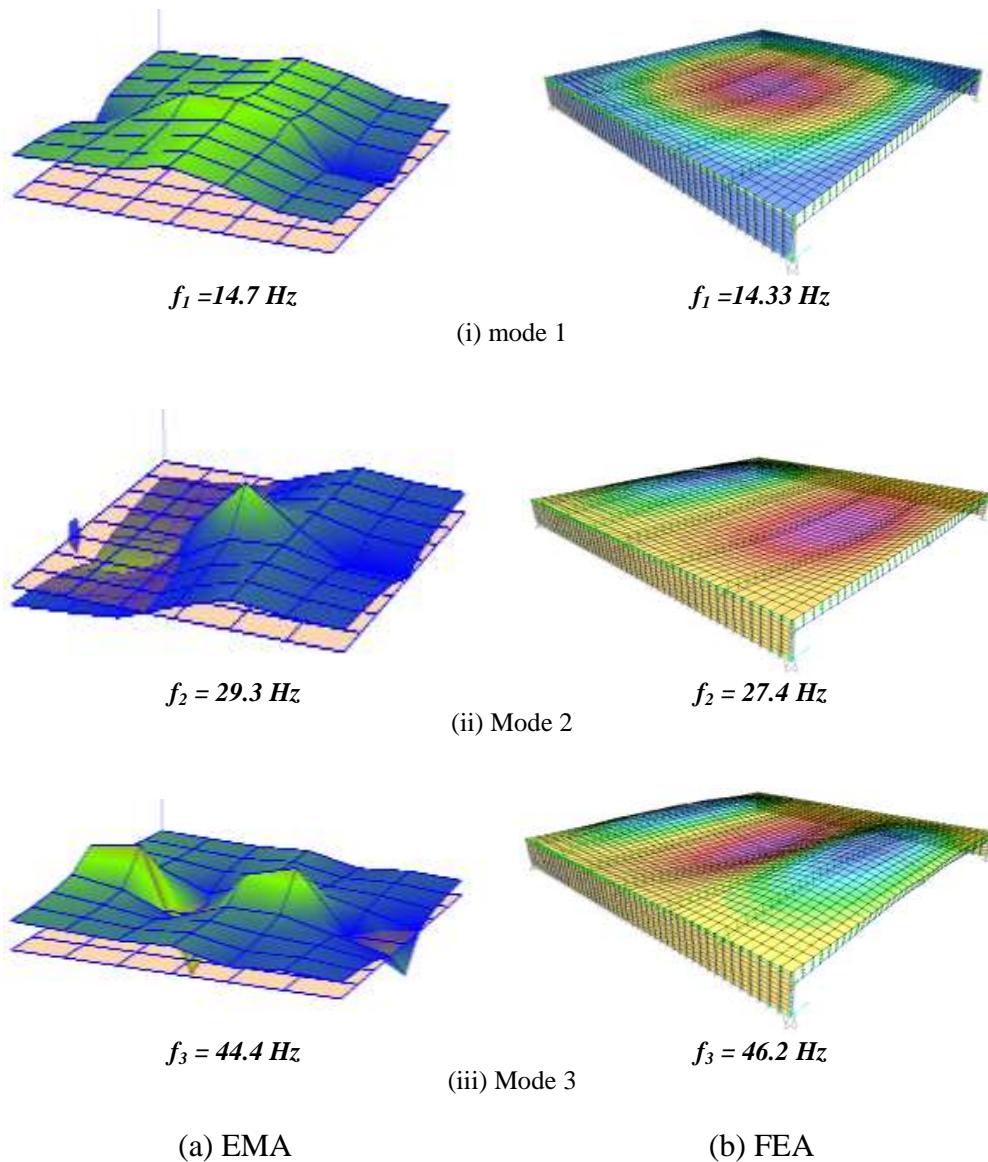


Figure 5-17 Comparative mode shapes for the single-bay LCC floor

## 5.5 Summary and Conclusions

The analytical modelling was performed to validate the experimental modal analysis (EMA) results using the modal analysis method in the SAP 2000 software package, for reduced-scale LCC T-joint specimens and floor. Only natural frequencies and mode shape were determined during the modal analysis. The vibration behaviour of the specimens and floor were more easily understood compared to the EMA, due to the effect of close mode frequencies.

The modal analysis showed local mode frequencies were very close and the number of close local modes was proportional to the number of spans due to the

identical properties for each span and storey. For multi-storey specimens, the top storey dominated the 1<sup>st</sup> mode behaviour since the sources of the excitation, the shaker was located at the top storey.

The differences between natural frequencies of multi-span and multi-storey specimens from EMA and FEA results were fairly high, especially for mode 1. A big percentage error was determined resulting from close mode natural frequencies which were difficult to isolate from the EMA data. By contrast, the FEA provided all natural frequencies of the specimens. However, the comparisons for the single-bay LCC floor were close due to the floor being only single-span and with no close mode effects.

The main conclusions from FE modelling of reduced-scale LCC T-joint specimens and floor can be summarised as follows:

1. There is a slight trend for the natural frequencies of the isolated components to decrease when they form part of a structural system.
2. Where two nominally identical floors make up either a two storey building or a two span beam, close mode natural frequencies occur.
3. A varying level of vibration transmission between two floors, having close mode natural frequencies has been identified.
4. Many of the mode shapes clearly show a discontinuity at the supports, which suggested the span responses are possible less influenced by adjacent span than they would be if the beams were continuous across the spans.
5. While the multi-span and multi-storey systems had slightly lower natural frequencies than the frequencies of the isolated components, this was not as significant as it was for the single-bay floor.
6. Conversely, there is still adequate connectivity for energy to be transmitted to distant spans (both vertical and horizontally) and cause sympathetic resonance.

## **CHAPTER 6      ANALYTICAL MODELLING OF FULL-SCALE T-JOIST LCC FLOOR**

This chapter discusses the analytical modelling of a full-scale T-joist LCC floor. The full-scale T-joist LCC floor model was an enlarged model based on the reduced-scale LCC specimens which were tested and modelled earlier (refer to Chapter 5). Due to limitations of space and time, the full-scale T-joist LCC floor could not be constructed. However, the reduced-scale LCC model was verified with the electrodynamic shaker test as discussed in Chapters 4 and 5.

The purpose of this chapter is to predict the vibration parameters and behaviour of the full-scale flooring system. The discussion also includes the influences of concrete topping thickness, LVL joist depth, stiffness of shear connector, and the boundary conditions on the vibration behaviour of a full-scale T-joist LCC floor. In addition, the full-scale floor was checked using the established design guide (CEN, 2004b) to make sure the floor would satisfy the serviceability limit state.

### **6.1 8 m x 7.8 m T-joist LCC floor model**

The full-scale T-joist LCC floor was modeled using the SAP 2000 software package, to determine the vibration behaviour. The full-scale model was implemented from the reduced-scale model (refer to Chapter 5), including the material cross-section and properties. The full-scale T-joist LCC floor was modeled up to an 8 m span length and 7.8 m width, using six (6) notched connectors located along the joist, as illustrated in Figure 6-1. The properties of the connectors were as discussed in Chapter 5.

Initially, a floor strip of 8 m x 0.6 m was implemented in the SAP 2000 software package, refer to Figure 6-1 . Later, the strip was expanded 13 times to build an 8 m x 7.8 m T-joist LCC floor, as illustrated in Figure 6-2. Since the concrete topping breadth of the strip was 0.6 m, it was not possible to model a square 8 m LCC floor.

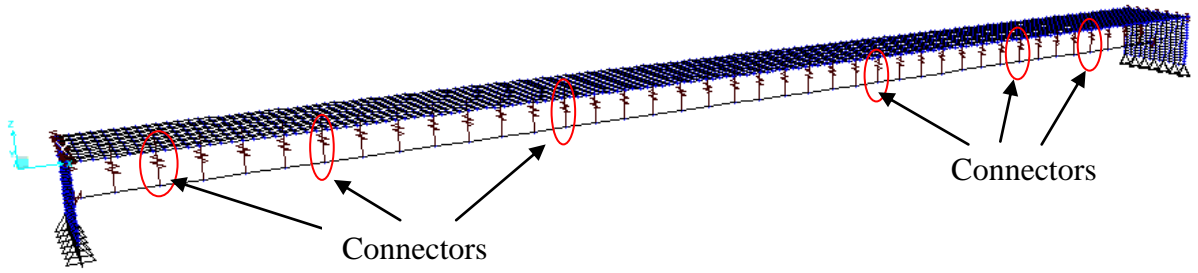


Figure 6-1 FE model of a floor strip of 8 m x 0.6

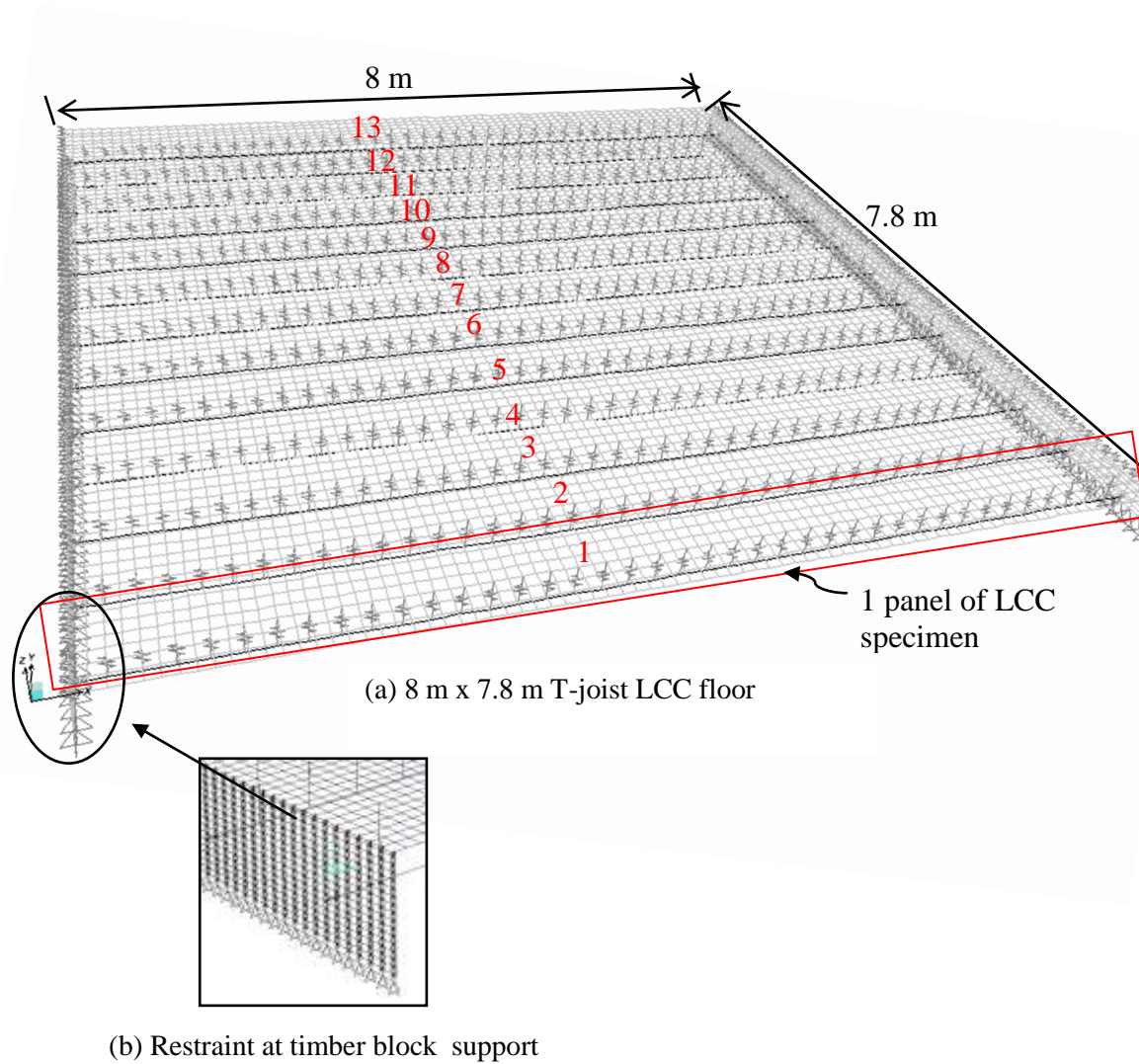


Figure 6-2 The model of an 8 m x 7.8 m T-joist LCC floor

The mesh size is one of the important parameters in the finite element modelling. To select an accurate size of mesh, the model needed to be run several times until the results converged to the same value of the natural frequency. The analyses were started from the bigger size to the smaller size of the mesh. The mesh ratio size (b/d) was kept lower than two (2). It is important to have a sufficiently dense mesh to ensure accuracy of the results at the same time. However, the number of elements should not be too large, to reduce computational time when carrying out the analyses. Thus, the mesh size that was selected based on the number of nodes in this study, as shown in Figure 6-3. The number selected from Figure 6-3 was for a one strip of LCC floor. Thus, for the complete LCC floor, the number of nodes used was  $121 \times 13 = 1573$ .

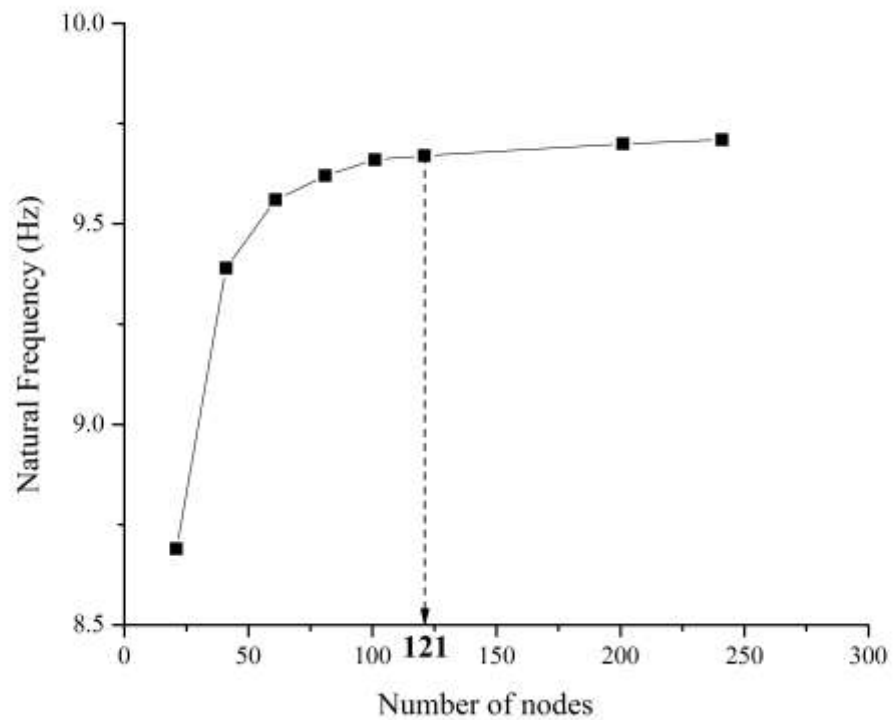


Figure 6-3 Natural frequency vs number of nodes for mesh size of the floor strip

During the analysis, a local mode behaviour was found, especially on the timber block supports. The local mode behaviour appears in the results, especially at high frequencies, and the results with local mode behaviour were eliminated. However, in some cases, the local mode behaviour on the timber blocks emerged at low frequencies. To eliminate the local mode behaviour, the timber block support model was restrained in translation in the x-direction (parallel to the joist axes), and in rotation

about the y- and z-axes. In the real situation, the timber blocks represent a main beam in the structure and have higher strength and stiffness compared to the LVL joist.

## 6.2 8 m x 7.8 m T-joist LCC floor behaviour

Four different types of support condition were selected to study the behaviour of the LCC floor system, as illustrated in Figure 6-4 and as listed below.

- (a) **B1** : fixed support at each end.
- (b) **B2** : restraint along the joist edge and fixed support at each end
- (c) **B3** : restraint along the joist edge
- (d) **B4** : restraint along four edges.

The support systems in this model were replicated as closely as possible to the supports in real conditions. The timber block, which acts as a beam, was modeled with the Young's modulus of the LVL ( $E_{LVL}$ ) applied parallel to the grain, to allow for the flexibility of the timber block.

Furthermore, during the analysis, the local mode behaviour of the timber block was pointed out, especially on the LCC floor with B1 support system (refer to Figure 6-4 (a)), not in global flooring system. In this study, only the global mode behaviour was of interest. However, the local mode behaviour influences the overall behaviour of the floor, which in this case, decreased the natural frequency.

Thus, fixed support was applied at each ends together with restraints at both edges of concrete topping, as illustrated in Figure 6-4 (b) known as B2 support system. This system was almost similar with actual situation. But, the local mode behaviour was detected as well although not as much as LCC floor with B1 support system.

Furthermore, the local mode was reduced by restraint on all the four edges of the LCC floor, as shown in Figure 6-4 (d). This system also against the vertical displacement on either timber blocks or edge of the joists, but increased the stiffness of the LCC floor system. However, the local mode behaviour happens on the high

frequency. The B2 support system (refer to Figure 6-4 (c)) was selected to understand the LCC floor behaviour with two edges restrained support system.

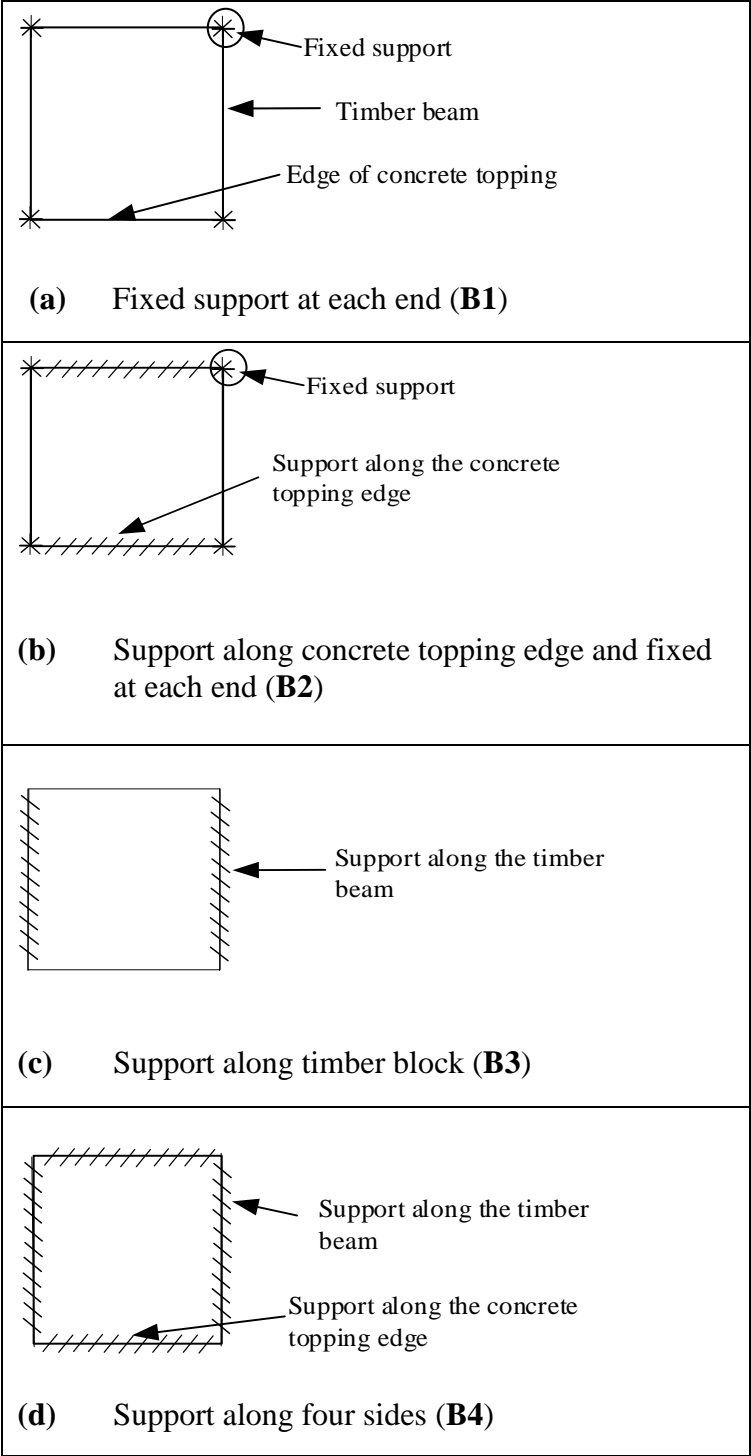


Figure 6-4 Different types of support system

Figure 6-5 illustrates the natural frequency for first six modes of the LCC floor with different types of support systems. From the overall results, the LCC floor with B4 support system presents the highest value of natural frequency for all modes, compared to other support systems. This is because restraint at all the edges increased the stiffness of the system and increased the natural frequency as well. Also related to this, the floor with B1 support system had the lowest value of natural frequency due to the diminished support stiffness.

However, the natural frequencies were close for modes 1 and 2, between 5.88 Hz to 9.12 Hz and 8.61 Hz to 11.28 Hz, respectively. At mode 3, the natural frequencies were close for except LCC floor with B4 system. The differences of the natural frequencies were large for higher mode frequencies.

The mode shapes of the LCC floor is illustrated in Figure 6-6 with different types of support systems. All the behaviour acted as a plate except for the LCC floor with B3 support system, which acted as a beam. It is because all the three support systems, B1, B2 and B4 have a restraint at each end and for B2 only restraint along the timber joist.

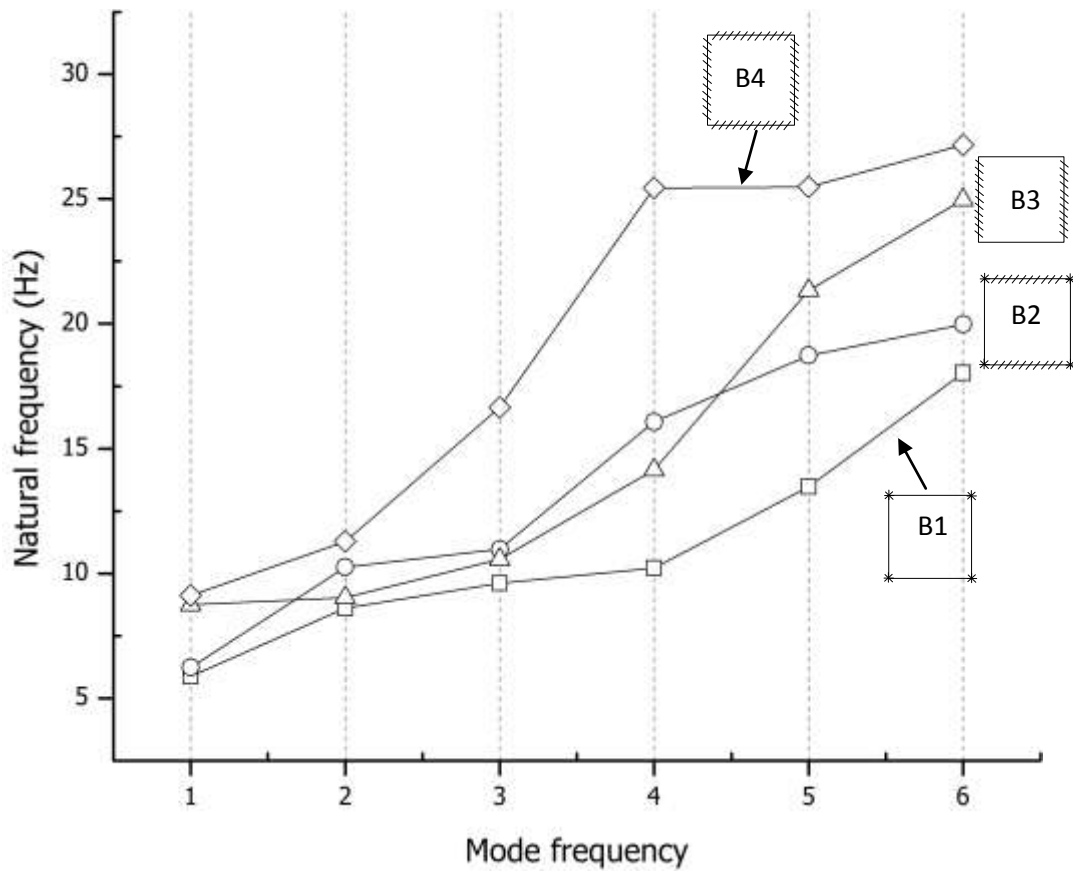


Figure 6-5 Natural frequency of different types of support systems

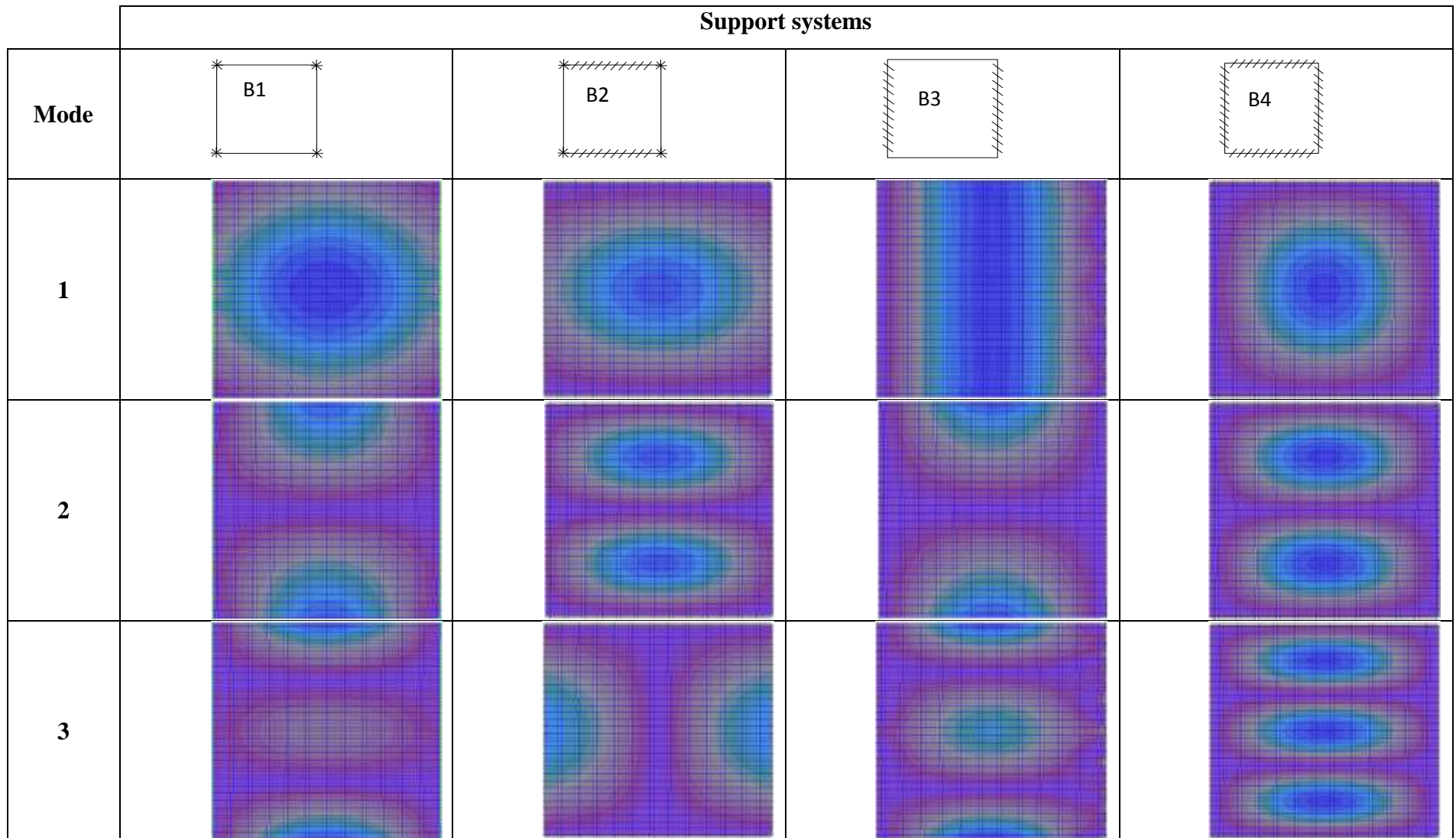


Figure 6-6 Mode shapes of LCC floor with different types of support system

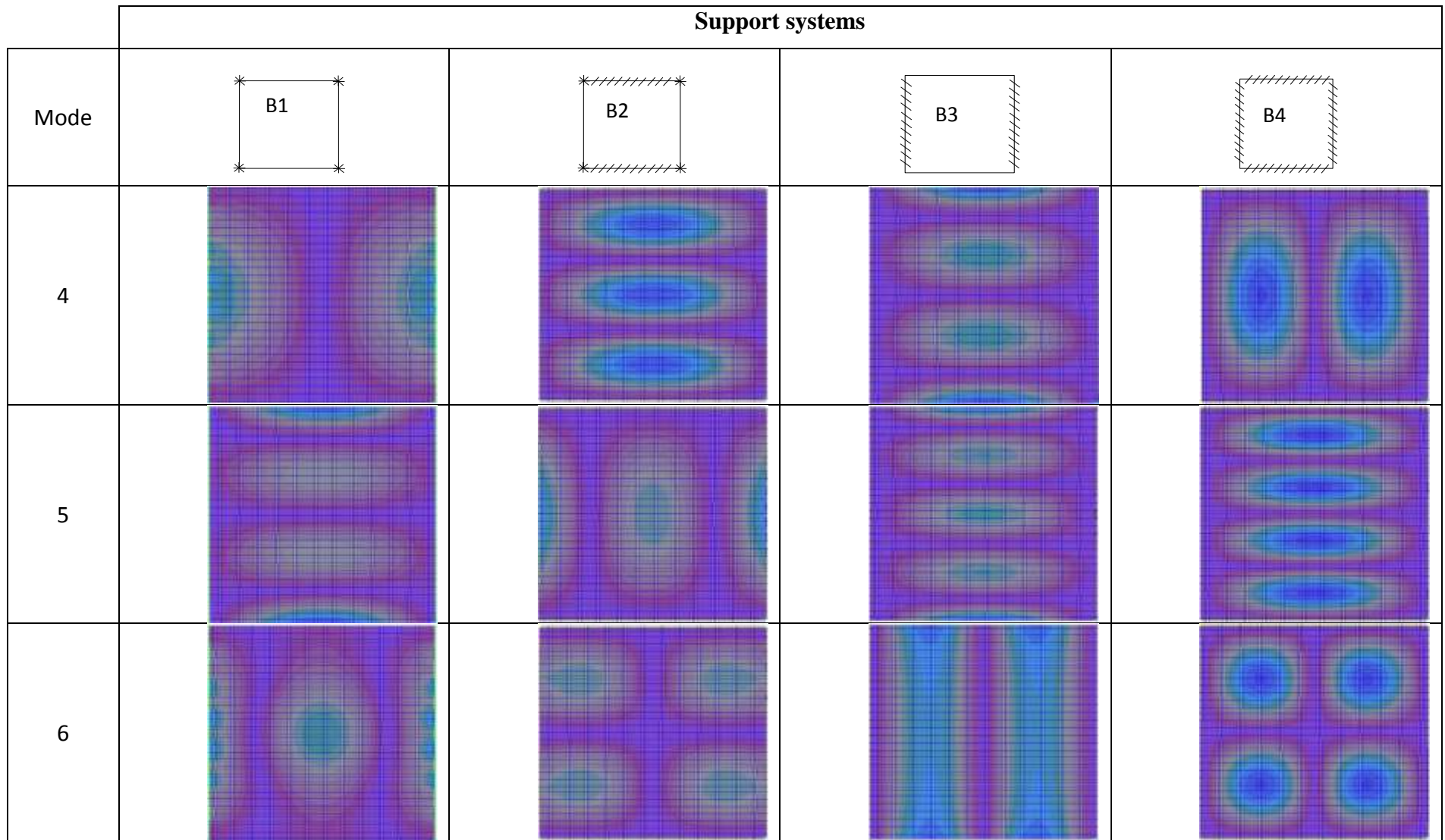
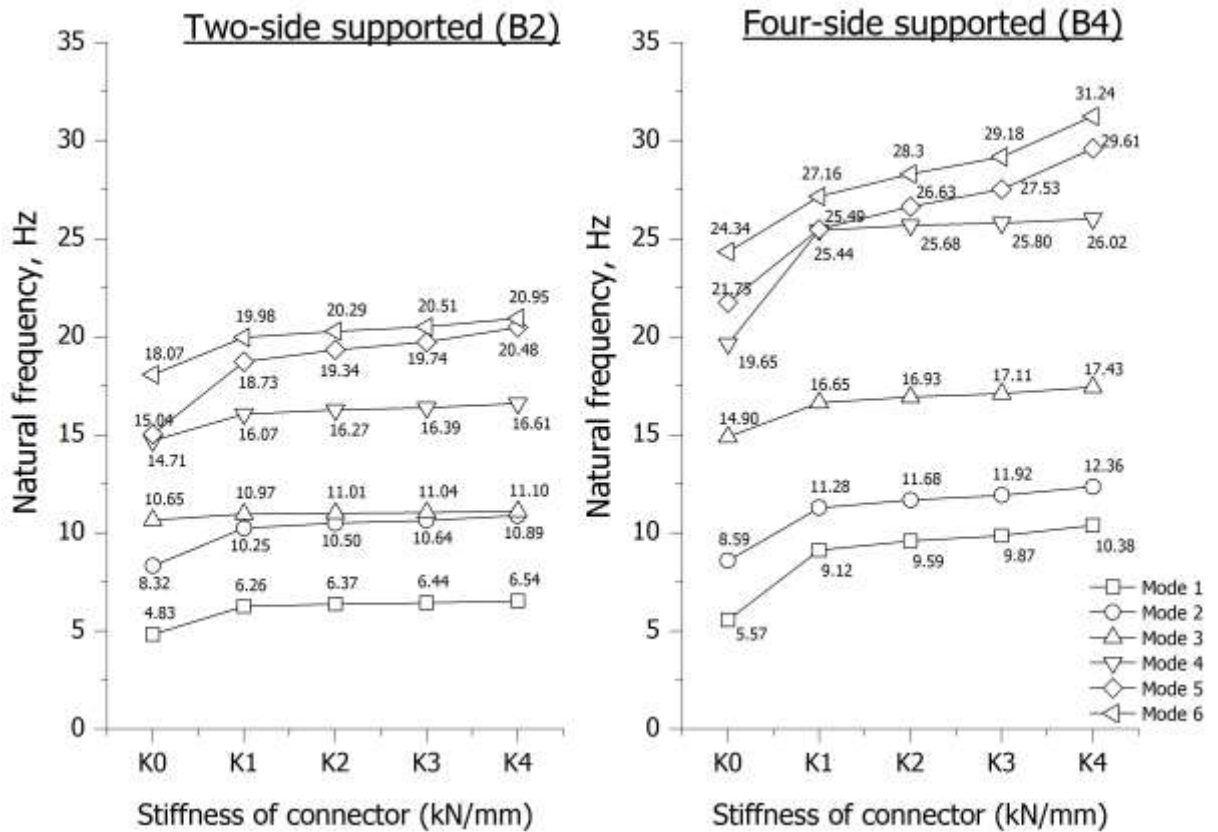


Figure 6-6 Mode shapes of LCC floor with different types of support system (continued)

### 6.3 Effect of connector stiffness

Figure 6-7 shows the first mode natural frequency of the full-scale LCC floor for five different types of connectors. Three connectors were selected as suggested by Yeoh (2010), with the stiffness of each connector being: (1)  $K_1 = 80.2$  kN/mm, (2)  $K_2 = 146$  kN/mm and (3)  $K_3 = 247$  kN/mm. Additionally two extra stiffnesses were added, of  $K_0 = 0$  kN/mm and  $K_4 = 10^8$  kN/mm to represent no slip and rigid stiffness connection of the LCC flooring system, respectively. The differences of the connector stiffnesses were generated between two types of support system, B2 and B4 (refer section 6.2 for details), with restraint on two side edges and restraint on four side edges, respectively.

Obviously, the flooring system with restraint on all the edges gave the higher value of natural frequency, with the increase of the floor stiffness. This behaviour was also applicable when the connector stiffness was changed. The natural frequency was rising with the increase of the connector stiffness. However, the differences are small for mode 1 until mode 4, except for the  $K_0$  connector stiffness. It seems clear that changing the stiffness of connectors did not greatly influence the vibration behaviour of the LCC floor especially for lower modes (from mode 1 until mode 4). In general however, the natural frequencies increased equivalent with the connector stiffness. The behaviour was changed for the higher modes, 5 and 6, as the domination of the higher stiffnesses were shown especially for the floor with B4 support system.



*Note : K0 = no slip,  
 K1,K2 & K3 = according to Yeoh (2010),  
 K4 = rigid stiffener connector*

Figure 6-7 Comparison of natural frequency for different types of connector stiffness

#### 6.4 Effect of concrete topping thickness

The effect of the concrete topping thickness on the dynamic behaviour of LCC floors was studied with a range of between 25 mm to 200 mm, with 25 mm intervals and in addition the 65 mm thickness due to the proposed design by Yeoh (2010) (refer to Chapter 3). The size of LVL joist for this modelling was 400 mm x 63 mm.

Theoretically, the natural frequency is influenced by the mass and stiffness of the floor. The natural frequency was increased by a lower mass or a higher stiffness of the floor and the natural frequency was reduced with a higher mass and a less stiff floor as found by Mertens et al (2007), Rijal et al (2010), Skinner (2013) and Abd. Ghafar et al (2008). However, the behaviour of the LCC floor did not agree with the theory in certain cases as illustrated in Figure 6-8 and

Figure 6-10.

Figure 6-8 shows the first six modes of behaviour of LCC floor, with variation of concrete topping thickness and using only 400 mm LVL joist depth. For mode 1 behaviour, the natural frequency was reduced when concrete topping thickness was increased from 25 mm up to 75 mm. When the thickness of concrete topping was increased to 200 mm, the natural frequency was lifted up as depicted in Figure 6-8. This behaviour also applied for mode 2. On the other hand, the behaviour was changed for mode 3 until mode 6, where the trend was not as smooth as for mode 1 and mode 2,. Again, this behaviour is a result of the local mode behaviour at the timber support block.

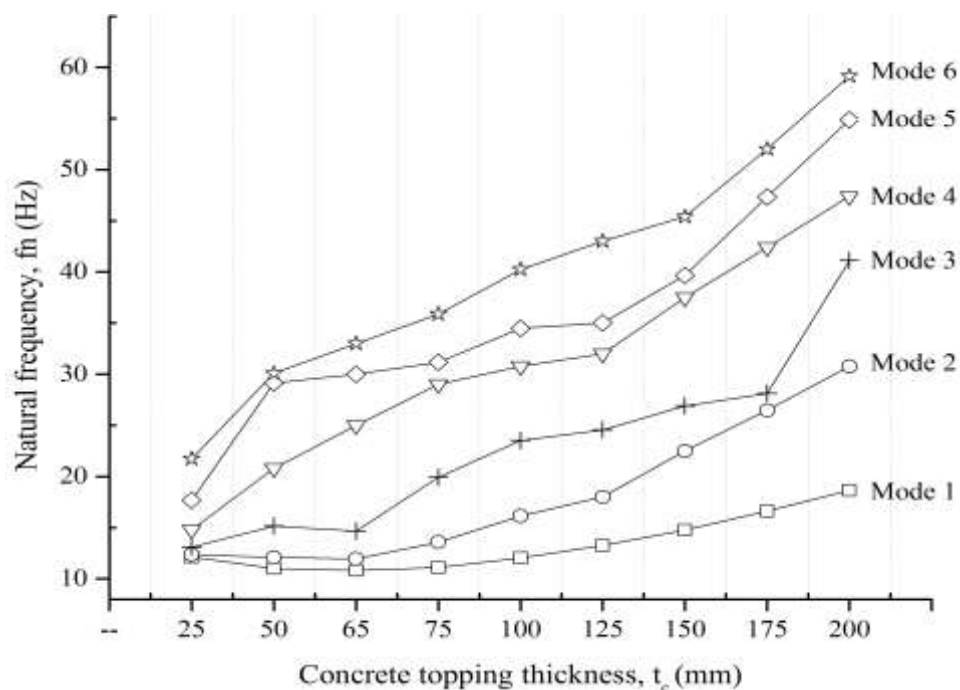


Figure 6-8 The first six modes of vibration with increasing concrete topping thickness

## 6.5 Effect of LVL joist depth

The size of LVL joist was used as manufactured by Carter Holt Harvey Wood products. The depths of the LVL considered were 150 mm, 170 mm, 200 mm, 240 mm, 300 mm, 360 mm and 400 mm with widths of 45 mm and 63 mm. However, in this research, 63 mm width LVL was used.

As mentioned before, the natural frequency was increased by a higher stiffness of the floor. By increasing the LVL depth, the natural frequency rose as well, as shown in Figure 6-9. This behaviour was true for mode 1 and mode 2 only. For higher modes, mode 3 to mode 6, the behaviour was changed due to the local mode of the timber block behaviour. For lower mode, mode 1 and mode 2, no local mode behaviour was detected. However, the mode behaviour with a local mode was ignored in this research.

The first mode natural frequency for LVL depth 150 mm was 6.02 Hz and the deeper LVL depth, 400 mm was 12.01 Hz. For the other types of LVL depth, 200 mm, 250 mm, 300 mm and 350 mm, the natural frequencies were 6.33 Hz, 6.85 Hz, 7.60 Hz, 8.82 Hz and 10.21 Hz, respectively. The percentage differences were increased from 5 % to 10 % comparing between LVL joist depths.

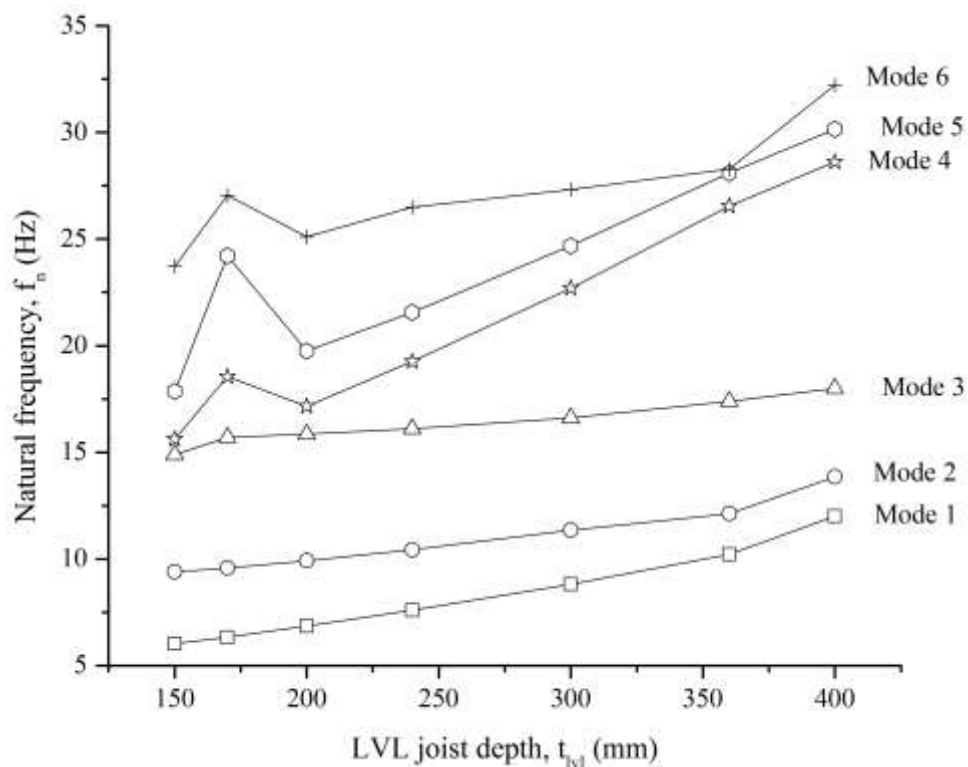


Figure 6-9 The first six modes of vibration with increasing depth of LVL joist

## 6.6 Relationship between concrete topping thickness and LVL joist depth

As shown in Figure 6-10, the vibration behaviour of the LCC floor was governed mainly by (1) mass and (2) stiffness, for linear elastic response. Furthermore, the damping ratio, support conditions and human occupancies also gave influences on the overall floor vibration behaviour. These results described the behaviour of mode 1 only. Figure 6-10 (a) and (b) show that the natural frequencies rose with increasing thickness of the concrete topping. However, when the LVL joist depth was varied from 150 mm to 200 mm, the behaviour was changed. The natural frequency decreased at the second point and rose up again at 65 mm of concrete topping thickness. In this case, vibration of the LCC floor system was governed by mass. This behaviour remained for the LCC floor with 240 mm and 300 mm depth of LVL joist. Later, for higher LVL joist depths, the natural frequency reduced at 25 mm to 75 mm of concrete topping thickness; refer to Figure 6-10 (c) to (e). And then, the natural frequency increased with the thickness of concrete topping as depicted in Figure 6-10 (f) and (g) when the LCC floor was dominated by stiffness of the system.

Figure 6-11 shows that the natural frequency generally increased linearly with the depth of the LVL. However, the differences between the natural frequencies were smaller when the concrete topping was thicker. This is probably due to the mass of the concrete which governed the behaviour of the LCC floor compared to the LVL joist. It indicates that the vibration behaviour of LCC was governed by the mass of the concrete topping and the stiffness of the LVL joist. For less deep LVL joists, the mass of the concrete controls the behaviour. But, when the depth of the LVL increased, at some point, the behaviour was dominated by the stiffness of the LVL. Probably, the composite action also affects the behaviour before the mass takes over the behaviour again.

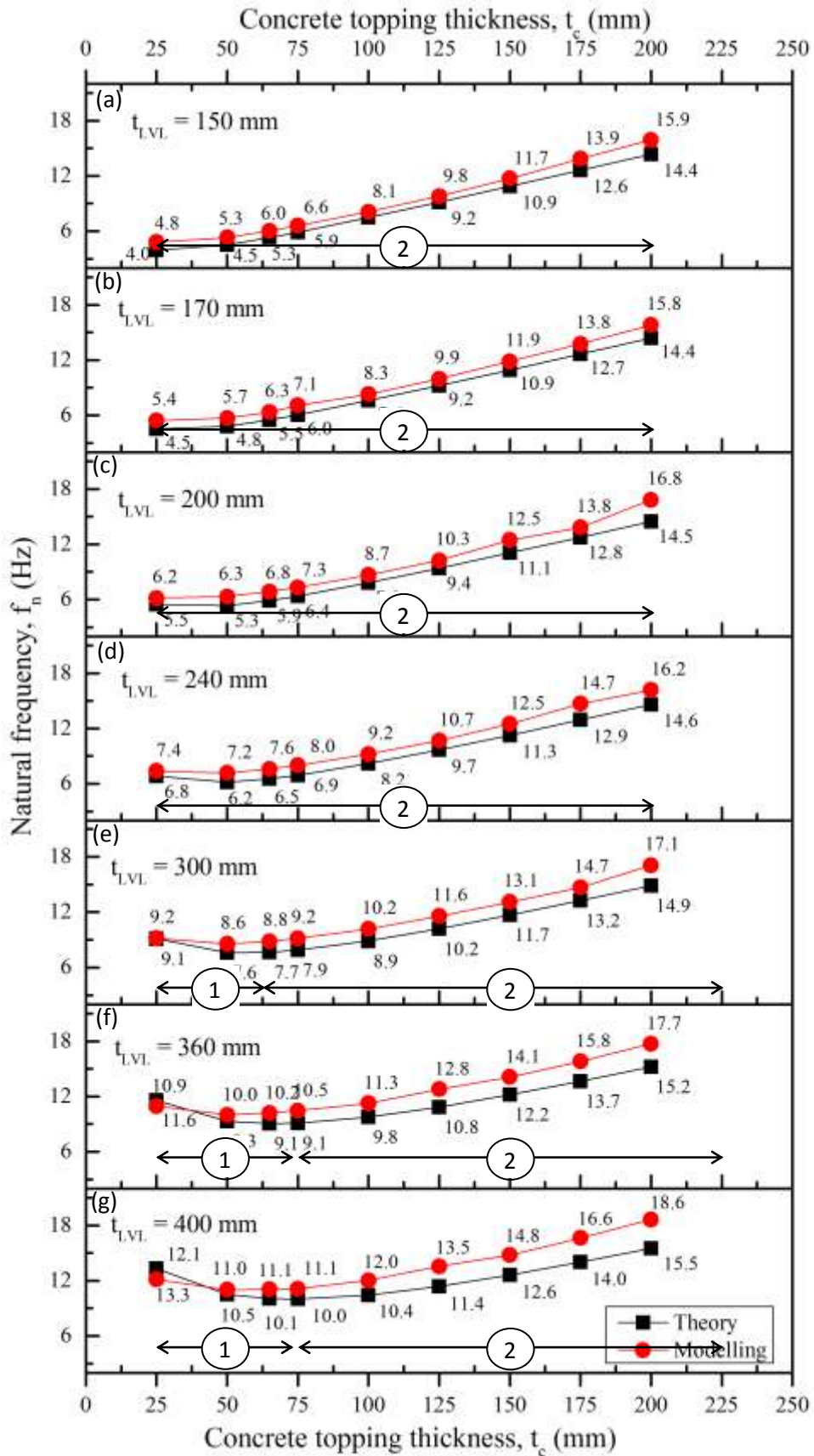
The results from analytical modelling were compared with theoretical calculations from Eurocode 5 (CEN, 2005) using the formula discussed in Chapter 2. The percentage difference between the two first mode natural frequencies for an 8 m x 7.8 m LCC floor with varying thickness of concrete topping and LVL joist depth is depicted in Table 6-2. The results show that the predicted behaviour was similar to the analytical modelling with the maximum percentage error about 21%. The pattern of the

natural frequency behaviour when increasing the concrete topping thickness or the LVL joist depth also agree with the behaviour from the analytical study. This shows that the analytical modelling results could be useful and acceptable.

Finally, recommendations can be made on the minimum concrete topping thickness for several categories of manufacturer standard sizes of LVL joist as tabulated in Table 6-1. For smaller LVL joists, between 150 mm to 240 mm depth, the minimum concrete topping thickness is 100 mm and for LVL joist from 300 mm to 400 mm depth, the minimum concrete topping is 65 mm. The suggestion was made based on the 8 Hz limitation of natural frequency as discussed in previous chapter.

Table 6-1 Limitation of concrete topping thickness for 8 m x 7.8 m LCC floor

<b>LVL joist (h x b) mm</b>	<b>Minimum concrete topping thickness (mm)</b>
150 x 63	100
170 x 63	
200 x 63	
240 x 63	
300 x 63	65
360 x 63	
400 x 63	



Note : The behaviour was governed by (1) mass or (2) stiffness

Figure 6-10 Comparison of natural frequencies for different concrete topping thickness

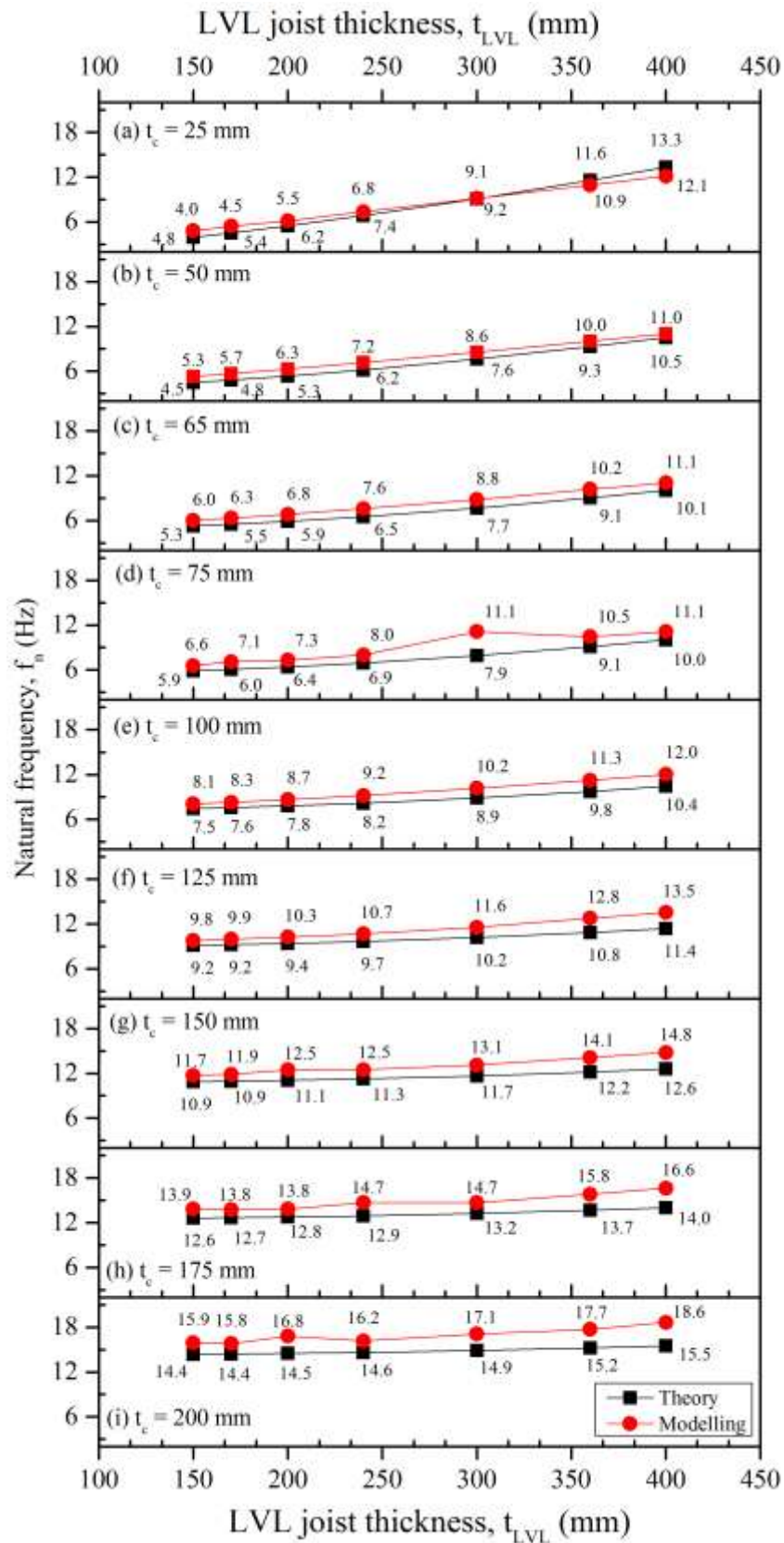


Figure 6-11 Comparison of natural frequencies for different LVL joist depths

Table 6-2 Percentage difference between SAP model and Eurocode 5 formula

LVL joist size (mm x mm)	Concrete thickness, $t_c$ (mm)	Fundamental natural frequency, $f_1$ (Hz)								
		25	50	65	75	100	125	150	175	200
150 x 63	SAP	4.81	5.31	6.02	6.58	8.09	9.78	11.72	13.85	15.9
	Euro 5	3.95	4.51	5.28	5.87	7.47	9.15	10.87	12.6	14.35
	<b>Different (abs)</b>	<b>0.86</b>	<b>0.8</b>	<b>0.74</b>	<b>0.71</b>	<b>0.62</b>	<b>0.63</b>	<b>0.85</b>	<b>1.25</b>	<b>1.55</b>
	<b>Error %</b>	<b>21.77</b>	<b>17.74</b>	<b>14.02</b>	<b>12.10</b>	<b>8.30</b>	<b>6.89</b>	<b>7.82</b>	<b>9.92</b>	<b>10.80</b>
170 x 63	SAP	5.43	5.69	6.33	7.09	8.29	9.95	11.86	13.76	15.81
	Euro 5	4.53	4.81	5.5	6.05	7.6	9.23	10.93	12.65	14.39
	<b>Different (abs)</b>	<b>0.9</b>	<b>0.88</b>	<b>0.83</b>	<b>1.04</b>	<b>0.69</b>	<b>0.72</b>	<b>0.93</b>	<b>1.11</b>	<b>1.42</b>
	<b>Error %</b>	<b>19.87</b>	<b>18.30</b>	<b>15.09</b>	<b>17.19</b>	<b>9.08</b>	<b>7.80</b>	<b>8.51</b>	<b>8.77</b>	<b>9.87</b>
200 x 63	SAP	6.15	6.31	6.85	7.31	8.65	10.3	12.46	13.82	16.81
	Euro 5	5.46	5.34	5.89	6.38	7.81	9.39	11.06	12.75	14.48
	<b>Different (abs)</b>	<b>0.69</b>	<b>0.97</b>	<b>0.96</b>	<b>0.93</b>	<b>0.84</b>	<b>0.91</b>	<b>1.4</b>	<b>1.07</b>	<b>2.33</b>
	<b>Error %</b>	<b>12.64</b>	<b>18.16</b>	<b>16.30</b>	<b>14.58</b>	<b>10.76</b>	<b>8.83</b>	<b>12.66</b>	<b>8.39</b>	<b>16.09</b>
240 x 63	SAP	7.37	7.16	7.60	8.00	9.21	10.67	12.5	14.68	16.17
	Euro 5	6.83	6.17	6.52	6.91	8.17	9.66	11.26	12.92	14.61
	<b>Different (abs)</b>	<b>0.54</b>	<b>0.99</b>	<b>1.08</b>	<b>1.09</b>	<b>1.04</b>	<b>1.01</b>	<b>1.24</b>	<b>1.76</b>	<b>1.56</b>
	<b>Error %</b>	<b>7.91</b>	<b>16.05</b>	<b>16.56</b>	<b>15.77</b>	<b>12.73</b>	<b>10.46</b>	<b>9.92</b>	<b>13.62</b>	<b>10.68</b>
300 x 63	SAP	9.16	8.55	8.82	11.14	10.17	11.56	13.1	14.67	17.09
	Euro 5	9.10	7.63	7.67	7.90	8.86	10.18	11.66	13.24	14.88
	<b>Different (abs)</b>	<b>0.06</b>	<b>0.92</b>	<b>1.15</b>	<b>3.24</b>	<b>1.31</b>	<b>1.38</b>	<b>1.44</b>	<b>1.43</b>	<b>2.21</b>
	<b>Error %</b>	<b>0.66</b>	<b>12.06</b>	<b>14.99</b>	<b>41.01</b>	<b>14.79</b>	<b>13.56</b>	<b>12.35</b>	<b>10.80</b>	<b>14.85</b>
360 x 63	SAP	10.95	10	10.21	10.46	11.26	12.8	14.11	15.81	17.72
	Euro 5	11.58	9.31	9.05	9.1	9.75	10.84	12.18	13.65	15.23
	<b>Different (abs)</b>	<b>0.63</b>	<b>0.69</b>	<b>1.16</b>	<b>1.36</b>	<b>1.51</b>	<b>1.96</b>	<b>1.93</b>	<b>2.16</b>	<b>2.49</b>
	<b>Error %</b>	<b>5.44</b>	<b>7.41</b>	<b>12.82</b>	<b>14.95</b>	<b>15.49</b>	<b>15.31</b>	<b>15.85</b>	<b>15.82</b>	<b>16.35</b>
400 x 63	SAP	12.12	11.00	11.1	11.12	12.03	13.5	14.77	16.62	18.63
	Euro 5	13.33	10.52	10.06	10.00	10.43	11.37	12.59	14	15.5
	<b>Different (abs)</b>	<b>1.21</b>	<b>0.48</b>	<b>1.04</b>	<b>1.12</b>	<b>1.6</b>	<b>2.13</b>	<b>2.18</b>	<b>2.62</b>	<b>3.13</b>
	<b>Error %</b>	<b>9.08</b>	<b>4.56</b>	<b>9.36</b>	<b>11.20</b>	<b>15.34</b>	<b>15.78</b>	<b>17.32</b>	<b>18.71</b>	<b>20.19</b>

## 6.7 Conclusion and Summary

A series of finite element modelling was carried out to analyse and understand the dynamic behaviour of the LCC flooring system. A few parameters were highlighted during the analysis including the thickness of concrete topping, the LVL joist depth and the stiffness of the connectors. As expected and discussed before, the higher stiffness increased the natural frequency of the system and the higher mass lowered the natural frequency.

Besides, local mode behaviour was found at the timber block supports, which reduced the natural frequency of the LCC floor. To reduce the effect of this local mode behaviour, all edges of the LCC floor should be restrained. However, too many restraints will increase the stiffness of the LCC floor system and this boundary condition should be applied carefully during the finite element analysis.

During the analysis, the vibration behaviour of the LCC floor was found to be governed by both stiffness and mass of LVL and concrete topping. When the concrete topping is increased, the stiffness of the LCC floor also increased due to (i) an increase in stiffness of the LCC floor with respect to the LVL only beam (which is a positive effect); and (ii) an increase in mass, due to the weight of the concrete (which is a negative effect in terms of vibration).

The limitation of concrete topping thickness and LVL joist depth was proposed in this chapter, especially for 8 m x 7.8 m LCC floor, based on the 8 Hz limitation of natural frequency. For the deeper LVL joists, from 300 mm to 400 mm depth, a minimum thickness of 65 mm is suggested. For smaller LVL joists between 150 mm to 240 mm depth, concrete topping with minimum thickness of 100 mm is recommended.

## CHAPTER 7      DESIGN FOR VIBRATION OF LVL- CONCRETE COMPOSITE (LCC) FLOORS

This chapter presents design guidance to estimate the dynamic behaviour of long span LCC floors, based on the 8 Hz limitation of fundamental natural frequency,  $f_1$ .

### 7.1      Introduction

The LVL-concrete composite (LCC) floor is one of the solutions for timber flooring systems. LVL is more flexible than steel and concrete, so the flexibility of the LVL causes large deflections if LVL is used with traditional timber floors which have long spans. Associated with this, the resonant frequency of the floor will decrease, and humans will feel uncomfortable if they can feel the vibration of the floor.

As discussed in Chapter 2, the traditional approach to verify the vibration limit has been to determine the deflection of the floor under 1 kN point load applied at midspan, and check that the deflection does not exceed 2 mm. However, due to design demand nowadays, which requires medium to long spans of floor, the natural frequency,  $f_n$  becomes more important. The limitation of  $f_n$  depends on the stiffness and mass of the flooring system.

Established standard design procedures (refer section 7.2) give guidance to estimate the fundamental natural frequency and recommend the limits that should be satisfied. This chapter provides some recommendation for the designer on the vibration limitation of long span LCC floors. The guidance includes both an advanced design method and a simple design method. The equations in the simple design method have been used to propose the recommended thickness of the concrete topping for different joist sizes of a LCC floor with a span of 8.0m.

## **7.2 Design criteria**

The design criteria have been discussed in detail in Chapter 2 (refer to 2.2.3). There are no specific requirements to classify floor behaviour exactly as comfortable or non-comfortable, because the vibration serviceability criterion is very subjective compared to limit state design for strength or deflection. However, lots of researchers have recommended a limitation of natural frequency, between 6 Hz to 10 Hz of fundamental natural frequency (Allen and Murray (1993), Ohlsson (1988), Wyatt (1989), Smith and Chui (1988), CEN (2004b), Pavic (2009) and Rijal (2013)). Thus, for this research, the 8 Hz fundamental natural frequency was preferred as a limitation of vibration serviceability for LCC floors.

## **7.3 Preliminary design**

### **I. Eurocode static design procedure**

The first step in any design will be to estimate the member sizes and the topping concrete thickness. The static design procedure from Eurocode 5 is recommended for this purpose.

### **II. Suggested concrete topping thickness**

Suggested values of the minimum concrete topping thickness are proposed below. The thickness is based on the standard sizes of LVL joists from manufacturers as illustrated in Table 7-1, but only applicable for 8 m spans. The minimum concrete topping thickness in Table 7-1 was obtained by using the finite element method in Section 7.4 and as discussed in Chapter 6. For a floor with a span of 8.0 m and a width of 7.8m. For LVL joist depth 150 mm to 240 mm with 63 mm breath, the minimum concrete thickness is 100 mm and for LVL joist depth 300 mm to 400 mm with 63 mm breath, the minimum concrete thickness is 65 mm. This is as a guide for designer to estimate the size of LCC floor accordingly to 8 Hz fundamental natural frequency of vibration serviceability limit. However, for different dimension of floor, the designer needs to design either by advanced design or simple design method as discussed in sections 7.4 and 7.5.

Table 7-1 Suggested topping thickness for LCC floors based on 8 Hz limitation

<b>LVL joist (h x b) mm</b>	<b>Minimum concrete topping thickness (mm)</b>
150 x 63	100
170 x 63	
200 x 63	
240 x 63	
300 x 63	65
360 x 63	
400 x 63	

#### **7.4 Advanced design method**

For the advanced design method, it is proposed to use finite element modelling (FEM) to determine the natural frequencies and mode shapes of the LCC floor. The FEM is useful particularly for complex structures. The use of finite element methods is the most suitable procedure to accurately assess the floor response and will give a better prediction than that given by the hand calculation method.

FEM is a numerical method, using several elements to create the structure and then analysis using the mathematical equations, with software aids. The SAP 2000 FEM that has been used in this research is similar to general FEM procedures, however some details need to be taken account of during the process. The advanced design method consist three major procedures as below:

##### **A. PRE-PROCESSING**

Pre-processing is the process to input all the data and to do the modelling of the structure into the SAP 2000 software package. No specific methodology is required, however a simple guideline as follow;

1. Insert the material properties

Generally, SAP 2000 requires input data for material properties as below;

For concrete:

- Modulus of Elasticity, E
- Poisson's ratio,  $\mu$
- Shear Modulus, G
- Weight per unit volume
- Mass per unit volume
- Compressive strength,  $f_c$

For LVL:

- Modulus of Elasticity, E in three directions ( $E_1$ ,  $E_2$  and  $E_3$ )
- Poisson's ratio,  $\mu$  for three planes ( $\mu_{12}$ ,  $\mu_{13}$ ,  $\mu_{23}$ )
- Shear Modulus, G for three planes ( $G_{12}$ ,  $G_{13}$  and  $G_{23}$ )
- Weight per unit volume
- Mass per unit volume

Note that a local coordinate system for LVL as orthotropic material is defined where Direction 1 is parallel to the grain, while Directions 2 and 3 are perpendicular to the grain.

2. Insert the section properties

The estimation of the dimension of the concrete topping and the LVL joists should be determined through the static design procedure, as proposed in Eurocode 5.

Insert the geometry of the structure. See Section 3.5 for more detailed advice on elements and masses in the finite element model.

- The concrete topping should be modelled as shell elements
- The LVL joists should be modelled as beam elements
- The shear connectors should be modelled as link or spring elements.

### 3. Model the structure

After all the properties have been assigned, the next step is model the structure. See Section 3.5 for more detailed advice. By following the step described below, the model of the floor can be constructed.

- Define the dimensions of the floor. i.e. the span, the width of the floor, the joist spacing, and number of beams.
- Determine the type of shear connection between the LVL joists and the concrete topping.
- Define the boundary conditions including the type of end supports, edge supports, and the number of continuous spans.
- Define the joist hangers or other end supports.
- Define a finite element grid and insert finite elements for the joists, the concrete topping, the shear connectors, and the end supports.

### 4. Applied load cases

To determine the dynamic floor behaviour, few load cases should be applied as list below;

- Normal design loads for static design
- 1 kN at mid span for simple estimation of dynamic response
- Modal analysis for detailed estimation of dynamic response with Ritz method.

## **B. PROCESSING**

The processing step is carried out by the computer. The computation time will depend on the complexity of the model.

## **C. POST- PROCESSING**

The results are determine in the post-processing step.

- Determine the deflections, natural frequency, mode shape.
- Modify the structural sizes or topping thickness as necessary. Re-run the analysis to get acceptable behaviour.

From the analysis previously described for LCC flooring system, it is clear that the following parameters and modelling details should be considered.

i. Local axis

The definition of the local axis of each point or member in finite element modelling is very important to understand especially for applying the material properties of LVL as an orthotropic material and the stiffness of the connectors. Wrong interpretation of the local axis will give inaccurate results.

ii. Local mode behaviour

LVL has lower Young's Modulus compared to other materials like steel or concrete, producing higher flexibility. This flexibility of the LVL will affect the local mode behaviours, especially on the timber beam. Local mode behaviour will change the behaviour of the LCC system and reduce the natural frequency. Thus, timber beam should be restrained to increase the stiffness as well as to avoid the local mode behaviour. Other than that, each edge support (which is represented as a column) should be assumed

as a fixed support to give more accurate results provided that all of the input variables are assessed correctly.

iii. Mass

The mass of the floor should be input equivalent to the self-weight of the floor and all other permanent loads that might be present.

iv. Stiffness of multi-span or multi-storey

It is quite complicated to model multi-span or multi-storey TCC floors. The stiffness of the continuity of the span over the supports or the stiffness of the structure between adjacent floors should be included. Column sections should be considered as pinned at both ends.

v. Joist hanger stiffness

The flexibility of joist hangers at the support end of the floor should be accounted for in the modelling, because the joist hanger flexibility will affect the floor behaviour. The stiffness should be calculated as described in Chapter 3.

vi. Mesh

There are no hard and fast rules for the size of the finite elements (or finite element mesh), but, in general, if the number of elements can be doubled without significantly changing the frequencies, then there are sufficient elements and the model should be adopted.

## 7.5 Simple design method

A simple design method is the easy way to make the first assumptions on the dynamic behaviour of the floor. By using the basic formulae given below, the fundamental natural frequency of the LCC floor could be determined.

In many cases the edge condition parallel to the floor joist may be neglected, and the frequency may be approximated by

$$f_n = \frac{\pi}{2l^2} \sqrt{\frac{(EI)_{com}}{m_{com}}} \quad (Hz) \quad (7-1)$$

where  $(EI)_{com}$  is the composite flexural stiffness ( $Nm^2$ ),  $m_{com}$  is the composite mass per unit length ( $kg/m$ ) and  $l$  is the span length ( $m$ ).

If the floor system consists of both joists and beams, the fundamental frequency of the floor system is reasonably well approximated by (Murray et.al, 2003):

$$f_{n, floor} = \sqrt{\frac{f_{n, joist}^2 \times f_{n, beam}^2}{f_{n, joist}^2 + f_{n, beam}^2}} \quad (7-2)$$

where

$$\begin{aligned} f_{n, floor} &= \text{fundamental natural frequency of the floor system (Hz),} \\ f_{n, joist} &= \text{fundamental natural frequency of the joist alone (Hz),} \\ f_{n, beam} &= \text{fundamental natural frequency of the beam supporting the joist (Hz)} \end{aligned}$$

Otherwise, to get more accurate result, the fundamental frequency,  $f_n$  of a LCC floor system, is calculated from the plate theory by Timoshenko (1964);

$$f_n = \frac{\pi}{2l^2} \sqrt{\frac{(EI)_{com}}{m_{com}}} \times \sqrt{1 + \left[ 2 \left(\frac{l}{b}\right)^2 + \left(\frac{l}{b}\right)^4 \right] \frac{(EI)_x}{(EI)_y}} \quad (Hz) \quad (7-3)$$

where  $(EI)_{com}$  is the composite flexural stiffness ( $Nm^2$ ),  $(EI)_x$  is the stiffness of floor joists and slab per unit width,  $(EI)_y$  is the stiffness of floor slab per unit width in a perpendicular direction to the joists,  $b$  is the floor width,  $m_{com}$  is the composite mass per unit length ( $kg/m$ ) and  $l$  is the span length ( $m$ ).

The flexural stiffness of the composite beam  $(EI)_{com}$  is obtained using the Equation 7.4, as recommended by Eurocode 5 (CEN, 2004b) and as mentioned in section 2.1.1;

$$(EI)_{com} = (EI)_c + (EI)_t + \gamma_1 E_c A_c a_c^2 + \gamma_2 E_t A_t a_t^2; \quad (7-4)$$

where  $(EI)_c$  is the flexural stiffness of concrete topping ( $Nm^2$ ),  $(EI)_t$  is the flexural stiffness of LVL joist ( $N/m^2$ ),  $E_c$  is the modulus elasticity of concrete topping

(N/m<sup>2</sup>),  $E_t$  is the modulus elasticity of LVL joist (N/m<sup>2</sup>),  $A_c$  is the concrete topping area (m<sup>2</sup>),  $A_t$  is LVL joist area (m<sup>2</sup>).

The  $a_c$  and  $a_t$  distances can be determined as below:

$$a_c = \frac{\gamma_t E_t A_t H}{\gamma_c E_c A_c + \gamma_t E_t A_t}, \quad a_t = \frac{\gamma_c E_c A_c H}{\gamma_c E_c A_c + \gamma_t E_t A_t}; \quad (7-5a, 7-5b)$$

Where;

$$H = \frac{t_c}{2} + t_p + \frac{t_{LVL}}{2}; \quad (7-6)$$

$$\gamma_c = \frac{1}{1 + \frac{\pi^2 E_c A_c s_{eff}}{k_s l^2}}, \quad \gamma_t = 1 \quad (7-7a, 7-7b)$$

where  $s_{eff}$  is the effective spacing (mm) of connection,  $k_s$  is the slip modulus of the connection (kN/m),  $t_c$  is the thickness of concrete topping,  $t_{LVL}$  is the thickness of LVL and  $t_p$  is the thickness of permanent formwork. The slip modulus was obtained from the push-out test as discussed in Chapter 2. However, when designing for floor vibration, the serviceability stiffness should be considered, as the dynamic stiffness of the floor was found to be 10 % higher than the static stiffness, where the  $k_{sls,dynamic} = 1.1 \times k_{sls,static}$ .

The effective spacing of connections can be calculated as below

$$s_{eff} = 0.75s_{min} + 0.25s_{max} \quad (7-8)$$

where  $s_{min}$  is minimum spacing of connections and  $s_{max}$  is maximum spacing of connections along the beam span.

## 7.6 Worked Example

The simple design method was applied to a simply-supported LVL-concrete composite floor spanning 8 m with 400 x 63 mm joists and a 600 x 65 mm concrete slab. The calculation was evaluated for the walking vibration of a residential or commercial office floor.

### **a. Material properties**

#### *i. Concrete*

$$\begin{aligned}\text{Concrete topping thickness, } t_c &= 0.065 \text{ m} \\ \text{Concrete topping width, } b_c &= 0.6 \text{ m} \\ \text{Density, } \delta_c &= 2400 \text{ kg/m}^3 \\ \text{Modulus Young, } E_c &= 30 \times 10^9 \text{ N/m}^2 \\ \text{Moment Inertia, } I_c &= bh^3/12 \\ &= 1.37 \times 10^{-5} \text{ m}^4 \\ \text{Mass, } m_c &= A_c \delta_c \\ &= 0.065 * 0.065 * 2400 \\ &= 93.6 \text{ kg/m}\end{aligned}$$

#### *ii. LVL*

$$\begin{aligned}\text{LVL thickness, } t_{LVL} &= 0.4 \text{ m} \\ \text{LVL width, } b_{LVL} &= 0.063 \text{ m} \\ \text{Density, } \delta_t &= 620 \text{ kg/m}^3 \\ \text{Modulus Young, } E_t &= 12.7 \times 10^9 \text{ N/m}^2 \\ \text{Moment Inertia, } I_t &= bh^3/12 \\ &= 3.36 \times 10^{-4} \text{ m}^4 \\ \text{Mass, } m_t &= A_t \delta_t \\ &= 0.063 * 0.4 * 620 \\ &= 15.62 \text{ kg/m}\end{aligned}$$

#### *iii. Permanent formwork*

$$\text{Thickness of permanent formwork, } t_p = 0.017 \text{ m}$$

### **b. Effective stiffness for composite, (EI)<sub>com</sub>**

The connection slip modulus,  $k_s = 2.47 \times 10^8 \text{ N/m}^2$ ,  
(Use a rectangular notch (50 mm x 300 mm) with 16 mm diameter coach screw (refer to Appendix A)),

Take,

$$\begin{aligned}\text{Maximum spacing, } s_{\max} &= 1.394 \text{ m} \\ \text{Minimum spacing, } s_{\min} &= 0.831 \text{ m}\end{aligned}$$

Use Equation (7-8)

$$\begin{aligned}\text{Effective spacing of connection, } s_{\text{eff}} &= 0.75 s_{\min} + 0.25 s_{\max} \\ &= 0.972 \text{ m}\end{aligned}$$

Concrete gamma coefficient from Equation (7-7a) is:

$$\gamma_1 = \frac{1}{1 + \frac{\pi^2 E_c A_c s_{\text{eff}}}{k_s l^2}} = 0.585$$

Use Equation (7-6) and (7-5a)

$$H = \frac{t_c}{2} + t_p + \frac{t_{LVL}}{2} = 0.25$$

$$a_c = \frac{\gamma_t E_t A_t H}{\gamma_c E_c A_c + \gamma_t E_t A_t} = 0.08$$

$$a_t = \frac{\gamma_c E_c A_c H}{\gamma_c E_c A_c + \gamma_t E_t A_t} = 0.17$$

Thus, Effective stiffness for composite,  $(EI)_{com}$  (refer to Equation 7-4)

$$(EI)_{com} = E_c I_c + E_t I_t + \gamma_1 E_c A_c a_c^2 + \gamma_2 E_t A_t a_t^2 = \mathbf{1.83 \times 10^7 \text{ N/m}^2}$$

### **c. Fundamental natural frequency**

Refer to Equation 7.1

$$f_n = \frac{\pi}{2l^2} \sqrt{\frac{(EI)_{com}}{m_{com}}}$$

$$= \mathbf{10 \text{ Hz} > 8 \text{ Hz}}$$

Thus, the floor is satisfactory as suggested in Eurocode 5 (CEN, 2004b).

### **d. Evaluation (refer Hu (2015))**

There no standard design methodology or guidance for timber-composite floor established, as mentioned by FPInnovation (2013). Therefore, another method is suggested to evaluate the satisfactory of the floor using Hu's (2015) method, as discussed in section 2.2.4. The reason is the wood-framed floor that proposed by Hu (2015) similar to the LCC floor, especially the wood-frame with concrete topping. However, the Hu (2015) method does not consider the composite action on the floor.

From Equation (2-18) ;

$$l \leq \frac{1}{8.22} \times \frac{EI_{com}^{0.284}}{(F_{scl}^{0.14})(m_{com}^{0.15})}$$

where;

$$F_{scl} = 0.0294 + 0.536 K_1^{0.25} + 0.516 K_1^{0.5} - 0.31 K_1^{0.75}$$

$$K_1 = \frac{K_J}{K_J + K_L}$$

$$K_j = \frac{EI_{com}}{l^3} = 3.57 \times 10^4 \text{ N/m,}$$

$$K_L = \frac{0.585 \times l \times E_c I_c}{b_1^3}$$

Use joist spacing,  $b_1 = 0.6 \text{ m}$

Thus,  $K_L = 8.9 \times 10^6 \text{ N/m,}$

$\therefore K_1 = 0.004$  and  $F_{scl} = 0.19$

Use Equation (2-18)

$$\frac{1}{8.22} \times \frac{EI_{com}^{0.284}}{(F_{scl}^{0.14})(m_{com}^{0.15})} = \mathbf{8.75 \text{ m}}, \text{ which is more than the trial span of 8 m,}$$

therefore the vibration-controlled span is satisfactory.

The example of this calculation method using Matlab code is given in Appendix B.

## 7.7 Summary

This chapter has given a methodology for design of LCC floors, either by hand calculation or sophisticated finite element modelling. Both methods will give a prediction of the dynamic floor behaviour, however, the finite element modelling will give a much more accurate prediction, provided that all of the input variables are assessed correctly.

## **CHAPTER 8 CONCLUSIONS AND RECOMMENDATIONS FOR FURTHER WORK**

This chapter summarises and concludes the complete work in this research project. Also, the recommendations for future research, which are mainly findings from this research, are provided in this chapter.

### **8.1 Research objectives**

The three objectives of this research were given in Chapter 1 as follows:

1. Experimentally characterise the dynamic performance (specifically the natural frequencies, equivalent viscous damping ratios and mode shapes) of full- and reduced-scale LVL-concrete composite floor system beams and floors.
2. Implement numerical finite element modelling of the tested structures, full- and reduced-scale beams and floors, using the results from experimental modal analysis to verify the models.
3. Propose a simple design method for control of vibration at the serviceability limit state based on finite element modelling results.

Objectives 1 and 2 have been met fully, as described in the thesis. Objective 3 has been addressed in Chapter 7, and is summarised below.

### **8.2 Research Summary**

The aim of this research was to improve the knowledge of the dynamic behaviour of LVL-concrete composite (LCC) T-joint flooring system, and to provide some recommendations to structural engineers to control the vibration of these structures. To get a better understanding of the vibration behaviour of LCC floors, experimental modal analysis (EMA) tests and finite element analysis (FEA) were carried out.

This research began with the experimental modal analysis (EMA) tests on the 6m, 8m and 10m LCC T-joint specimens, to study the vibration behaviour, as discussed

in Chapter 3. Then, the experimental works were verified with finite element analysis (FEA) using the SAP 2000 software package. Both EMA and FEA results show that the fundamental natural frequencies for 6 m, 8 m and 10 m LCC specimens were 15 Hz, 9 Hz and 6 Hz, respectively. It showed that the 6 m and 8 m LCC specimens were over the limitation of 8 Hz natural frequency as suggested by Ohlsson (1988) and Eurocode 5 (CEN, 2004b). However, the natural frequency of the 10 m LCC specimens was under the limitation of 8 Hz natural frequency.

As expected, the longer the specimen, the lower the natural frequency. Thus, it is suggested that the suitable limitation span length for the tested floor geometry should not be more than 8 m. In addition, the rigidity of the boundary conditions had a big influence on the vibration behaviour. Changing the boundary support condition from flexible (steel roller) to stiffer (timber block) increased the natural frequency of the floor system, helping to push the natural frequency above 8 Hz.

The experimental results show a general trend for the natural frequencies of isolated flooring components to decrease when they form part of a larger structural system, and there is a slight trend for the natural frequencies of the isolated components to decrease in proportion to the number of similar spans and storeys.

Further research on the effect of topping thickness and LVL joist thickness was discussed in Chapter 6. The elastic vibration behaviour of the LCC floor was governed by both stiffness and mass of the LVL and the concrete topping. When the concrete topping thickness is increased, the stiffness of the LCC floor also increases due to (i) an increase in stiffness of the LCC floor with respect to the LVL only beam (which is a positive effect); and (ii) an increase in mass, due to the weight of the concrete (which is a negative effect in terms of vibration).

The transmission of vibration energy was determined through the multi-span and multi-storey specimens. With multiple floor systems, the vibration energy was found to be dissipated and transmitted between spans and storeys. The outer span received more vibration energy compared to the inner span as illustrated in Chapters 4 and 5. Also, the local mode natural frequency of each span or storey was dominated by the global mode natural frequency, according to the mode shape behaviour of the specimens.

### 8.3 Recommendations for designers

1. The recommended design criterion for LCC floors is the widely accepted limit of 8Hz for the natural frequency of vibration. Floors with a lower frequency than this will often be unacceptable to users.
2. There is a hierarchy of design methods for assessing the vibration performance of LCC floors, listed in order of increasing accuracy and increasing work for the designer:
  - a. Static deflection of 1mm under a point load of 1kN.
  - b. Equations for the Simple Design Procedure described in Chapter 7.
  - c. Detailed finite element analysis, for the Advanced Design Procedure, as described in Chapter 7.
3. To obtain accurate results, even for simple floors, a finite element analysis is recommended. However, the input parameters and the modelling techniques should be considered carefully, as discussed in Chapter 7, especially for the local mode behaviour.
4. For complex floors that are quite impossible to design by hand, a finite element analysis is the only way of assessing the vibration frequency of the floor.
5. The longest practical span for an LCC flooring system such as described herein, is recommended to be 8m. For spans greater than 8m, the floors may have an issue with deflections and vibration problems may occur. For floors spanning more than 8 m, the stiffness would need to be increased by using bigger joists or a thicker topping, or both. Another possibility would be to try a reduced joist spacing, or find a way to increase the damping.
6. Designers of some buildings may need to take precautions to ensure that floor vibrations in one part of the building are not transmitted to other sections of flooring at the same level, or to floors on other storeys of the building.

## **8.4 Recommendations for Further Research**

1. A methodology has been presented in this thesis for the verification of analytical models through experimental testing of component parts of real structures. However, due to the limited time and resources available to this project, only a small number of structures were actually tested in the laboratory. Thus, it is recommended that more testing be carried out on full scale floors in real buildings, so that the vibration behaviour may be understood better, leading to improved design guidelines.
2. In this research, the effects of adjacent beams on multi-span flooring systems were investigated using only limited number of tests of a reduced-scale (one-third scale) 4-span LVL-concrete composite T-joist specimen. It is recommended that, to increase the confidence of the conclusion drawn in this thesis, a larger number of tests are required on full-scale TCC flooring systems, including tests in real buildings.
3. The effect of boundary conditions was partly investigated during the experimental work. Some end moment fixity was provided by letting the specimen stand by its own on the laboratory floor. It is recommended that in future tests, a wider range of support conditions should make sure that there is no movement at both ends of the specimens during the testing.
4. The propagation of vibration waves was observed during the impact tests on multi-span LVL-concrete specimens. Future studies should include the effects of wave propagation in detail, to understand the effect on adjacent beams and on other floors, where the vibration energy is transmitted between floors.
5. Finite Element Analysis was applied to all the tested LVL-concrete composite specimens and multi-span LVL-concrete composite specimens. For realistic floors, the FEA was only applied to one typical floor. Hence, it is recommended that the FEA should be applied to a much wider range of full-scale LVL-concrete composite flooring systems.
6. There should be more experimental study of the vibration criteria for a floor subject to human walking excitation, including the effects of damping.

## REFERENCES

- Abd Ghafar, N. H. (2008). Forced vibration testing on LVL-concrete composite floor system, *7<sup>th</sup> Fib Phd Symposium in Stuttgart*, Germany, pp. 1-6.
- Abd Ghafar, N.H., Deam, B., Fragiacomio, M. & Buchanan, A. (2008). Vibration performance of LVL-concrete composite floor systems. *10<sup>th</sup> World Conference on Timber Engineering WCTE*, vol. CD. Miyazaki, Japan.
- Abd Ghafar N H, Deam, B., Fragiacomio, M., Buchanan, A. (2008). Susceptibility to Vibrations of LVL-Concrete Composite Floors. *Workshop Italiano Sulie Composite*. Benevento, Italy: University Degli Studi Del Sannio.
- Allen, D. E., & Murray, T. M. (1993). Design criterion for vibrations due to walking. *Engineering Journal*, 30(4), 117–129.
- ARUP (2012). Technical Report on Nelson Marlborough Institute of Technology Arts and Media Building - Vibration and Acoustic Study, Opus, Australia.
- AS/NZS, (2002). AS/NZS 1170.0:2002 Structural design actions. *Part 0: General Principles*. Sydney and Wellington (Jointly publish).
- Bachmann, H. & Ammann, W. ,(1987). *Vibrations in Structures: Induced by Man and Machines*, IABSE-AIPCIVBH, Zurich, Switzerland.
- Bernard, E. S. (2008). Dynamic Serviceability in Lightweight Engineered Timber Floors. *Journal of Structural Engineering*, 134(2), 258–268.
- Bernard, S. (2003). *Vibration of composite timber and concrete flooring*. Victoria, Australia: Forest & Wood Products Research & Development Corporation.
- Benitez, M.F. (2000). Development and testing of timber/concrete shear connector. *Proceedings of the World Conference on Timber Engineering 2000*. Vancouver, BC, Canada, paper 8.3.2
- Blakeborough, A., & Williams, M. S. (2003). Measurement of floor vibrations using a heel drop test. *Proceedings of the Institution of Civil Engineers: Structures and Buildings*, 156(4), 367-371.
- Brunner, M., Romer, M., & Schnuriger, M. (2007). Timber-concrete-composite with an adhesive connector (wet on wet process). *Materials and Structures/Materiaux et Constructions*, 40(1), 119–126.
- Canadian Construction Materials Centre (CCMC), (1997). Development of Design Procedures for Vibration Controlled Spans using Engineered Wood Members. Canadian Wood Council, DMO associates, Quaille Engineering Ltd., Forintek Canada Corp. Ottawa.
- Ceccotti, A. (1995). Timber-Concrete Composite Structures. *Timber Engineering, Step 2* (1st Edition). Centrum Hout, The Netherlands.

- Ceccotti, A. (2002). Composite concrete-timber structures. *Progress in Structural Engineering and Materials*, 4(3), 264–275.
- CEN (2004b). Design of timber structures. In *Part 1-1: General rules and rules for buildings*. Brussels, Belgium.
- Crocetti, R, Sartori, T & Flansbjerg, M. (2010). Timber-Concrete Composite Structures with Prefabricated FRC Slab, *World Conference on Timber Engineering*, Italy.
- Crocetti, R, Sartori, T & Tomasi, R (2015). Innovative Timber-Concrete Composite Structures with Prefabricated FRF Slabs, *Journal of Structural Engineering*, 141(9), 1-10
- Deam B, Fragiaco M, Gross LS (2008). Experimental behaviour of prestressed LVLconcrete composite beams. *Journal of Structural Engineering - ASCE*. 134(5), 801-809.
- Devine, P.J, Smith, A.L. & Hicks, S.J (2007). Design Guide on the Vibration Floors (2<sup>nd</sup> Edition). *The Steel Construction Institute (SCI)*. Berkshire, United Kingdom
- Dolan, J. D. et al. (1999). Preventing Annoying Wood Floor Vibrations. *Journal of Structural Engineering*, Vol.125 (1), 19-24.
- Ebrahimpour, A et. al, (1996). Measuring and Modeling Dynamic Loads Imposed by Moving Crowds. *Journal of Structural Engineering*, 122(12), 1468–1474.
- Ebrahimpour, A., & Sack, R. L. (1989). Modeling Dynamic Occupant Loads. *Journal of Structural Engineering*, 115(6), 1476–1496.
- Ebrahimpour, A., & Sack, R. L. (1992). Design Live Loads for Coherent Crowd Harmonic Movements. *Journal of Structural Engineering*, 118(4), 1121–1136.
- El-Dardiry, E., & Ji, T. (2006). Modelling of the dynamic behaviour of profiled composite floors. *Engineering Structures*, 28(4), 567–579.
- Ellingwood, A. & Tallin, B. (1984). Structural serviceability: floor vibrations. *Journal of Structural Engineering*, 110(2), 410–419.
- Franklin K & Hough R., (2014). Modelling and measurement of the dynamic performance of a timber concrete composite floor. In *Wood Engineering Conference* (p. CD). Quebec City, Canada.
- Fuller, A. H. (1924). Dynamic effects of moving floor loads - stresses measured in the floor and balcony of a college gymnasium. *Am Arch Arch*, 126(11), 455–456.
- FPIInnovations (2013). Technical Guide for the Design and Construction of Tall Wood Building in Canada. Quebec.
- Gross, S. L. (2004). *Experimental testing on prestressed timber-concrete composite beams*. *Civil Engineering*. University of Canterbury, New Zealand.

- Gutkowski, R, Balogh, J., Natterer, Brown, K., Koike, E. & Etournaud, P, (2000). Laboratory tests of composite wood-concrete beam and floor specimens. *Sixth World Conference on Timber Engineering*. Whistler.
- Hehhl, S., Tannert, T., Meena, R. and Vallee, T., (2014). Experimental and Numerical Investigations of Groove Connections for a Novel Timber-Concrete Composite System. *Journal of Performance of Constructed Facilities*, 28(6), A4014010
- Hu, L.J., (2007). Design Guide for Wood-framed Floor Systems. Canadian Forest Service Report NO. 32. Quebec:FPInnovations.
- Hu, L. J., (2015). Mid-rise Wood-Frame Construction Handbook, First Edition, FPInnovations, Quebec.
- ISO (1989). ISO 2631-2:1989 evaluation of human exposure to whole-body vibration - part 2: Continuous and shock-induced vibration in buildings (1 to 80Hz).
- Lenzen, K. H. (1966). Vibration of steel joist-concrete slab floors. *American Institute of Steel Construction -- Engineering Journal*, 3(3), 133–136.
- Ljunggren, F., (2006). Floor Vibration - Dynamic Properties and Subjective Perception, Lulea University of Technology, Sweden.
- Mertens, C., Martin, Y., & Dobbels, F. 2007. Investigation of the vibration behaviour of Timber-Concrete composite floors as part of a performance evaluation for the Belgian building industry. *Building Acoustics*, 14 (1), 25-36.
- Murray, T.M, Allen, D.E. & Ungar, E.E., (2003). *Floor Vibration due to Human Activity*. United States of America: American Institute of Steel Construction.
- Natterer, J., Hamm, J., & Favre, P., (1996). Composite wood-concrete floors for multistorey buildings. In *Wood Engineering Conference* (Vol. 3, pp. 3425–3431). Omnipress, Madison, WIs.
- National Research Council (NRC), (2010). National Building Code of Canada (NBC). National Research Council of Canada, Ottawa.
- Nauta, F. (1970). *Composite Glulam beam-reinforced concrete deck bridges*. Test report 364, Central labs.
- Nelson, F. C. (1974). Subjective rating of building floor vibration. *Sound and Vibration*, 8, 34–37.
- Nguyen, T., Gad, E., Wilson, J. & Haritos, N., (2012). Improving a current method for predicting walking-induced floor vibration, *Steel and Composite Structures*, 13 (2), pp 139-155.
- Nguyen, T., Gad, E., Wilson, J. & Haritos, N. (2014). Mitigating foot fall induced vibration in long-span floors, *Australian Journal of Structural Engineering*, 15(1), pp. 97-109,

- Ohlsson, S (1988). *Springiness and human-induced floor vibrations – A design guide*. Swedish Council for Building Research, Stockholm, Sweden
- Pavic, A., & Reynolds, P. (2003). Modal testing and dynamic FE model correlation and updating of a prototype high-strength concrete floor. *Cement and Concrete Composites*, 25(7), 787–799.
- Pavic, A., Widjaja, T., & Reynolds, P. (2002). The use of modal testing and FE model updating to investigate vibration transmission between two nominally identical building floors. In *International Conference on Structure Dynamics Modeling–Test, Analysis, Correlation and Validation* (pp. 347-355).
- Pernica, G., & Allen, D.E, (1982). Floor vibration measurements in a shopping centre. *Canadian Journal of Civil Engineering*, 9(2), 149.
- Rainer, J. H. (1980). Dynamic tests on a steel-josit concrete-slab floor. *Canadian Journal of Civil Engineering*, 7(2), 213–224.
- Reiher, H., & Meister, F. (1931). The effect of vibration on people. *Forschung Im Ingenieurwesen*, 2(11), 381–386 (in German). Retrieved from
- Reynolds, P., Pavic, A. (2000). Quality Assurance Procedures for the Modal Testing of Building Floor Structures. *Experimental Techniques*, 24(4), 36-41.
- Rijal, R., Samali, B. & Crews, K. (2010). Dynamic performance of the timber-concrete composite flooring systems, *Australasian Conference on the Mechanics of Structures and Materials (ACMSM) 21*, Melbourne, Australia.
- Rijal, R. (2013). *Dynamic performance of timber and timber-concrete composite flooring systems*. University of Technology, Sydney.
- SAP2000. (1997). User Manual : Integrated Finite Element Analysis and Design Structures: Computer and Structures, Inc.
- Seibold, E. (2004). *Feasibility study for composite concrete-timber floor systems using laminated veneer lumber in New Zealand*. University of Karlsruhe, Germany.
- Setareh, M. & Hanson, R. (1992). Tuned mass dampers for balcony vibration control. *Journal of Structural Engineering – ASCE*, 118( 3), pp. 723-740.
- Skinner J. M. (2013). *Thin topping timber-concrete composite floors*. University of Bath.
- Skinner J., Harris R., Paine K., Walker P., and B. J. (2013). Ultra-thin topping upgrades for improved serviceability performance. *Advanced Materials Research*, (778), 673–681.
- Smith, I. and Chui, Y. H., (1988). Design of lightweight wooden floors to avoid human discomfort. *Canadian Journal of Engineering*, 15(2), 254-262.
- Soltis L.A. & Hunt M.O, (2002). Vibration testing of timber floor systems. *Forest Products Journal*, 52(10), 75–81.

- Stojić, D., & Cvetković, R. (2001). Analysis of a composite timber-concrete structures according to the limit states design and innovative methods in coupling of a timber and concrete. *Facta Universitatis Series: Architecture and Civil Engineering*, v.2(No3), p.169–184.
- Thornton, C. H., Cuoco, D. A. & Velivasakis, E.E.( 1990), “Taming Structural Vibrations”, *Civil Engineering – ASCE*, Vol. 60, No. 11, pp. 57-59.
- Timoshenko, S. (1964). *Theory of Plates and Shells*. London:McGraw-Hill, 2nd ed.
- Tilden, C. J. (1913). Kinetic effects of crowds. *Proceedings of the American Society of Civil Engineers*, 34(3), 325-340.
- Tuan, C. Y., & Saul, W. E. (1985). Loads due to spectator movements. *Journal of Structural Engineering*, 111(2), 418–434.
- Ungar, E. E. (1978). Footfall-induced vibrations of floors supporting sensitive equipment. *The Journal of the Acoustical Society of America*, 64(S1), S26-S26
- Van der Linden, M. L. R. (1999). *Timber-Concrete Composite Floor Systems*. TU Delft, Delft University of Technology.
- Webster, A. & Vaicaitis, R. 1992, “Application of tuned mass dampers to control vibrations of composite floor systems”, *Engineering Journal of the American Institute of Steel Construction*, 29( 3), pp. 116-124.
- Wiss, J. F., & Parmelee, R. A. (1974). Human perception of transient vibrations. *American Institute of Steel Construction*, 100(4), 773–787.
- Wyatt, T. A. (1989). *Design Guide on The Vibration of Floors (SCI Publication 076)*. Ascot, UK: SCI.
- Yeoh Fragiacom, M., Abd. Ghafar, N.H, Buchanan, A., Deam, B., D. (2008). Behaviour of timber-concrete composite floor systems. *Australasian Structural Engineering Conference*. Melbourne, Australia.
- Yeoh, D. (2010). *Behaviour and design of timber-concrete composite floor system*. University of Canterbury, New Zealand.
- Zivanovic, S., & Pavic, A. (2009). Probabilistic Modeling of Walking Excitation for Building Floors. *Journal of Performance of Constructed Facilities*, 23(3), 132–143.

## APPENDIX A MATERIAL PROPERTIES

Material properties of concrete and LVL is shown in Table A1 and A2. The slip modulus of connection is adopted from Yeoh (2010) is illustrated in Table A3 and the characteristic load of joist hanger is shown in Table A4.

Table A1 Properties of Concrete

Concrete Properties			
Modulus of elasticity	$E_c$	30,000	MPa
Modulus of rigidity	$G_c$	1,875	MPa
Density	$\rho_c$	2400	kg/m <sup>3</sup>

Table A2 Properties of LVL

Concrete Properties			
Modulus of elasticity	$E_t$	12,700	MPa
Modulus of rigidity	$G_t$	660	MPa
Density	$\rho_t$	620	kg/m <sup>3</sup>

Table A3 Comparison of mean strength and secant slip moduli for different connectors

Type of connections	Slip moduli (kN/mm)		Shear strength (kN)
	$k_{s,0.4}$	$k_{s,0.6}$	$F_{max}$
$\phi 16$ lag screw only	28.9	6.3	46.4
150 mm notch only	105.0	59.3	48.3
150 mm NLS $\phi 12$	77.9	74.5	66.0
150 mm NLS $\phi 16$	80.2	75.4	73.0
300 mm NLS $\phi 16$	247.2	241.4	138.9

Note: NLS = Notched connection reinforced with Lag Screw (source: Yeoh,2010)

Table A4 Characteristic load of joist hanger

Type of Joist Hanger	Characteristic load- Nails			Characteristic load- Screws		
	No. Of Nails per Flange*	Down (kN)	Uplift (kN)	No. Of Nails per Flange	Down (kN)	Uplift (kN)
47 x 90	3	9.0	6.0	1	7.0	7.4
47 x 120	5	15.0	10.0	2	14.0	12.0
47 x 190	9	27.0	18.0	3	21.0	18.0
95 x 165	8	24.0	16.0	3	21.0	18.0
70 x 180	8	24.0	16.0	3	21.0	18.0

(source: MITEK New Zealand Ltd)

## APPENDIX B WORKED EXAMPLE

```
% Design for 8 m LCC floor according to Hu (2015), vibration-controlled
% span

l= 8; % (floor span,m)
%% Material Properties

% concrete
tc = 0.065; % (concrete topping thickness, m)
bc = 0.6; % (concrete topping width,m)
Ec = 30e9; % (Modulus Young of concrete, N/m^2)
dc = 2400; % ( Density of concrete, kg/m^3)
Ic = (bc*tc^3)/12; % (Moment inertia of concrete, m^4)
mc = dc*tc*bc; % (concrete mass, kg/m)

%LVL joist
tj = 0.4; % (LVL thickness, m)
bj = 0.063; % (LVL width,m)
Ej = 12.7e9; % (Modulus Young of LVL, N/m^2)
dj = 620; % ( Density of LVL, kg/m^3)
Ij = (bj*tj^3)/12; % (Moment inertia of LVL, m^4)
mj = dj*tj*bj; % (LVL mass, kg/m)

%% Effective stiffness for composite, (EI)com

k = 2.47e8; % (Connection slip modulus, N/m^2)
H = tc/2 + tj/2 + 0.017;
max = 1.394; % (maximum connection spacing)
smin = 0.831; % (minimum connection spacing)
seff = 0.75*smin + 0.25*smax; % (effective spacing of connection)

gamma_c = 1/((1+(3.142^2*Ec*tc*bc*seff)/(k*l^2)));
gamma_t = 1;

ac = (gamma_t*Ej*tj*bj*H)/((gamma_c*Ec*tc*bc)+(gamma_t*Ej*tj*bj));
at = (gamma_c*Ec*tc*bc*H)/((gamma_c*Ec*tc*bc)+(gamma_t*Ej*tj*bj));

EIcom = (Ec*Ic)+(Ej*Ij)+(gamma_c*Ec*tc*bc*ac^2)+(Ej*tj*bj*at^2);

%% Fundamental natural frequency, fn (Hz)

fn2 = (3.142/(2*l^2))*sqrt(EIcom/(mc+mj));

%% Calculate Fsc1
% Fsc1 = 0.0294 + 0.536K1^0.25 + 0.516K1^0.5 - 0.31K1^0.75

kj = EIcom/l^3;
kl = (0.585*l*Ec*Ic)/bc^3;
k1 = kj/(kj+kl);
Fsc1 = 0.0294 + (0.536*(k1^0.25)) + (0.516*(k1^0.5)) - (0.31*(k1^0.75));

%% vibration-span control
% l<= 1/8.22 x ((EIeff)^0.284)/Fsc1^0.14 x mL^0.15

lcontrol = (1/8.22)* (EIcom^0.284/(Fsc1^0.14*((mc+mj)^0.15)));
% = 8.75 m
```

% The required span, 8 m less than the vibration-controlled span, 8.75 m,  
% Thus, the design can be accepted.